ISSN: 2408-2384 (Online)
ISSN: 1686-5456 (Print)

Environment and Natural Resources Journal

Volume 17, Number 1, January - March 2019

Scopus® Clarivate Analytics EBSCO HOST DOAJ DIRECTORY OF OPEN ACCES JOURNALS ASEAN CITATION INDEX TCI

Environment and Natural Resources Journal (EnNRJ)

Volume 17, Number 1, January-March 2019 ISSN: 1686-5456 (Print)
ISSN: 2408-2384 (Online)

AIMS AND SCOPE

The Environment and Natural Resources Journal is a peer-reviewed journal, which provides insight scientific knowledge into the diverse dimensions of integrated environmental and natural resource management. The journal aims to provide a platform for exchange and distribution of the knowledge and cutting-edge research in the fields of environmental science and natural resource management to academicians, scientists and researchers. The journal accepts a varied array of manuscripts on all aspects of environmental science and natural resource management. The journal scope covers the integration of multidisciplinary sciences for prevention, control, treatment, environmental clean-up and restoration. The study of the existing or emerging problems of environment and natural resources in the region of Southeast Asia and the creation of novel knowledge and/or recommendations of mitigation measures for sustainable development policies are emphasized.

The subject areas are diverse, but specific topics of interest include:

- Biodiversity
- Climate change
- Detection and monitoring of polluted sources e.g., industry, mining
- Disaster e.g., forest fire, flooding, earthquake, tsunami, or tidal wave
- Ecological/Environmental modelling
- Emerging contaminants/hazardous wastes investigation and remediation
- Environmental dynamics e.g., coastal erosion, sea level rise
- Environmental assessment tools, policy and management e.g., GIS, remote sensing, Environmental Management System (EMS)
- Environmental pollution and other novel solutions to pollution
- Remediation technology of contaminated environments
- Transboundary pollution
- Waste and wastewater treatments and disposal technology

Schedule

Environment and Natural Resources Journal (EnNRJ) is a quarterly published journal in January-March, April-June, July-September and October-December.

Publication Fees

There is no cost of the article-processing and publication.

Ethics in publishing

EnNRJ follows closely a set of guidelines and recommendations published by Committee on Publication Ethics (COPE) (http://publicationethics.org/).

Editorial Office Address
Research and Academic Services Section,
Faculty of Environment and Resource Studies, Mahidol University
999, Phutthamonthon Sai 4 Road, Salaya, Phutthamonthon, Nakhon Pathom, Thailand, 73170
Phone +662 441 5000 ext. 2108, 2132 Fax. +662 441 9509-10
Website: https://www.tci-thaijo.org/index.php/ennrj/
E-mail: ennrjournal@gmail.com

Environment and Natural Resources Journal (EnNRJ)

Volume 17, Number 1, January-March 2019 ISSN: 1686-5456 (Print)
ISSN: 2408-2384 (Online)

EXECUTIVE CONSULTANT TO EDITOR

Associate Professor Dr. Kampanad Bhaktikul
(Mahidol University, Thailand)
Associate Professor Dr. Sura Pattanakiat
(Mahidol University, Thailand)

EDITOR

Associate Professor Dr. Benjaphorn Prapagdee
(Mahidol University, Thailand)

EDITORIAL BOARD

Professor Dr. Anthony SF Chiu
(De La Salle University, Philippines)
Professor Dr. Chongrak Polprasert
(Thammasat University, Thailand)
Professor Dr. Gerhard Wiegleb
(Brandenburgische Technische Universitat Cottbus, Germany)
Professor Dr. Hermann Knoflacher
(University of Technology Vienna, Austria)
Professor Dr. Jurgen P. Kropp
(University of Potsdam, Germany)
Professor Dr. Mark G. Robson
(Rutgers University, USA)
Professor Dr. Nipon Tangtham
(Kasetsart University, Thailand)
Professor Dr. Pranom Chantaranothai
(Khon Kaen University, Thailand)
Professor Dr. Shuzo Tanaka
(Meisei University, Japan)
Professor Dr. Warren Y. Brockelman
(Mahidol University, Thailand)
Professor Dr. Yeong Hee Ahn
(Dong-A University, South Korea)
Associate Professor Dr. Kathleen R Johnson
(Department of Earth System Science, USA)
Associate Professor Dr. Sate Sampattagul
(Chiang Mai University, Thailand)
Associate Professor Dr. Sompon Wanwimolruk
(Mahidol University, Thailand)

Associate Professor Dr. Takehiko Kenzaka
(Osaka Ohtani University, Japan)
Associate Professor Dr. Tamao Kasahara
(Kyushu University, Japan)
Associate Professor Dr. Uwe Strotmann
(University of Applied Sciences, Germany)
Assistant Professor Dr. Devi N. Choesin
(Institut Teknologi Bandung, Indonesia)
Assistant Professor Dr. Said Munir
(Umm Al-Qura University, Saudi Arabia)
Dr. Manish Mehta
(Wadia Institute of Himalayan Geology, India)
Dr. Marzuki Ismail
(University Malaysia Terengganu, Malaysia)
Dr. Mohamed Fassy Yassin
(University of Kuwait, Kuwait)
Dr. Norberto Asensio
(University of Basque Country, Spain)
Dr. Thomas Neal Stewart
(Mahidol University, Thailand)

ASSISTANT TO EDITOR

Associate Professor Dr. Kanchana Nakhapakorn
Dr. Chitsanuphong Pratum
Dr. Kamalaporn Kanongdate
Dr. Paramita Punwong
Dr. Witchaya Rongsayamanont

JOURNAL MANAGER

Isaree Apinya

JOURNAL EDITORIAL OFFICER

Supalak Wattanachalarmyot
Parynya Chowwiwattanaporn

Environment and Natural Resources Journal (EnNRJ)

Volume 17, Number 1, January-March 2019 ISSN: 1686-5456 (Print)
ISSN: 2408-2384 (Online)

CONTENT

Assessment of Air and Noise Pollution from Industrial Sources in Ibadan, Southwest, Nigeria

Ogunyemi Akinsanmi*, Oguntoke Olusegun and Adeofun Clement

Department of Environmental Management and Toxicology, Federal University of Agriculture, Abeokuta, Nigeria

ARTICLE INFO

Received: 17 Apr 2018
Received in revised:
25 Jun 2018
Accepted: 4 Jul 2018
Published online:
14 Sep 2018
DOI: 10.32526/ennrj.17.1.2019.01

Keywords:
Air pollution/ Noise/ Industries/ Assessment/ Health effects/ Standards

*** Corresponding author:**
E-mail:
essackyy2k3@yahoo.com

ABSTRACT

This study assessed air quality and noise parameters in Oluyole, an industrial zone in Southwest Nigeria. Twenty three sampling points were randomly selected in the industrial and residential areas, while four points control. The assessment was carried out for eight weeks each during rainy and dry seasons. A multi-gas monitor was used to determine sampling CO, SO_2, H_2S, and Hydrocarbon (HC), while a Personal Data RAM-1200 was used to measure suspended particulate matter (SPM). Noise levels were measured using a sound level meter, while the co-ordinates of sampling points were taken with a Garmin GPS. Data were subjected to descriptive analysis and one-way analysis of variance (ANOVA) to separate means. Selected air quality parameters varied significantly ($p<0.05$) for different locations and seasons. Residential and industrial areas showed significant variation in their levels of Noise, SPM and CO. SPM and H_2S levels were higher during dry season while Noise, CO and Hydrocarbon levels were higher during the wet season. Levels of Noise, SPM, H_2S and CO decreased with increasing distance from the industrial area but the reverse was the case for Hydrocarbon. Hence, there is a need for adoption of cleaner technologies by the industries and enforcement of environmental standards by regulatory agencies.

1. INTRODUCTION

Air pollution can be defined as the presence of pollutants, such as sulphur dioxide (SO_2), particle substances (PM), nitrogen oxides (NO_x) and ozone (O_3) in the air that we inhale at levels which can create some negative effects on the environment and human health (Turk and Kavraz, 2011). It can be classified into natural air pollution which includes wind-blown dust, volcanic ash, and gases, smoke and trace gases from forest fires, and anthropogenic air pollution which includes products of combustion such as nitrogen oxides (NO_x), carbon oxides (CO_x), sulphur dioxide (SO_2) (Oyekanmi et al., 2010). Pollutants that are pumped into the atmosphere and directly pollute the air are called primary pollutants while those that are formed in the air when primary pollutants react or interact are known as secondary pollutants (Agbaire, 2009).

Industrial pollution adversely affects human health, sometimes leading to chronic diseases of permanent nature. It is a serious threat to environmental health in many cities with a wide range of symptoms such as low birth weight, increased hospitalization, sudden infant death and high mortality (Brook et al., 2004). According to WHO, more than two million premature deaths each year can be attributed to the effects of urban outdoor and indoor air pollution and more than half of this disease burden is borne by the populations of developing countries (Mohammed, 2009). Chemicals found in polluted air could cause cancer, birth defects, brain and nerve damage and long term injury to the lungs and breathing passages in certain circumstances while long term exposure to high concentrations can cause severe injury or even death (Oyekanmi et al., 2010). Effects of air pollutants on structures include discolouration of buildings, while impairment of normal visibility often leads to disruptions in transportation system, death and stunted growth of crops, and acute toxicological effect in humans (Abdulkareem and Kovo, 2006). The costs of this burden of illness would include lost years of life and income, health care costs, and quality of life related costs. Beyond the toll on human health, there will also be corresponding impacts on domestic animals and food production (Bikkhu et al., 2009).

Studies have reported high concentrations of gaseous pollutants such as NO, CO, SO_2 and hydrocarbon above permissible limits. Rene (2008)

measured high levels of particulate matter, CO, NO_2, SO_2 and Ozone above the environmental regulation limits in Vaal air shed of South Africa with warnings of serious health implications for residents, while Nkwocha and Egejuru (2008) revealed a strong association between air pollution indices and diseases such as cough, cold, bronchitis, sinusitis and phlegm among some school children in Nigeria with the strongest effect recorded among those below two years of age. Noise from industrial areas is often overlooked and has received very little attention over the years. In Nigeria, many industrial estates are located within the heart of towns and cities, while residential and commercial buildings might just find their way into industrial zones as a result of poor enforcement of town planning laws. Without strict environmental regulation and control laws in many developing countries, industrial noise sources can pose severe health risks (Nwobodo et al., 2004). The observed effects of noise on motivation, as measured by persistence with a difficult cognitive task, may either be independent or secondary to cognitive impairments (SRC, 2007). Homes, schools, hospitals and other structures found in industrial areas could be adversely affected by environmental noise. Depending on its duration and volume, the effects of noise on human health and comfort are divided into four categories; physical effects, such as hearing defects; physiological effects, such as increased blood pressure, irregularity of heart rhythms and ulcers; psychological effects, such as disorders, sleeplessness and going to sleep late, irritability and stress; and finally effects on work performance, such as reduction of productivity and misunderstanding what is heard (Ozer, 2009). Similarly, Olayinka et al. (2008), found that the noise exposure level (LAeq) in minerals crushing mills, soft drinks bottling, beer brewing, bottling and tobacco making industries was above 85 dBA and noise level was well above 60 dBA recommended by World Health Organization in five selected processing and manufacturing industries in Ilorin, Nigeria.

Air pollutions from industrial sources and their possible effects have been widely studied and this has improved the understanding of the link between air pollution and health effects thereby driving improvements of air quality in many countries. However, many challenges remain especially in the developing countries like Nigeria which are not heavily industrialised but still experience significant air pollutions in their cities. Many of these challenges include inadequate monitoring of air quality, high pollution index, scarce air pollution epidemiological research and weak enforcement of standards among others (Agbaire, 2009).

Table 1. Noise exposure limits for Nigeria (NESREA, 2009)

Facility	Maximum permissible noise limit (dBA)	
	Day	Night
Hospital, convalescence home, home for the aged, sanatorium and institutions of higher learning, conference rooms, public library, environmental and recreational sites.	45	35
Residential buildings	50	33
Mixed residential (with some commercial and entertainment)	55	45
Residential + industry or small-scale production + commerce	60	50
Industrial (outside perimeter fence)	70	60

Table 1 and Table 2 shows the National Environmental Standards Regulation Agency (NESREA) limits for noise and emissions. It specified the benchmark for noise level in various types of premises while indicating the acceptable limits for some air pollutants for long-term and short-term exposures rates.

The broad objective of this study was to evaluate the level of noise and some air pollutants, determine exceedance of ambient air quality standard and draw up management plan where necessary, while the specific objectives were:

- To evaluate the general level of some air pollutants in the study area.
- To determine seasonal variations in air qualities.
- To assess the level of noise pollution in the industrial estate.

- To establish the impact of industrial activities on ambient air qualities.
- To determine a possible exceedance of ambient air quality standards.

Table 2. National emission limits for some air pollutants

Pollutant	Emission limits (mg/m^3)	
	Long-term limits	Short-term limits
CO	1.0	5.0
HC (Total)	2.0	5.0
H_2S	0.008	0.008
SO_2	0.1	0.5
SPM	0.2	0.2
Pb	0.005	0.002
Hg	0.0003	-
O_3	0.1	0.2

2. METHODOLOGY

2.1 Site description

The study area, as shown in Figures 1 and Figure 2, was Oluyole industrial Scheme situated within Ibadan metropolis of Oyo state, Southwest Nigeria. Its geographical coordinates are Latitude 7º 21′ 19″ N and Longitude 3º 51′ 1″ E and covers about 1,926,600 m^2. Also located within the scheme are high and medium density residential areas, schools, clinics, places of religious and commercial centre. The Oluyole area of the metropolis has a population of about 282,585 according to the 2006 national population census.

The metropolis has a tropical wet and dry climate, with a lengthy wet season and relatively constant temperatures of about 32ºC throughout the year. The wet season runs from April through October, though a lull in precipitation is experienced in August which nearly divides the rainy season into two segments of wet season.

2.2 Sampling measurement

Twenty three randomly selected sampling points as illustrated in Figure 2, separated by at least 200 m covered the study area (industrial and residential) while the control area had four points, making twenty seven points altogether. The sampling design for the study area covered the industrial area with thirteen (13) points while the residential area had five (5) points on the east and west of the industrial area. Similarly, in the control (Government Residential Area devoid of Industrial Activities) within the metropolis, four randomly selected sampling points were assessed. The average value for repeated readings at each sampling point were recorded while assessment of noise and air quality parameters was carried out fortnightly for eight weeks during two periods of wet season (August to September) and dry season respectively (February to March). Concentrations of carbon monoxide (CO), sulphur-dioxide (SO_2), hydrogen sulphide (H_2S), and hydrocarbon (HC) were measured with an ITX Multi-gas Monitor while suspended particulate matter (SPM) was determined with a Personal Data RAM-1200 (Park Davis) and noise level dBA using a sound level meter (Extech Instruments 407730). Other parameters including air temperature, wind speed and wind pressure were determined by a portable weather station as a guide in the positioning of sampling equipment. Temperature and relative humidity were measured using a Pen monitor while wind speed and wind pressure were determined with a portable weather station and the coordinates of sampling points were taken with Garmin GPS. Iyaganku was selected as a control because of its serene environment.

Data obtained from the assessment were subjected to descriptive analysis and one-way analysis of variance (ANOVA) to separate means using the statistical package for social sciences (SPSS).

Table 3. Sampling points in the study

S/N	Location	Latitude	Longitude
1	Residential area	N 06º 35.489	E 003º 22.331
2	Residential area	N 07º 21.821	E 003º 51.460
3	Residential area	N 07º 21.803	E 003º 51.417
4	Residential area	N 07º 21.832	E 003º 51.348
5	Residential area	N 07º 21.762	E 003º 51.376
6	Industrial area	N 07º 21.498	E 003º 50.983
7	Industrial area	N 07º 21.448	E 003º 50.946
8	Industrial area	N 07º 21.373	E 003º 51.037
9	Industrial area	N 07º 21.231	E 003º 50.932
10	Industrial area	N 07º 21.405	E 003º 50.869
11	Industrial area	N 07º 21.371	E 003º 50.834
12	Industrial area	N 07º 21.323	E 003º 50.773
13	Industrial area	N 07º 21.360	E 003º 50.728
14	Industrial area	N 07º 21.400	E 003º 50.607
15	Industrial area	N 07º 21.438	E 003º 50.733
16	Industrial area	N 07º 21.539	E 003º 50.730
17	Industrial area	N 07º 21.726	E 003º 50.742
18	Industrial area	N 07º 21.786	E 003º 50.751

Table 3. Sampling points in the study (cont.)

S/N	Location	Latitude	Longitude
19	Residential area	N 07 º 21.802	E 003 º 50.674
20	Residential area	N 07 º 21.802	E 003 º 50.525
21	Residential area	N 07 º 21.901	E 003 º 50.251
22	Residential area	N 07 º 21.911	E 003 º 50.175
23	Residential area	N 07 º 21.916	E 003 º 50.117
24	Control area	N 07 º 21.900	E 003 º 50.253
25	Control area	N 07 º 21.900	E 003 º 50.253
26	Control area	N 07 º 21.900	E 003 º 50.253
27	Control area	N 07 º 21.900	E 003 º 50.253

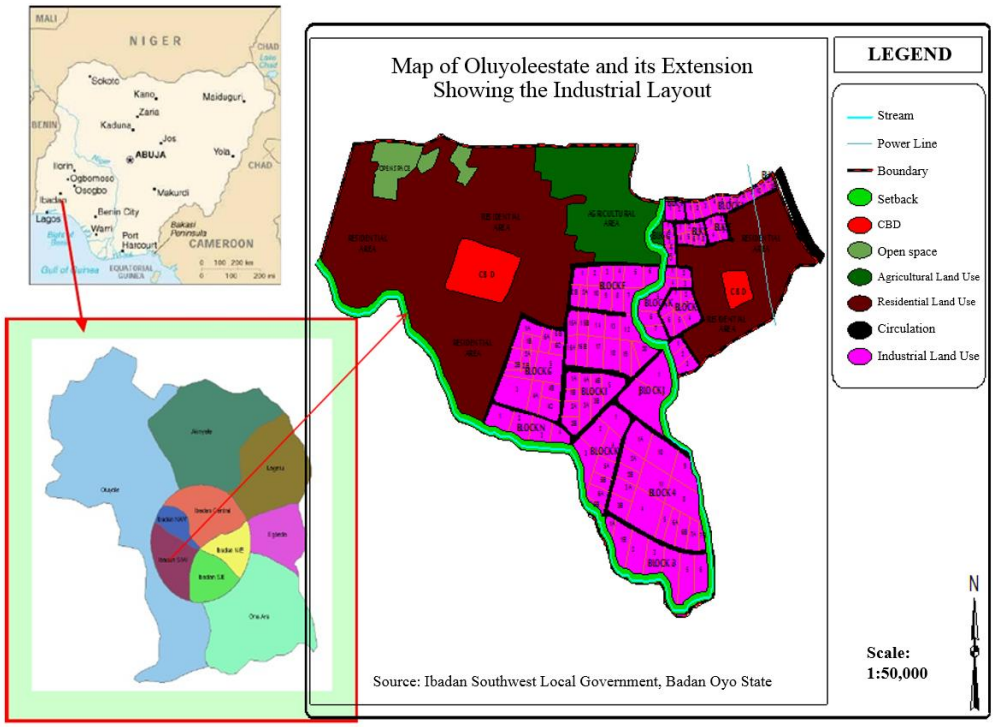

Figure 1. Map showing the study area

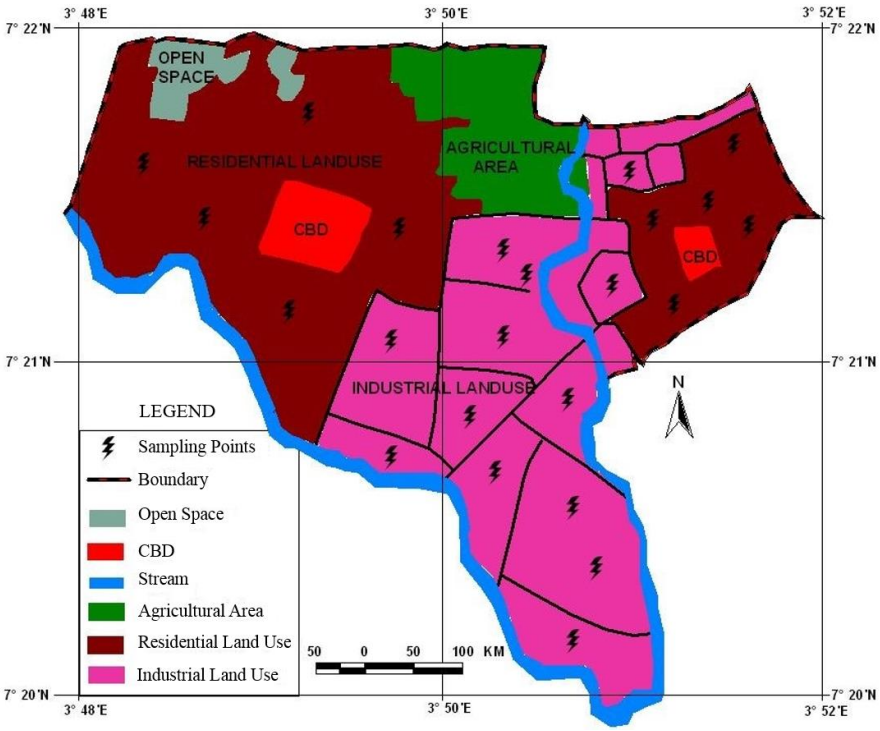

Figure 2. Map of study area showing land use and sampling points

3. RESULTS AND DISCUSSION

In the dry season, as illustrated in Table 4, within the residential area, noise level, SPM, CO and HC ranged between 46.19-68.47 dBA, 9.0-206 mg/m^3, 0.0-4.0 mg/m^3, and 0.0-6.0 mg/m^3 respectively, with mean values of 55.85 dBA, 48.91 mg/m^3, 1.23 mg/m^3 and 2.10 mg/m^3 respectively. CO was above the long-term exposure limit of 1.0 mg/m^3. HC level was generally above the 2.0 mg/m^3 long-term exposure limit while some sampling points had values as high as 7.5 mg/m^3 which is above the short-term exposure limit. SO_2 in the residential area was less than 0.001 mg/m^3 all through. This could be due to either a low level of sulphur release from production processes in many of the industries or due to dissolution, dispersion, mixing or any other atmospheric reaction leading to a low ground level concentration. Generally, the residential area is free from SO_2 and H_2S pollution at levels less than 0.01 mg/m^3.

For the industrial area, noise levels have a clustered range of 53.06-82.36 dBA with a mean of 66.98 dBA. In five of the sampling areas, the mean noise level was found with values as high as 273 dBA. SPM was low in places close to residential areas but measured up to as much as 721 mg/m^3 in the core industrial zone with a mean of 192.08 mg/m^3 and values ranging between 25-721 mg/m^3. The range of all values for CO was 0-8 mg/m^3 while the mean is 2.14 mg/m^3 which is higher than the long-term national emission limits. HC ranged between 0-6 mg/m^3 with a mean of 0.56 mg/m^3 while concentrations were above both short-term and long-term limit in a few parts of the industrial zone. SO_2 levels were generally below 0.01 mg/m^3, while hydrogen sulphide ranged between 0-11 mg/m^3 with a mean of 0.62 mg/m^3. Dispersion or fall out could be responsible for these low values. Meanwhile, in the control area, the noise level ranged between 38.72-46.48 dBA with a mean of 43.60 dBA, while SPM had a mean of 6.0 mg/m^3 and values that ranged between 2.0-11 mg/m^3. CO, H_2S and SO_2 levels were less than 0.01 throughout the sampling period of the season, but HC levels ranged between 0-5 mg/m^3 while the mean was 2.13 mg/m^3.

Table 4. Variation in the values of air parameters during dry season

Parameter	Locations		
	Residential	Industrial	Control
T (^OC)	34.45 ± 0.30^b	35.60 ± 0.21^a	28.19 ± 0.33^c
RH (%)	62.08 ± 1.42^b	54.44 ± 1.22^c	77.63 ± 1.29^a
WS (m/s)	7.23 ± 0.43^a	7.47 ± 0.36^a	5.37 ± 0.38^b
WP (mm Hg)	1.51 ± 0.38^a	1.29 ± 0.21^{ab}	0.39 ± 0.18^b
NOISE (dB)	55.85 ± 0.83^b	66.98 ± 0.93^a	43.60 ± 0.61^c
SPM (mg/m^3)	48.91 ± 5.28^b	192.08 ± 26.68^a	6.00 ± 0.52^c
CO (mg/m^3)	0.80 ± 0.21^b	2.14 ± 0.31^a	0.00 ± 0.00^b
H_2S (mg/m^3)	0.00 ± 0.00^b	0.62 ± 0.31^a	0.00 ± 0.00^b
SO_2 (mg/m^3)	0.00 ± 0.00^a	0.00 ± 0.00^a	0.00 ± 0.00^a
HC (mg/m^3)	2.10 ± 0.29^a	0.56 ± 0.20^b	2.13 ± 0.38^a

Values in the same row and with different superscript are significantly different at $p<0.05$

In the rainy season, as shown in Table 5, noise levels ranged between 52.50-81.90 dBA with a mean of 62.15 dBA, while SPM ranged between 5.0-100 mg/m^3 with a mean value of 35.56 mg/m^3. CO was found to be within the range of 0.0-8.0 mg/m^3 with a mean of 2.88 mg/m^3, while HC level ranged between 0.0-3.50 mg/m^3 with a mean of 1.34 mg/m^3. H_2S and SO_2 levels were not detectable.

Noise levels in the industrial area ranged between 62.50-89.60 dBA with a mean of 75.96 dBA. Moreover, SPM ranged from 6.0-521 mg/m^3 with an average value of 107.52 mg/m^3, while CO ranged between 0.00-10 mg/m^3 having a mean of 6.10 mg/m^3. Hydrocarbon level was within 0.00-4 mg/m^3 with a mean value of 1.55 mg/m^3, while SO_2 and H_2S levels were very low and almost undetectable.

Noise levels within the control area was in the range of 45.2-62.7 dBA with an average of 54.81 dBA, while the measured level of the suspended particulate matter was in the range of 16-54 mg/m^3

with a mean value of 28.36 mg/m^3. The measured level of CO in the area falls within the range of 0-7 mg/m^3 with a mean value of 1.94 mg/m^3, while the hydrocarbon level was between 0-3 mg/m^3 with an average value of 0.88 mg/m^3. Similarly, H_2S and SO_2 levels were below detectable limits.

Table 5. Variation in the values of air parameters for wet season

Parameter	Locations		
	Residential	Industrial	Control
T (^{O}C)	29.10±0.28^b	30.61±0.17^a	30.51±0.21^a
RH (%)	68.18±1.23^a	61.54±0.80^b	61.70±0.61^b
WS (m/s)	8.67±0.29^b	9.82±0.27^a	8.59±0.52^b
WP (mm Hg)	1.90±0.15^b	2.41±0.13^a	1.85±0.26^b
NOISE (dB)	62.15±0.95^b	75.96±1.03^a	54.61±1.07^c
SPM (mg/m^3)	35.58±3.44^b	107.52±16.32^a	29.55±2.53^b
CO (mg/m^3)	2.88±0.3475^b	6.10±0.43^a	2.05±0.46^b
H_2S (mg/m^3)	0.00±0.00^a	0.00±0.00^a	0.00±0.00^a
SO_2 (mg/m^3)	0.00±0.00^a	0.00±0.00^a	0.00±0.00^a
HC (mg/m^3)	1.34±0.17^{ab}	1.55±0.16^a	0.85±0.21^b

Values in the same row and with different superscript are significantly different at $p<0.05$.

Seasonal variation as shown in Table 6 indicated a significant variation ($p<0.05$) in noise levels during the dry (55.85±0.82, 66.98±0.97 and 43.60±0.61) and wet season (62.15±0.95, 75.96 ±1.03 and 55.23±1.23) at all locations. The level of SPM within the Residential and Industrial areas was significantly higher ($p<0.05$) during the dry season (48.91±5.28 and 192.08±26.68) than the wet season (35.58±3.44 and 107.52±16.32) except for the control area with reverse situation.

Also, there was a significant variation ($p<0.05$) in CO concentrations during the dry (0.80±0.21, 2.14±0.32 and 0.00±0.00) and wet season (2.89±0.35, 6.10±0.43 and 2.13±0.54) at all three locations. Meanwhile, there was no significant variation ($p>0.05$) in the values of H_2S except in the Industrial area in wet season. A similar situation was recorded for SO_2 concentrations. However, the values of HC varied significantly ($p<0.05$) among locations during both dry and wet seasons.

The comparison of air pollutant levels with permissible limits, as shown in Table 7, the noise level in residential areas during both wet and dry seasons were found to be above 50 dBA which is the standard limit stipulated by NESREA while that of the control area was not above limit. There was exceedance during the dry season in the industrial area with values above 70 dBA while the mean value during the wet season was not above the standard limit. Generally, noise levels were higher during the dry season.

Similarly, Table 8 illustrates that during the dry season, there was exceedance in the level of suspended particulate matter for long and short-term exposure limits in all locations, while there was exceedance in CO and HC for short-term exposure limit in both residential and control area. The levels of SO_2 and H_2S with values below 0.001 mg/m^3 did not exceed both standards, while in the industrial area the level of suspended particulate matter and H_2S exceeded standards for both long and short-term exposure limits. CO and HC showed exceedance only for long-term exposure limit. SO_2 levels were less than 0.001 mg/m^3 which does not exceed exposure limits.

For the wet season, the level of suspended particulate matter exceeded limits for both long-term and short-term exposures in all location, but CO, HC and H_2S levels only exceeded long-term exposure standards in all locations, whereas the level of SO_2 was generally not above standard with a mean value of 0.001 mg/m^3.

This study showed that industrial activities contributed significantly to the noise level in the surrounding residential areas, making it higher than the permissible limit. Noise levels within the industrial area were above the permissible limit during dry season. Industrial noise impact was found to decrease with increasing distance from the

industrial area, which means that there is an inverse relationship between distance and industrial noise pollution in surrounding residence. There was also an exceedance of permissible noise limit in the control area during the dry season, and this could be attributed to frequent honking from trucks venturing into the area. Exceedance in permissible noise level in the study area poses a serious threat to the health and general well-being of the residents. Ozer et al. (2009) revealed a very high noise level in some areas of Tokat city, Turkey which includes public structures, hospitals, schools and houses with noise levels over 75 dB, while Osemeikhian and Anomohanran (2006) recorded noise levels above 90 dBA in Warri, Nigeria. High noise levels may predispose residents of this study area to health problems such as noise-induced hearing loss, tinnitus, insomnia and headache, as reported by Bisong et al. (2004) that members of the community that are exposed to 105.8±9.24 dBA of noise level suffered from noise-induced hearing loss, tinnitus, insomnia and headache. There is a special concern for the children attending the various schools located very close to the industrial area as it could be a serious source of distraction among other effects. Similarly, Kankal and Gaikwad (2011) concluded that residential areas and vulnerable institutions and hospitals face noise levels which are much higher than the acceptable limit. The level of SPM in the residential, industrial and control areas was far above both short and long-term permissible limits. In a similar development, Ideriah and Stanley (2008) observed that the concentrations of SPM were found to exceed permissible limits at all locations while Assimakopoulos et al. (2008) discovered that SPM were found at levels above the specified limits in different areas of usage in Athens. It was observed that SPM level in the residential area decreased with increasing distance from the industrial area meaning there is an inverse relationship between the distance from the industrial area and level of SPM and this implies that industrial activities are the main sources of SPM. The inverse relationship between distance and pollutant concentration observed in this study agrees with the findings of Nwaogu and Onyeze (2010), where mean values of all the air quality indices decreased as the distance from the flaring site increased while Al-Salem and Khan (2008) also noted that distance and winds are the strongest influencing parameters for the disposal of gaseous pollutants.

Carbon monoxide level was above long-term exposure limit in all areas in both seasons. Meanwhile, short term exposure limit was exceeded only in the industrial area in wet season. The higher level of CO in the wet season could also be attributed to less dispersion and mixing. Ideriah and Stanley (2008) reported a CO value between 1-5 mg/m^3 which is in line with the results of this study while high levels of pollutants were further attributed to vehicular emission and domestic activities which is also similar to the situation in the area of study. CO combines ten times more readily with haemoglobin than oxygen. Therefore people exposed to it for long hours could experience dizziness and fatigue more often. CO is a poisonous gas having a life time of two to four months in the atmosphere and affects the oxygen carrying capacity of haemoglobin (Ideriah and Stanley, 2008). People who already have ailments like asthma, bronchitis or other respiratory diseases could have their conditions worsened by this situation. Exceedance of permissible limits was found in all measured parameters in the industrial, residence and control areas except for SO_2.

The health of people working and living in the area could be negatively impacted by a high concentration of air pollutants. Kowalska et al. (2006) found that measured concentrations of airborne particulate and gaseous pollutants in the Katowice Conurbation (0.035 mg/m^3 and 0.049 mg/m^3 of SO_2 and SPM respectively) influenced daily mortality pattern among the inhabitants of the region while the largest impact was seen in relation to the elderly and the case of cardiovascular mortality and SO_2 remained the most powerful determinant among the examined air pollutants. The effects of long-term exposure to ambient PM apply to cardiopulmonary mortality and probably to lung cancer also (WHO, 2004). Peng et al. (2008) revealed that a 10 mg/m^3 increase in PM2.5-PM10 was associated with 0.36% increase in cardiovascular disease admissions on the same day while Yang et al. (2008) found CO and SO_2 to be significantly associated with chronic obstruction pulmonary disease (COPD).

Table 6. Variation in the values of air parameters for dry and wet seasons

Parameter	Residential (dry season)	Residential (wet season)	Industrial (dry season)	Industrial (wet season)	Control (dry season)	Control (wet season)
T (^{O}C)	34.42±0.30^{a}	29.096±0.28^{b}	35.60±0.22^{a}	30.61±0.17^{b}	28.19±0.33^{b}	30.52±0.26^{a}
RH (%)	62.08±1.42^{b}	68.175±1.23^{a}	54.44±1.22^{b}	61.54±0.80^{a}	77.63±1.29^{a}	61.31±0.72^{b}
WS (m/s)	7.23±0.432^{b}	8.665±0.29^{a}	7.47±0.36^{cb}	9.82±0.27^{a}	5.37±0.38^{b}	8.71±0.62^{a}
WP (mm Hg)	1.51±0.38^{b}	1.8962 ±1.45^{a}	1.29±0.21^{b}	2.41±0.13^{a}	0.39±0.18^{b}	1.92±0.31^{a}
NOISE (dB)	55.85± 0.82^{b}	62.15±0.95^{a}	66.98±0.97^{b}	75.96±1.03^{a}	43.60±0.61^{b}	55.23±1.23^{a}
SPM (mg/m^{3})	48.91±5.28^{a}	35.58±3.44^{b}	192.08±26.68^{a}	107.52±16.32^{b}	6.00±0.52^{b}	28.75±2.67^{a}
CO (mg/m^{3})	0.80±0.21^{b}	2.89±0.35^{a}	2.14±0.32^{b}	6.10±0.43^{a}	0.00±0.00^{b}	2.13±0.54^{a}
H_2S (mg/m^{3})	0.00±0.00^{a}	0.00±0.00^{a}	0.62±0.31^{a}	0.00±0.00^{b}	0.00±0.00^{a}	0.00±0.00^{a}
SO_2 (mg/m^{3})	0.00±0.00^{a}	0.00±0.00^{a}	0.00±0.00^{a}	0.00±0.00^{a}	0.00±0.00^{a}	0.00±0.00^{a}
HC (mg/m^{3})	2.10±0.30^{a}	1.34±0.17^{b}	0.56±0.20^{b}	1.55±0.16^{a}	2.13±0.38^{a}	0.72±0.20^{b}

Values in the same row and with different superscript are significantly different at $p<0.05$.

Table 7. Noise level in comparison with permissible limits of NESREA

Facility	Maximum permissible limit (dBA)	Mean value for wet season (dBA)		Mean values dry season (dBA)	
		Residential	Control	Residential	Control
Residential buildings	50	55.85	43.6	62.15	54.81
Industrial area (Outside perimeter fencing)	70	66.98		75.96	

Table 8. Air pollutant concentrations in comparison with permissible limits of NESREA

Pollutant	Long-term limits (mg/m^{3})	Short-term limits (mg/m^{3})	Dry season			Wet season		
			Residential (mg/m^{3})	Industrial (mg/m^{3})	Control (mg/m^{3})	Residential (mg/m^{3})	Industrial (mg/m^{3})	Control (mg/m^{3})
SPM	0.20	0.20	48.91	192.01	6.00	35.58	107.52	28.38
CO	1.00	5.0	1.23	2.13	2.14	2.88	6.10	1.94
H_2S	0.008	0.008	0.00	0.62	0.00	0.00	0.00	0.00
SO_2	0.10	0.50	0.00	0.00	0.00	0.00	0.00	0.00
HC (Total)	2.00	5.00	2.10	0.56	2.13	1.34	1.55	0.88

4. CONCLUSIONS

Emissions released from industries located in the industrial scheme contributed significantly to the ground level concentration of H_2S, PM, and noise in surrounding residential areas while exceedance of exposure limits by NESREA was recorded for all parameters except in SO_2. Seasonal variation played an important role in the difference between ground level concentrations of pollutants. The presence of industries contributed significantly to high ground level concentrations of air pollutants in the surrounding and distant residential areas therefore reductions in air pollution will be of significant benefits to both living and non-living resources in and around the metropolis.

There is the need for air quality monitoring on the part of a relevant government agency while the residence should be enlightened on the inherent danger posed by air pollution and how to seek redress though they may rather feel that the industries are important to them regarding economic opportunity.

ACKNOWLEDGEMENTS

We seek this medium to appreciate the support and cooperation received from the staffs of the planning department of Oluyole Local Government, Ibadan without whom this project would be impossible.

REFERENCES

Abdulkareem AS, Kovo AS. Urban air pollution by process industry in Kaduna, Nigeria. Assumption University Journal of Technology 2006;9:172-4.

Agbaire PO. Air pollution tolerance indices (APTI) of some plants around erhoike-kokori oil exploration site of delta state, Nigeria. International Journal of Physical Science 2009;4:366-8.

Al-salem SM, Khan AR. Comparative assessment of ambient air quality in two urban areas adjacent petroleum downstream/upstream facility in Kuwait. Brazilian Journal of Chemical Engineering 2008; 25:683-5.

Assimakopoulos VD, Saraga D, Helmis CG, Stathopoulou OI, Halios CH. An experimental study of indoor air quality in areas of different use. Global NEST Journal 2008;10:192-200.

Bhikkhu V. Negative Impacts of Industrialization Along Lumbini Road, Nepal. Lumbini institutions. Birgitta, Berglund and Lindvall, H: A Draft Document of Community Noise. 2009.

Bisong SA, Umana AN, Onoyom-ita V, Osim EE. Hearing acuity loss of operators of food grounding machine in Calabar, Nigeria. Nigerian Journal of Physiological Sciences 2004;19:20-7.

Brook RD, Franklin B, Cascio W, Hong Y, Howard G, Lipsett M, Luepker R, Mittleman M, Samet J, Smith SC, Tager I. Air pollution and cardiovascular disease: a statement for healthcare professionals from the expert panel on population and prevention science. American Heart Association 2004;109:2655-71.

Ideriah JK, Stanley HO. Air quality around some cement industries in Port Harcourt, Nigeria. Scientia Africana 2008;7:27-34.

Kankal SB, Gaikwad RW. Studies on noise and air quality monitoring at Shirdi (Maharashta), India. Advances in Applied Sciences Research 2011;2:63-75.

Kowalska M, Zejda JE, Hubicki L, Osrodka L, Krajny E, Wojtylak M. Effect of ambient air pollution on daily mortality in Katowice Conurbation, Poland. Polish Journal of Environmental Studies 2006;16:227-32.

Mohammed IN. Risk Assessment in Air; Qualitative Analysis for Industrial Process [dissertation]. University of Technology, Malaysia; 2009.

National Environmental Standard Regulations Agency (NESREA). Federal Republic of Nigeria Official Gazette; National Environmental Regulations. 2009;96:1299-389.

Nkwocha EE, Egejuru RO. Effect of industrial air pollution on the respiratory health of children. International Journal of Environmental Science and Technology 2008;5:509-16.

Nwaogu LA, Onyeze GOC. Environmental impact of gas flaring in ebocha-egbema, Niger-Delta. Nigerian Journal of Biochemistry and Molecular Biology 2010;25:25-30.

Nwobodo ED, Ighoroje ADA, Marchie C. Noise induced hearing impairment as an occupational risk factor among Nigerian traders. Nigerian Journal of Physiological Sciences 2004;19:14-9.

Olayinka OS, Abdullahi SA. An overview of industrial employees' exposure to noise in sundry processing and manufacturing industries in Ilorin metropolis, Nigeria. Industrial Health 2008;4:123-33.

Osemeikhian JEA, Anomohanran O. Day and night pollution study in some major towns in Delta State, Nigeria. Ghana Journal of Science 2006;46:47-54.

Oyekanmi A, Obidairo K, Ekop G, Medupin C. EMS 311: Air and noise pollution, school of science and technology, National Open University [Internet]. 2010 [cited 2017 Nov 15] Available from: http://nouedu.net/sites/default/files/2017-03/ESM% 20311.pdf

Ozer S, Hasan Y, Murat Y, Pervin Y. Evaluation of noise pollution caused by vehicles in the city of Tokat, Turkey. Science Research and Essay 2009;4:1205-12.

Peng RD, Chang HH, Bell ML, McDermott A, Zeger SL, Samet JM. Coarse particulate matter, air pollution and hospital admissions for cardiovascular and respiratory diseases among medicare patients. Journal of the American Medical Association 2008;299:2172-9.

Rene GT. An Air Quality Baseline Assessment for the Vaal Airshed in South Africa [dissertation]. University of Pretoria; South Africa: 2008.

Spire Research and Consulting (SRC). Air Pollution-China's Public Health Danger. 2007. p. 1-11.

Turk YA, Kavraz M. Air pollutants and its effects on human health: the case of the city of Trabzon. In: Moldoveanu A. editor. Advanced Topics in Environmental Health and Air Pollution Case Studies. Croatia: In Tech Europe; 2011. p. 251- 68.

Yang Q, Chen Y, Krewski D, Burnett RT, Shi Y, McGrail KY. Effect of short-term exposure to low levels of gaseous pollutants on chronic obstruction pulmonary disease hospitalization. Environmental Research 2008;1(99):99-105.

World Health Organisation (WHO). Systematic review of health aspects of air pollution in Europe [Internet]. 2004 [cited 2017 Nov 15]. Available from: http://www.euro.who.int/__data/assets/pdf_file/0003/74730/E83080.pdf?ua=1

Effect of the Waste Heat Recovery System to Buoyancy and Momentum Flux of Combustion Stack in the Cement Industry

Jutarat Keawboonchu[1,2], Wissawa Malakan[1,2], Wisit Thongkum[3] and Sarawut Thepanondh[1,2*]

[1]Department of Sanitary Engineering, Faculty of Public health, Mahidol University, Bangkok 10400, Thailand
[2]Center of Excellence on Environmental Health and Toxicology (EHT), Bangkok 10400, Thailand
[3]Faculty of Public Health, Mahasarakham University, Mahasarakham 44150, Thailand

ARTICLE INFO

Received: 9 Apr 2018
Received in revised:
5 Jul 2018
Accepted: 17 Jul 2018
Published online:
4 Oct 2018
DOI: 10.32526/ennrj.17.1.2019.02

Keywords:
Buoyancy flux/ Momentum flux/ PM-10/ Waste heat recovery

*** Corresponding author:**
E-mail:
thepanondh@gmail.com

ABSTRACT

Buoyancy and momentum fluxes are important parameters to determine the plume rise which is related to the ability to dilute air pollutants emitted from combustion stack sources. The change of temperature due to waste heat recovery directly affects these fluxes. This study analyzed buoyancy and momentum fluxes and evaluated the ground level concentration of PM-10 prior and after implementation of waste heat recovery in the area surrounding one of the largest cement production plants in Thailand. The results showed that the ambient temperature was the significant parameter affecting buoyancy and momentum fluxes. The buoyancy flux was found to be the dominant force to the rise of plume for both scenarios. There were no differences in the predicted PM-10 ground level concentrations at receptors around the cement plant for the model simulation under two scenarios. Therefore, it was concluded that decreasing of stack gas exit temperature does not affect the dispersion of air pollutants in the cement industry.

1. INTRODUCTION

Nowadays, a large number of pollutants emitted from various anthropogenic sources into the atmosphere cause damage to human health and the environment in the world (Liu et al., 2017; Cao et al., 2011; Kampa and Castanas, 2008; Brook et al., 2010). Approaches to manage and control air pollution problems in order to reduce ground level concentrations of pollutants can be classified into three general approaches. Firstly, increase the opportunity for air pollution to diffuse from emission sources. Secondly, modification of raw materials and production processes to reduce emissions of air pollutants from the source, and thirdly, by applying technology to the control and treatment of air pollutants. (Vallero, 2014; Dimmick and Wehe, 1999)

Under the first approach, increasing the chances of diffusion of air pollutants from the source leads to an increase of the volume of air dilution. Therefore, the ground level concentrations of pollutants at the receptor sites are reduced. The industry has applied this approach using tall stacks. Theoretically, increasing the vertical displacement of pollutants from ground level will contribute to the reduction of ground level concentrations and result in a lower intake fraction (Bhargava, 2016; Parvez et al., 2017).

It is well recognized that the diffusion of air pollutants from stack sources is not at the constant height as the physical stack height (h_s) but the pollutants can travel in the vertical direction. The distance from the top of the stack to the center of the plume is described as a plume rise (Δh) (Hoven, 1975), while, the distance from the ground level to the center of the plume (include the physical stack height) is the effective stack height (H). It is an important factor in atmospheric dispersion modeling and may have a significant influence on modeled concentration values (Essa et al., 2006; Masters, G.M., 1997; Turner, D.B., 1970) as shown in Figure 1.

Plumes can move downwind of a source and expand by diffusion in both horizontal and vertical dimensions. From Figure 1, the increasing of plume rise (Δh) value leads to an increase in vertical distance before pollutants spread in the horizontal dimension. Therefore, the rising of plume induces

the reduction of ground level concentrations. Stack plume rise is a phenomenon which is mainly dependent on two factors. Firstly, thermal buoyancy or buoyancy flux dominated by temperature difference between the stack and ambient air at discharge point. Secondly, mechanical momentum or momentum flux dominated by difference of stack exit gas velocity and wind velocity at discharge point. Both of these data are specific in each stack and area.

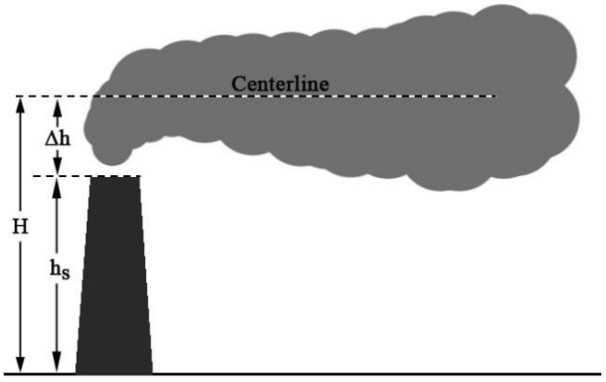

Figure 1. A Gaussian plume model

The cement industry is one of the world's largest energy consumers. Massive energy consumption for cement production occurs in the calcination process and clinker production process (Madlool et al., 2011; Madlool et al., 2013). Under the business as usual (BAU) for this type of industry, a large amount of heat is vented to the atmosphere passing through a combustion stack without utilization. Therefore, many cement plants have installed Waste heat recovery (WHR) systems to return escaping heat within processes and across the industry (Fang et al., 2013; United States Department of Energy, 2008; Demirkaya et al., 2013). WHR system may lead to a decreasing in the temperature of the discharged gas. The heat or temperature reduction will directly affect the buoyancy flux of gas, and may result in a decrease in the plume rise value. As a result, the ability to disperse and dilute air pollutants into atmosphere will drop off. Hence, ground level concentrations of air pollutants may be increased due to lower dilution ability caused by decreasing of stack plume rise. This research aims to analyze the effect of temperature changes in waste heat recovery system on buoyancy and momentum fluxes of the combustion plume from stacks in the cement industry. Results are further analyzed and illustrated for their impact on ground level concentrations of PM-10 prior and after implementing of the WHR system. Findings from this study will be very useful to elaborate whether there are any demerits of process modification (installation of WHR system) to pollution control and management of the cement industry or not.

2. METHODOLOGY

2.1 Study area

This study is conducted at a cement plant located in Saraburi, Thailand as shown in Figure 2. The area is classified as a complex terrain (mountainous area) with mountain peak elevations of about 800 to 1,300 m above mean sea level. This area is the home of the cement industry in Thailand (TCMA, 2016). The selected cement plant is located about 110 km northeast of Bangkok.

2.2 Meteorology

Thailand is located in the tropical area between latitudes 5˚37'N to 20˚27'N and longitude 97˚22'E to 105˚37'E. The climate is under the influence of the monsoon wind of seasonal character as southwest monsoon and northeast monsoon. The climate of Thailand can be divided into three seasons: summer from mid-February to mid-May, winter from mid-October to mid-February, and rainy season from mid-May to mid-October (TMD, 2018). The study area is located in the central part of Thailand that usually encounters a long period of warm weather. The surface meteorological data were derived from the Na-Pha-Lan ambient air monitoring station operated by the Pollution Control Department (PCD). This station is about 22 km away from the reference point. In this study, meteorological characteristics over five years (1st January 2012 to 31th December 2016) were used for the analysis. Analyzed data is as presented in Table 1. Measured meteorological data indicated that the area is arid with little rain in winter. The warmest period of the year is from March to May. Average monthly temperature is about 24.4-34.3˚C. These values for daytime and nighttime are about 29.4-34.3˚C and 24.4-28.8˚C, respectively. April is the hottest month of the year, while February is the coldest month. High wind speed is observed during winter with the highest average of 6.4 m/s in February. Average wind speeds during daytime and nighttime are

around 1.5-2.6 m/s and 0.6-1.1 m/s respectively. Figure 3 depicts the wind rose diagram of the study area. Most of the wind prevails from the south direction as illustrated in Figure 3.

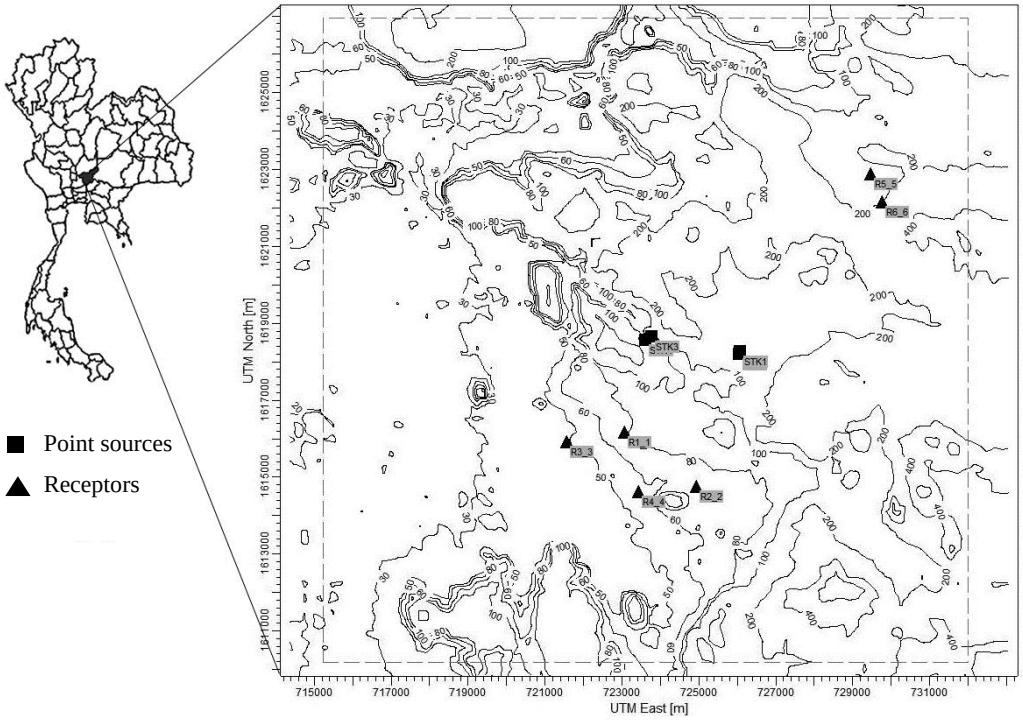

Receptors	Distance from the reference point (km)	Direction from the reference point
R1	2.8	SW
R2	3.6	SW
R3	4.3	SW
R4	4.6	SW
R5	7.1	NE
R6	7.6	NE

Figure 2. Location of emission sources and receptors in the modeling area

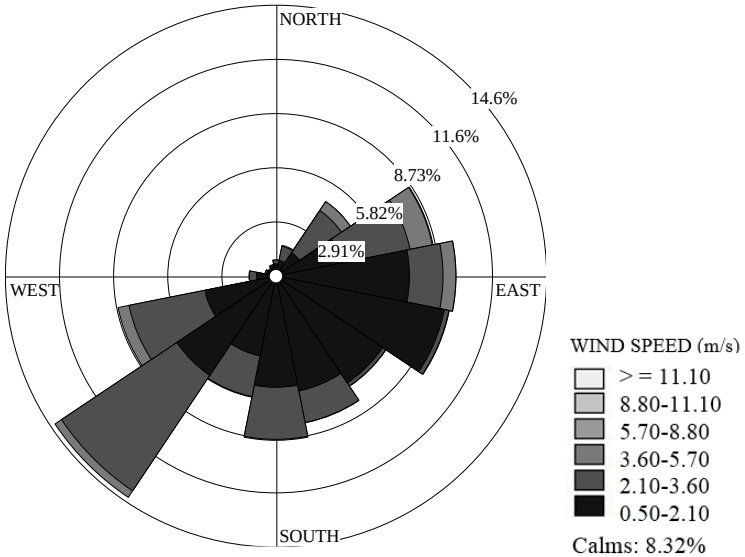

Figure 3. Wind rose of the study area (2012-2016)

Table 1. Summary of meteorological characteristics of the study area (data from 2012-2016)

Months	Relative humidity (%)	Average wind speed in day time[1] (m/s)	Average wind speed in night time[2] (m/s)	Average temperature in day time (˚C)	Average temperature in night time (˚C)	Minimum temperature (˚C)	Maximum temperature (˚C)
January	59.0	2.2	1.1	29.8	24.4	14.2	36.5
February	60.8	2.3	0.7	31.8	26.2	11.6	27.8
March	62.4	2.5	1.0	33.3	27.7	21.8	39.9
April	60.3	2.5	1.0	34.4	28.8	22.8	41.2
May	63.1	2.5	0.9	33.7	28.7	22.3	41.0
June	71.4	2.3	0.7	31.8	27.2	23.3	39.2
July	74.2	2.1	0.7	31.2	27.0	22.6	38.8
August	76.5	1.9	0.7	30.9	26.2	14.3	37.9
September	80.7	1.5	0.6	30.1	25.8	16.3	36.7
October	75.4	1.6	0.6	30.6	25.8	22.5	36.5
November	68.8	2.0	0.7	31.0	25.9	14.5	37.1
December	58.6	2.6	1.0	29.4	24.8	16.0	36.1

[1] Daytime is defined when the global radiation is less than or equal to 5 w/m^2

[2] Nighttime is defined when the global radiation is greater than 5 w/m^2

2.3 Evaluation of Buoyancy and Momentum fluxes

Screen View model (Lakes Environmental, 2011), a Window interface for the U.S. Environmental Protection Agency screening model SCREEN3 (USEPA, 1995a), provides a simple method of estimating contaminant concentrations. It is capable of measuring the worst-case dispersion (maximum concentration) of various pollutants. However, in this study, Screen View model is only used to estimate Buoyancy and momentum fluxes of combustion stack in the cement plant. For most plume rise situations, the value of the Briggs buoyancy flux parameter (F_b (m^4/s^3)) given by (1) and the momentum flux parameter (F_m (m^4/s^2)) given by (2) are needed.

$$\text{Buoyancy flux, } F_b = g v_s d_s^2 \left(\frac{T_s - T_a}{T_s}\right) \quad (1)$$

$$\text{Momentum flux, } F_m = \left(\frac{T_a}{T_s}\right) v_s^2 d_s^2 \quad (2)$$

where, T_s is the stack gas temperature (K), T_a is ambient temperature (K), g is gravity, 9.8 m/s^2, v_s is stack exit velocity (m/s), and d is top inside stack diameter (m)

The effects of buoyancy and momentum fluxes on plume rise are analyzed by using two data sets, meteorological data and stack characteristics. Meteorological data measured over the year 2012-2016 from the Na-Pha-Lan station are used to represent the meteorological conditions occurring in each month separated for daytime and nighttime data (Table 1). Information on the stack characteristics such as emission rate, stack height, stack diameter, stack gas exit velocity, stack gas exit temperature (designed data from the plant) are obtained from the factory (Table 2). The influences of implementing the waste heat recovery program in the factory on stack plume rise are evaluated under two scenarios.

Scenarios I. No waste heat recovery installation (No WHR) and

Scenarios II. Waste heat recovery installation (WHR)

Table 2. Input data

Cases	Emission rate (g/s)	Stack height (m)	Stack diameter (m)	Velocity (m/s)	Gas temperature (K)	Ambient temperature (K)	Wind speed (m/s)
I	43.94	120	5.2	17.85	598	Using measured meteorological data	Using measured meteorological data
II	43.94	120	5.2	17.85	413		

2.4 PM-10 ground level concentrations

The AERMOD air quality dispersion model (version 9.4.0) is used to predict the concentrations of PM-10 at receptor points located in the vicinity of the factory in this study. AERMOD is recommended and designed as a regulatory model by U.S. EPA. The model performs under the Gaussian plume theory for the vertical and horizontal distributions. The model is composed of three components: AERMOD Meteorological Pre-processor (AERMET), AERMOD Terrain Pre-processor (AERMAP), and the control module and modeling preprocessor (AERMOD). The AERMET processes the hourly surface data and a profile data file. The AERMAP is used to process the terrain data in conjunction with a layout of receptor and sources for AERMOD control files. The AERMOD is a dispersion model (USEPA, 2018).

The study domain covered an area of 16 x 16 km^2 with a finest grid resolution of 250 x 250 m^2 grid resolution. One stack emission source is set as a reference point (UTM 723618E and 1618563N). The hourly surface and upper air meteorological data from the year 2015 were used. The upper meteorological data were derived from the measurement in Bangkok (about 120 km in the southwestern direction of the plant).

Ground level concentrations of PM-10 are predicted for 6 receptor points located within community areas. Affected communities were selected based on their location along the prevailing winds of the study area (Figure 2). The nearest receptor to the reference point is about 2.8 km. Data of amount of dust (total Suspended Particulate, TSP) emitted from combustion stacks in cement plant are obtained from direct measurement. About 88% of them are estimated as PM-10 (Gupta et al., 2012) with 60 $\mu g/m^3$ of background concentration. The background concentration of PM-10 in this area was obtained from Department of Primary Industries and Mines, Thailand. Emission characteristics of each stack source are summarized in Table 3.

Table 3. Emission characteristics of four stacks in the cement plant

Stack number	Height (m)	Diameter (m)	Gas temp. (K)		Gas velocity (m/s)	PM-10 (g/s)
			No WHR	WHR		
S1	102	4	598	413	20	19.22
S2	102	4	598	413	16.5	19.49
S3	120	5.2	598	413	18	25.64
S4	120	5.2	598	413	17.9	43.94

3. RESULTS AND DISCUSSION

The effects of implementing waste heat recovery system in the factory to the alteration of plume rise were estimated under two difference scenarios. In the first scenario, plume rise was calculated under the condition with no waste heat recovery system were utilized in the factory. The hot gas was released directly to the atmosphere with the same temperature after exiting the combustion activity. Implementing of waste heat recovery system in the target industry which could be affected in decreasing of stack exit temperature of the exhaust gas was evaluated under the second scenario. Results are presented and discussed as follows:

3.1 Contribution of momentum and buoyancy fluxes to the plume rise

Many research studies have reported that buoyancy and momentum fluxes are associated factors affecting plume rise and ground level concentration of pollutants. In an unstable condition, the buoyancy of the plume increases as it rises, increasing the plume height. (Bhargava, 2016; Ilaboya et al., 2011). The business as usual (BAU) of the cement factory which the exhaust gas were released directly to the atmosphere (scenario I) was used to evaluate the contribution of buoyancy and momentum fluxes to the plume rise. Calculated results are presented in Table 4 and Table 5. The lowest buoyancy flux was predicted to occur during daytime in April while the highest value occurred during the nighttime in January. These findings could be resulted from the fact that buoyancy flux is mainly driven by the difference between stack exhausted gas and ambient temperature. April is the warmest month in Thailand (Average daytime temperature=34.4^{o}C), which leads to a smaller calculated buoyancy flux as compared with the

nighttime in January, which is the coldest period (Average nighttime temperature=24.4°C). The buoyancy flux was predicted to be highest during the nighttime periods. Average buoyancy flux during the day and nighttime were estimated as about 581.0 and 590.81 m^4/s^2, respectively. There were slight differences between the values of each month as indicated by low standard deviations (S.D.), However, buoyancy and momentum fluxes of daytime and nighttime are significantly different with statistically highly significant p-value<0.001 (Independent t-test)

On the other hand, the maximum momentum flux (1106.8 m^4/s^2) was estimated to occur during the daytime in April and the lowest value (1071.2 m^4/s^2) was predicted during the nighttime in January. Average momentum flux was 1096.7 and 1078.9 m^4/s^3 for day and nighttime, respectively. The values were not much difference among each month.

After implementing the waste heat recovery system in the factory (2nd Scenario), the results shows that decreasing of stack temperature lead to reduction of buoyancy flux while the momentum flux had the same tendency to the first scenario. The lowest and highest buoyancy fluxes occurred during daytime in April and nighttime in January, respectively.

Table 4. Temporal variation of buoyancy and momentum fluxes on a monthly basis in case of no waste heat recovery installation

Month	Buoyancy flux (m^4/s^3)		Momentum flux (m^4/s^2)	
	Daytime	Nighttime	Daytime	Nighttime
January	584.3	595.0	1090.6	1071.2
February	580.4	591.5	1097.8	1077.7
March	577.4	588.5	1103.2	1083.1
April	575.4	586.4	1106.8	1086.8
May	576.6	586.5	1104.7	1086.7
June	580.4	589.5	1097.8	1081.3
July	581.6	589.9	1095.7	1080.5
August	582.2	591.5	1094.6	1077.7
September	583.8	592.3	1091.7	1076.2
October	582.8	592.3	1093.5	1076.2
November	582.0	592.1	1095.0	1076.6
December	585.1	594.2	1089.2	1072.6
Average[1]	581.0	590.8	1096.7	1078.9
S.D.	2.9	2.5	5.2	4.6

[1] p-value<0.001 (Independent t-test)

In most EPA dispersion models, in order to calculate the plume rise, the buoyancy flux and momentum flux parameters are required. For cases of unstable condition with stack gas temperature greater than or equal to ambient temperature, it must be determined whether the plume rise is dominated by momentum or buoyancy forces. The dominant flux can be determined following the procedure of Briggs as showed in the ISC Users' Guide, Section 1.1.4.3 (USEPA, 1995b).

For Fb<55,

$$(\Delta T)_c = 0.00297 T_s \frac{v_s^{1/3}}{d_s^{2/3}} \quad (3)$$

and for Fb≥55,

$$(\Delta T)_c = 0.00575 T_s \frac{v_s^{2/3}}{d_s^{1/3}} \quad (4)$$

If the difference between the stack gas and ambient temperature (ΔT) is greater than or equal to the crossover temperature difference $(\Delta T)_c$ as shown in (3 and 4), then the plume rise is assumed to be buoyancy dominated. Using the stack and meteorological data in this study, we found that buoyancy is the dominant flux over the calculated plume rise. Even though in the case of implementing waste heat utilization, in which the temperature of exhausted gas decreased from their business as usual, the buoyancy flux still plays the key factor in controlling the plume rise. Results are as summarized in Table 6.

Table 5. Temporal variation of buoyancy and momentum fluxes on a monthly basis in case of waste heat recovery installation

Month	Buoyancy (m^4/s^3)		Momentum (m^4/s^2)	
	Daytime	Nighttime	Daytime	Nighttime
January	315.9	331.3	1579.2	1551.0
February	310.1	326.2	1589.6	1560.4
March	305.8	321.9	1597.4	1568.2
April	303.0	318.9	1602.6	1573.7
May	304.7	319.0	1599.5	1573.4
June	310.1	323.3	1589.6	1565.6
July	311.8	323.9	1586.5	1564.6
August	312.7	326.2	1584.9	1560.4
September	315.0	327.3	1580.7	1558.3
October	313.6	327.3	1583.3	1558.3
November	312.4	327.0	1585.4	1558.8
December	317.0	330.2	1577.1	1553.1
Average[1]	311.0	325.2	1588.0	1562.2
S.D.	4.3	3.8	7.8	6.9

[1] p-value<0.001 (Independent t-test)

Table 6. Dominated flux over the plume rise

Scenarios	$(\Delta T)_c$	$T_s - T_a$		Dominated flux
		Daytime	Nighttime	
No waste heat recovery				
January	13.56	295.2	300.6	Buoyancy flux
February		293.2	298.8	
March		291.7	297.3	
April		290.7	296.3	
May		291.3	296.3	
June		293.2	297.8	
July		293.8	298	
August		294.1	298.8	
September		294.9	299.2	
October		294.4	299.2	
November		294.0	299.1	
December		295.6	300.2	
Waste heat recovery				
January	9.36	110.2	115.6	Buoyancy flux
February		108.2	113.8	
March		106.7	112.3	
April		105.7	111.3	
May		106.3	111.3	
June		108.2	112.8	
July		108.8	113.0	
August		109.1	113.8	
September		109.9	114.2	
October		109.4	114.2	
November		109.0	114.1	
December		110.6	115.2	

3.2 PM-10 spatial distributions

Predicted 24-hour concentrations of PM-10 were calculated using AERMOD. Results are presented in Table 7. It was found that predicted PM-10 concentrations at every receptor were within the Thailand's ambient standard of 120 μg/m^3. There were no differences between predicted concentrations at receptors prior and after installation of the waste heat recovery system. However, the predicted maximum concentration of the second scenario over the modeling domain was found higher than its base line value. The predicted maximum concentration of 129 μg/m^3 under the utilization of waste heat recovery scenario was higher than the ambient PM-10 standard. High concentrations were predicted to occur in January which is the dry season with low humidity (Chaurasia et al., 2014). Predicted ground level concentrations of PM-10 in this study agree well with the results reported in other studies. It confirmed that increasing the stack gas temperature will increase the value of the effective stack height and lead to lower ground level concentrations (Ahmed, 2013). Differences between the temperature of ambient and emission sources affected the rise of plumes and played an important role in the dilution ability of air and ground level concentrations of air pollutants (El-Gazar and Tawfik, 2013). The pollution maps of predicted 24-hour average PM-10 concentration over the modeling domain for each scenario are illustrated in Figure 4 and Figure 5.

Table 7. Maximum 24-hour predicted concentration for PM-10

Stack temperature	Receptor no.	Max. concentration	Occurred duration	Thai Std. PM-10 (μg/m^3)
598 K (No WHR)	Maximum	115	January	120
	R1	64	January	
	R2	63	April	
	R3	66	January	
	R4	63	April	
	R5	62	September	
	R6	62	July	
413 K (WHR)	Maximum	129	January	120
	R1	65	December	
	R2	63	April	
	R3	66	January	
	R4	63	April	
	R5	62	September	
	R6	62	September	

4. CONCLUSIONS

The effect of utilizing waste heat recovery systems on the rise of plumes from combustion stacks in the cement industry was evaluated in this study. The results revealed that the buoyancy flux played a more dominant force than momentum flux on the rise of plumes. Decreases in the stack exit temperature due to implementation of waste heat recovery did not much affect the value of plume rise. Low ambient temperature is found to be a key factor influencing the increase of the plume rise. Spatial distribution of PM-10 concentrations were simulated under two different scenarios (with and without installation of waste heat recovery) in order to evaluate the effect of changing of stack gas exit temperature on the dispersion of an air pollutant emitted by the cement industry. Results indicated that there were no differences of the predicted PM-10 ground level concentrations at the receptors prior and after utilization of waste heat recovery. However, it should be noted that the maximum predicted concentration within the modeling domain in the scenario of using waste heat recovery was increased. This value was also higher than the ambient PM-10 concentration standard (>120 μg/m^3, daily average). Results, derived from this study can confirm that the implementation of waste heat recovery in this cement plant is not only a valuable energy source but also, in general, does not cause air pollution problems to the surrounding area of the factory.

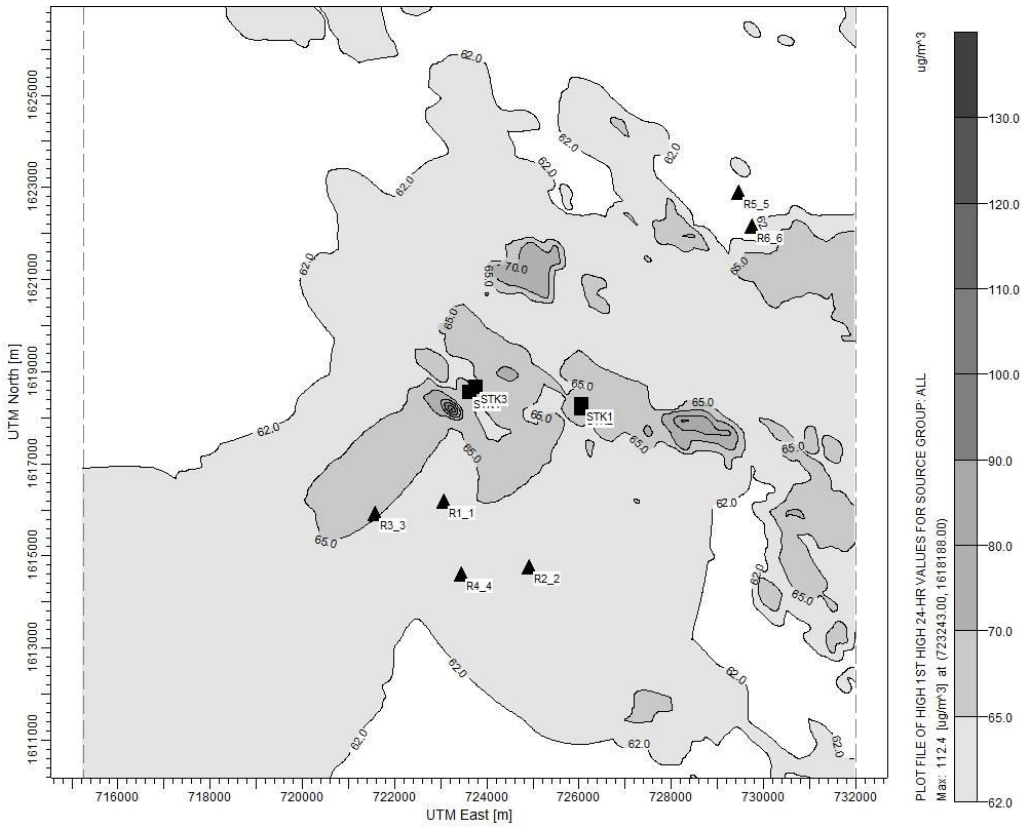

Figure 4. Daily simulation results of PM-10 spatial distribution (no waste heat recovery installation)

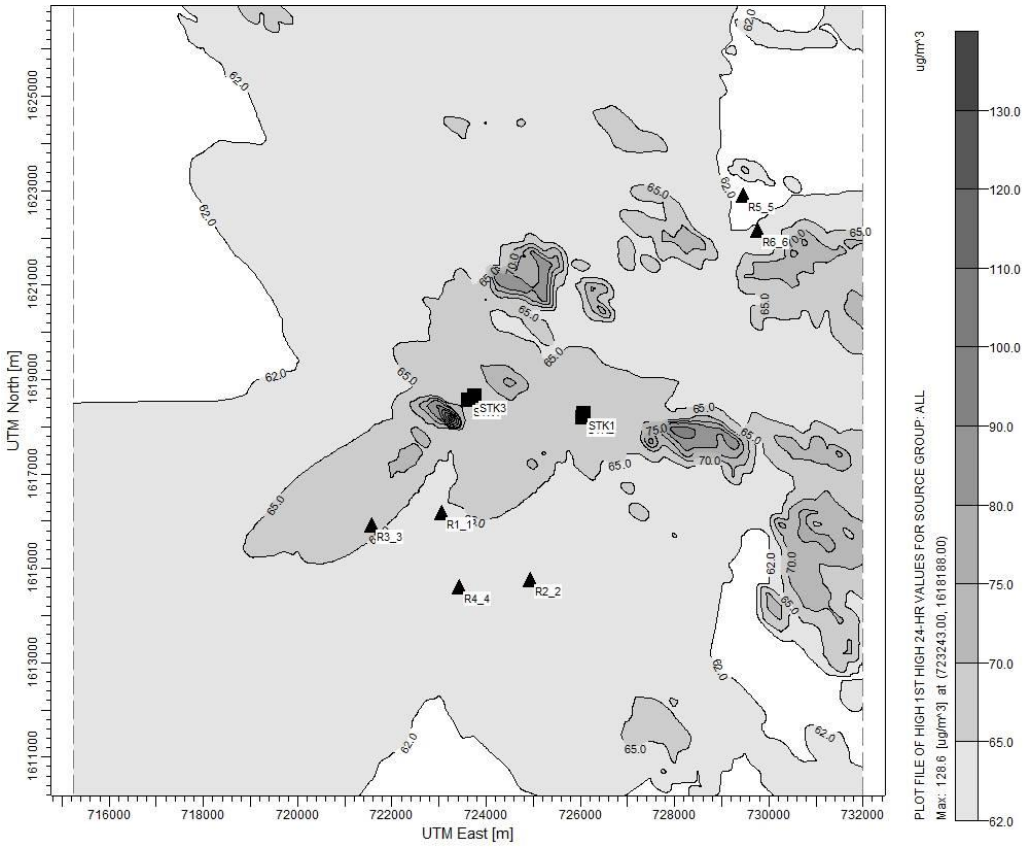

Figure 5. Daily simulation results of PM-10 spatial distribution (waste heat recovery installation)

ACKNOWLEDGEMENTS

The authors sincerely thank the Pollution Control Department and the cement plant for providing input data used in this study. This study was partial supported for the Center of Excellence on Environmental Health and Toxicology (EHT), Faculty of Public Health Mahidol University, Thailand. This study was partially supported for publication by the China Medical Board (CMB).

REFERENCES

Ahmed OS. Assessment and modeling of the effective stack height for different types of atmospheric stability class. Arab Journal of Nuclear Science and Applications 2013;46(1):179-91.

Bhargava A. Effect of wind speed and stack height on plume rise using different equations. International Journal of Engineering Science and Computing 2016;6(4):3228-34.

Brook RD, Rajagopalan S, Pope CA III, Brook JR, Bhatnagar A, Diez-Roux AV, et al. Particulate matter air pollution and cardiovascular disease: an update to the scientific statement from the American Heart Association. Circulation 2010;121(21):2331-78.

Cao J, Yang C, Li J, Chen R, Chen B, Gu D, Kan H. Association between long-term exposure to outdoor air pollution and mortality in China: a cohort study. Journal of Hazardous Materials 2011;186(2-3):1594-600.

Chaurasia S, Ahmed I, Gupta AD, Kumar S. Assessment of air pollution emission from cement industries in Nimbahera, India. International Journal of Current Microbiology and Applied Sciences 2014;3(3):133-9.

Demirkaya G, Padilla RV, Goswami DY. A review of combined power and cooling cycles. Wiley Interdisciplinary Reviews: Energy and Environment 2013;2(5):534-47.

Dimmick WF, Wehe AH. 41 - Technology and costing of air pollution abatement1 A2 -Holgate. In: Maynard R, Holgate S, Koren H, Samet J, Maynard R, editors. Air Pollution and Health. London: Academic Press; 1999. p. 931-45.

El-Gazar MM, Tawfik BBS. Analysis of the factors affecting the distribution of chimney emissions to the atmosphere - simulation approach. International Journal of Computer Science Engineering and Information Technology Research 2013;2(2):367-78.

Essa KSM, Mubarak F, Elsaid SEM. Effect of the plume rise and wind speed on extreme value of air pollutant concentration. Meteorology and Atmospheric Physics 2006;93(3):247-53.

Fang H, Xia J, Zhu K, Su Y, Jiang Y. Industrial waste heat utilization for low temperature district heating. Energy Policy 2013;62(Supplement C):236-46.

Gupta RK, Majumdar D, Trivedi JV, Bhanarkar AD. Particulate matter and elemental emissions from a cement kiln. Fuel Processing Technology 2012;104 (Supplement C):343-51.

Hoven IVD. Effects of time and height on behavior of emissions. Environmental Health Perspectives 1975;10:207-10.

Ilaboya IR, Atikpo E, Umukoro L, Omufuma FE, Ezugwa MO. Analysis of the effects of mixing height and other associated factors on the effective dispersion of plume. Iranica Journal of Energy and Environment 2011;2(2):153-60.

Kampa M, Castanas E. Human health effects of air pollution. Environmental Pollution 2008;151(2):362-7.

Lakes Environmental. Screen View 4.0.0 edition. Ontario, Canada: Lakes Environmental Software; 2011.

Liu H, Fang C, Zhang X, Wang Z, Bao C, Li F. The effect of natural and anthropogenic factors on haze pollution in Chinese cities: a spatial econometrics approach. Journal of Cleaner Production 2017;165(Supplement C):323-33.

Madlool NA, Saidur R, Hossain MS, Rahim NA. A critical review on energy use and savings in the cement industries. Renewable and Sustainable Energy Reviews 2011;15(4):2042-60.

Madlool NA, Saidur R, Rahim NA, Kamalisarvestani M. An overview of energy savings measures for cement industries. Renewable and Sustainable Energy Reviews 2013;19(Supplement C):18-29.

Masters GM. Introduction of Environemntal Engineering and Sciecne. Prentice Hall, USA; 1997.

Parvez F, Lamancusa C, Wagstrom K. Primary and secondary particulate matter intake fraction from different height emission sources. Atmospheric Environment 2017;165(Supplement C):1-11.

Thai Cement Manufacturers Association (TCMA). TCMA 2016. Thailand: Thai Cement Manufacturers Association; 2016.

Thai Meteorological Department (TMD). Season of Thailand [Internet]. 2018 [cited Jun 2018]. Available from: https://www.tmd.go.th/info/info.php?FileID=23

Turner DB. Workbook of Atmospheric Dispersion Estimates. U.S. Environmental Protection Agency; USA; 1970.

United States Department of Energy. Waste Heat Recovery: Technology and Opportunities in U.S. Industry. Industrial Technologies Program, U.S. Department of Energy. United State; 2008.

United States Environmental Protection Agency (USEPA). SCREEN3 model User's Guide. EPA-454/B-95-004, U.S. Environmental Protection Agency; USA; 1995a.

United State Environmental Protection Agency (USEPA). User's Guide for the Industrial Source Complex (ISC3)

Dispersion Models. Volume II - Description of Model Algorithms. North Carolina; 1995b.

United State Environmental Protection Agency (USEPA). User's Guide for the AMS/EPA Regulatory Model (AERMOD). Research Triangle Park, North Carolina; 2018.

Vallero D. Air pollution control technologies. In: Vallero D, editor. Fundamentals of Air Pollution (5th edition). Boston: Academic Press; 2014. p. 829-79.

Urban Land Cover Mapping and Change Detection Analysis Using High Resolution Sentinel-2A Data

Saravanan Vigneshwaran and Selvaraj Vasantha Kumar*

School of Civil and Chemical Engineering, Vellore Institute of Technology (VIT), Vellore-632014, Tamil Nadu, India

ARTICLE INFO

Received: 31 May 2018
Received in revised:
23 Jul 2018
Accepted: 8 Aug 2018
Published online:
5 Oct 2018
DOI: 10.32526/ennrj.17.1.2019.03

Keywords:
Land cover map/ Unsupervised classification/ Sentinel-2A/ Natural resources/ Change detection/ Urban sprawl

*** Corresponding author:**
E-mail: svasanthakumar1982@gmail.com

ABSTRACT

Land cover information is essential data required by urban planners and policy makers to understand existing development and to protect natural resources in a city or town. With the availability of high resolution satellite images from Sentinel-2A, it is now possible to prepare accurate land cover maps and the present study is an attempt in this direction. An approach based on unsupervised classification plus a post-classification editing (recoding) by referring to Google satellite images is proposed in this study and has been tested for the city of Chennai, India. An unsupervised classification using ISODATA technique with 150 clusters and 36 iterations was carried out first and then Google satellite images were used on the background to assign each cluster to a particular land cover type. The proposed approach is very promising as the overall accuracy was found to be 96% with Kappa coefficient of 0.94. It was found that the proposed approach performs well when compared to the supervised and object based classification. The land cover map from Sentinel-2A was compared with the topographical map of 1971 and it was found that there was a fourfold increase in built-up area over the years. Built-up area was induced to develop in proximity to important highways in Chennai as ribbon type of sprawl is noticed. The results showed that the availability of green space is only 7.626 m^2 per person in Chennai against the recommended value of 9 m^2. It was also found that almost 6 km^2 of water bodies have disappeared in Chennai and buildings were constructed over them illegally. The government should ensure proper land use planning and control built-up area development in order to protect the natural resources in the city.

1. INTRODUCTION

Increasing population in cities is a major concern to urban planners, especially in developing countries like India as it results in unprecedented growth of cities in recent decades. More people are migrating from rural to urban areas for better job opportunities and living conditions and this is one of the major reasons for urbanization in the country. Urbanization is inevitable in a developing country like India. However, if urbanization is not controlled properly, it may result in decrease in agricultural land and productivity, cutting down of trees, crowded habitats, air and noise pollution, water distribution problems, public health issues, road traffic congestion, etc. Accurate and up-to-date urban land cover information is an essential data required by urban planners and policy makers for various purposes such as detection of human encroachment on natural resources, urban infrastructure facilities planning, preparation of master plan and detailed development plans, identification of open and green spaces, selection of suitable site for solid waste disposal, etc. In recent years, high resolution satellite data are increasingly being used for urban land cover mapping and monitoring of natural resources as it is possible to differentiate among various earth surface features due to high spatial and spectral resolution (Gaur et al., 2015; Akay and Sertel, 2016; Malarvizhi et al., 2016; Thanvisitthpon, 2016; Salako et al., 2016; Mondal and Debnath, 2017; Guan et al., 2017; Goldblatt et al., 2018; Ongsomwang et al., 2018). Sentinel-2A launched on June 23, 2015 by European Space Agency (ESA) as part of Copernicus Programme is a milestone in the field of satellite remote sensing as it provides high resolution satellite images at free of cost for a wide range of applications. Out of 13 spectral bands of Sentinel-2A, the four bands (B2, B3, B4 and B8) in the visible and near infrared region has a high spatial

resolution of 10 m with a high revisit period of 5 days and hence could potentially be used for various urban related applications (Topaloglu et al., 2016; Abdikan et al., 2016; Elhag and Boteva, 2016; Djerriri et al., 2017; Marangoz et al., 2017; Hansen et al., 2017; Sekertekin et al., 2017; Clerici et al., 2017; Schlaffer and Harutyunyan, 2018).

In many studies, it is reported that the use of Sentinel-2A for land cover classification yields better results than using Landsat-8 (Topaloglu et al., 2016; Sekertekin et al., 2017). For example, Topaloglu et al. (2016) reported that the overall accuracy of land cover classification by Landsat-8 is in the range of 71% to 82% whereas the classification accuracy of Sentinel-2 is in the range of 76% to 84%. Sekertekin et al. (2017) found that the overall accuracy of land cover map derived from Sentinel-2 is 89% whilst that of Landsat-8 is only 84%. This shows that Sentinel-2 is superior to Landsat-8 in land cover classification. However the maximum accuracy reported by existing studies is only 89% (Sekertekin et al., 2017). None of the reported studies on the use of Sentinel-2A optical data for land cover map preparation reported more than 89% accuracy. This was the main motivation behind the present study, i.e., to propose an image classification approach which can give accuracy more than what has been reported in the existing studies. The unsupervised classification plus a post-classification editing (recoding) by referring to Google satellite images was proposed in the present study for land cover map preparation using optical data of Sentinel-2A. The land cover map prepared was then checked for its overall accuracy and Kappa coefficient using randomly generated points. After that, land use/land cover change detection analysis was carried out by comparing the land cover map prepared using Sentinel-2A with the land cover map of 1971 prepared using Survey of India topographical maps. The analysis of land cover maps will help to ascertain the level of urban growth over the years. The direction-wise urban growth analysis was also carried out to find the direction in which the urban growth is oriented. The fundamental question behind the present research work is, "How can the open source satellite data like Sentinel-2A and Google images be best utilized to prepare accurate land cover maps and perform change detection analysis?" The specific objectives of the research work are: (1) to propose an image classification approach for accurate land cover map preparation using Sentinel-2A and Google satellite images. (2) to perform change detection analysis to understand how the city grew over the years, in what direction, the causative factor behind its growth and the type of urban sprawl. (3) to analyze the impact of urbanization on water bodies.

2. METHODOLOGY

Chennai (formerly called Madras), the capital of the Tamil Nadu state in India is the fourth largest metropolitan city of the country. For land cover map preparation using Sentinel-2A data, Chennai Corporation which extends to an area of 430 km^2 was taken into account. Figure 1 shows the areal extent of Chennai Corporation and its location in Tamil Nadu and India. The Chennai Corporation is headed by a Mayor and it comprises 15 zones and 200 wards. Until 2011, Chennai Corporation covered only an area of 176 km^2. After that, several municipalities, town panchayats and panchayat unions adjacent to the city which were expanded along with the city were merged with the corporation and hence its areal extent has been increased from 176 km^2 to 430 km^2.

The Sentinel-2A data were acquired, processed, and generated by the European Space Agency and repackaged by U.S. Geological Survey (USGS) into 100 km × 100 km tiles. The Sentinel-2A satellite data acquired on August 24, 2016 was used in the present study to extract the land cover information. The satellite data was downloaded from USGS Earth Explorer (USGS, 2018). As the revisit frequency is 5 days, a large number of images acquired at different dates were available for download. However, selecting an image without any cloud cover was difficult as the percentage of cloud cover was high in most of the images. The satellite image taken on August 24, 2016 had a cloud cover of only 0.41% and hence the same was considered in the present study for land cover map preparation. The processing level of the downloaded image was Level-1C which includes radiometric and geometric correction, ortho rectification and spatial registration on a global reference system, namely, the WGS84 datum and Universal Transverse Mercator (UTM) Projection. There are 13 spectral bands in Sentinel-2A which extends from visible and near-infrared (VNIR) portion to Short-wave infrared (SWIR) portion. Out of 13 bands, four bands have 10 m

spatial resolution, six bands are at 20 m resolution and the remaining three bands at 60 m resolution. Since the purpose of the present study is to prepare urban land cover map, an image with high spatial resolution is generally preferred. Hence only the three bands of the Sentinel-2A data were considered. They are green (Band 3 at 560 nm), red (Band 4 at 665 nm) and near-infrared (Band 8 at 842 nm). The classical blue (Band 2 at 490 nm) was not considered as only green, red and near-infrared is sufficient for generating the false colour composite (FCC). After downloading Sentinel-2A data, clipping of the image within the study area was carried out as the downloaded image is of 100 km × 100 km size. The next step of generation of FCC was done by assigning band-3 (green) to blue, band-4 (red) to green, band-8 (near-infrared) to red. In the present study, four land cover classes were considered, namely, built-up, open land, vegetation and water bodies. The built-up area includes all buildings and roads; open land includes rocky, barren, scrubland, play grounds and residential layouts; vegetation includes parks, forest and agricultural lands; water bodies consist of lakes, rivers, ponds and tanks.

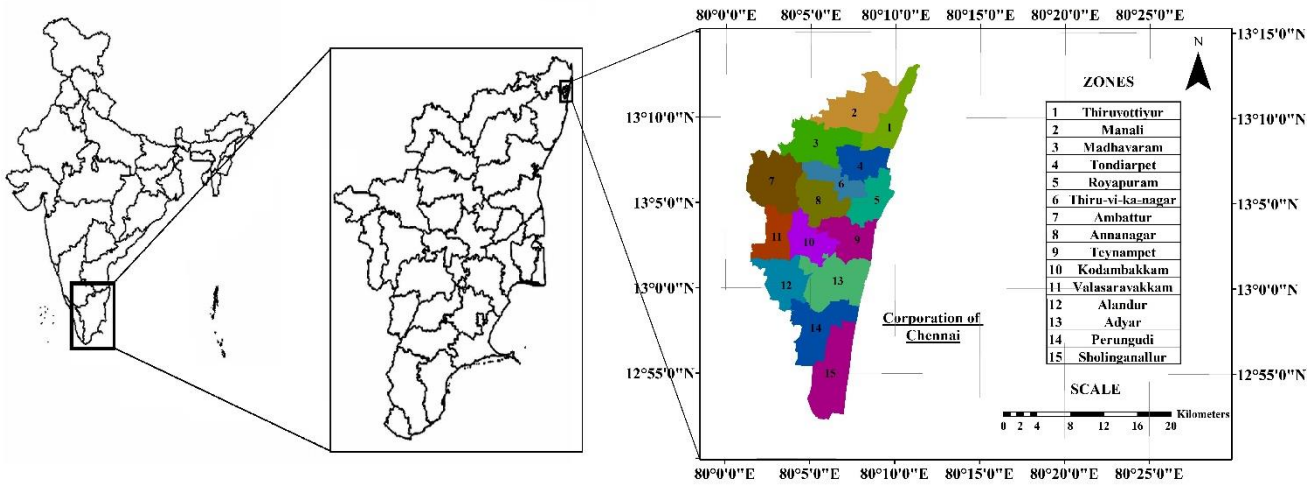

Figure 1. Map showing the location of Tamil Nadu state in India (left), location of Chennai Corporation in Tamil Nadu (middle) and Chennai Corporation (right)

In the present study, digital image processing using one of the popular unsupervised classification techniques called ISODATA was applied first and then visual interpretation using Google satellite images was carried out. The Iterative Self-Organizing Data Analysis Techniques Algorithm (ISODATA) is basically a clustering algorithm that uses an iterative procedure to group image pixels into spectrally similar clusters based on their position in the spectral space. The algorithm begins with an initial clustering of the data and the calculation of cluster means. During each iteration, the algorithm compares the spectral distance of each pixel to the cluster means and assigns them to the cluster whose mean is closest. Once all pixels are assigned, the cluster means are recalculated, and the pixels are again compared and clustered based on spectral distance to the cluster means. This process is repeated until the maximum number of iterations is reached. In the present study, ISODATA classification was applied with 150 clusters or classes and 36 iterations. After running the ISODATA algorithm using ERDAS Imagine software, the classified image was obtained with 150 classes. In order to assign each of these 150 classes to a particular land cover type, the traditional approach is to see the original satellite image used for classification and identify which land cover a particular cluster belongs to. But the problem with this approach is sometimes we may wrongly assign a cluster and this may happen especially in situations where the spatial resolution of the image is low. Even though the present study uses high resolution Sentinel-2A data of 10 m for classification, however, it may not be possible to see individual buildings, roads, etc. on the image. Hence it has been decided to use the satellites images from Google maps on the back ground to identify the land cover type of a given cluster as it is possible to see buildings, roads, etc. very clearly on the Google maps because of its

high resolution images. An open source software called Portable Base Map Server (PBMS) was used to get the Web Map Tile Service (WMTS) link of Google Maps and the link was used in ArcGIS software to bring the Google maps in background while assigning each cluster to a particular land cover type. Finally the land cover map with four classes, namely, built-up, open land, vegetation and water bodies was checked for its accuracy using 100 points generated randomly over the classified map using 'Create Accuracy Assessment Points' tool in ArcGIS software. For each of the random point generated, the type of land cover from classified image was compared with that of the actual land cover identified from Google maps satellite image to get the overall accuracy and Kappa statistic. A comparison with the supervised classification and object based classification was also attempted to check the performance of the proposed approach in land cover map preparation.

For preparing the land cover map of 1971, four toposheets, namely, 66C4, 66C8, 66D1 and 66D5 of 1:50000 scale covering Chennai corporation was obtained from Survey of India and then scanned & georeferenced using known ground control points and projected to the UTM Zone 44N. The land cover map was obtained by on-screen digitizing of built-up, open land, vegetation and water bodies in the toposheets within the study area. The areal extent of various land covers were found and compared with that of the land cover map prepared using Sentinel-2A to assess the urban growth. The direction-wise urban growth analysis was also carried out by calculating the built-up area in 16 cardinal directions (N-NNE, NNE-NE, etc.) using the land cover maps of 1971 and 2016. The direction-wise analysis helped to find the direction in which the urban growth was oriented. The results are discussed in the following section.

3. RESULTS AND DISCUSSION

The land cover maps of 1971 and 2016 are shown in Figure 2. The results of accuracy assessment of land cover map prepared using Sentinel-2A is presented in Table 1.

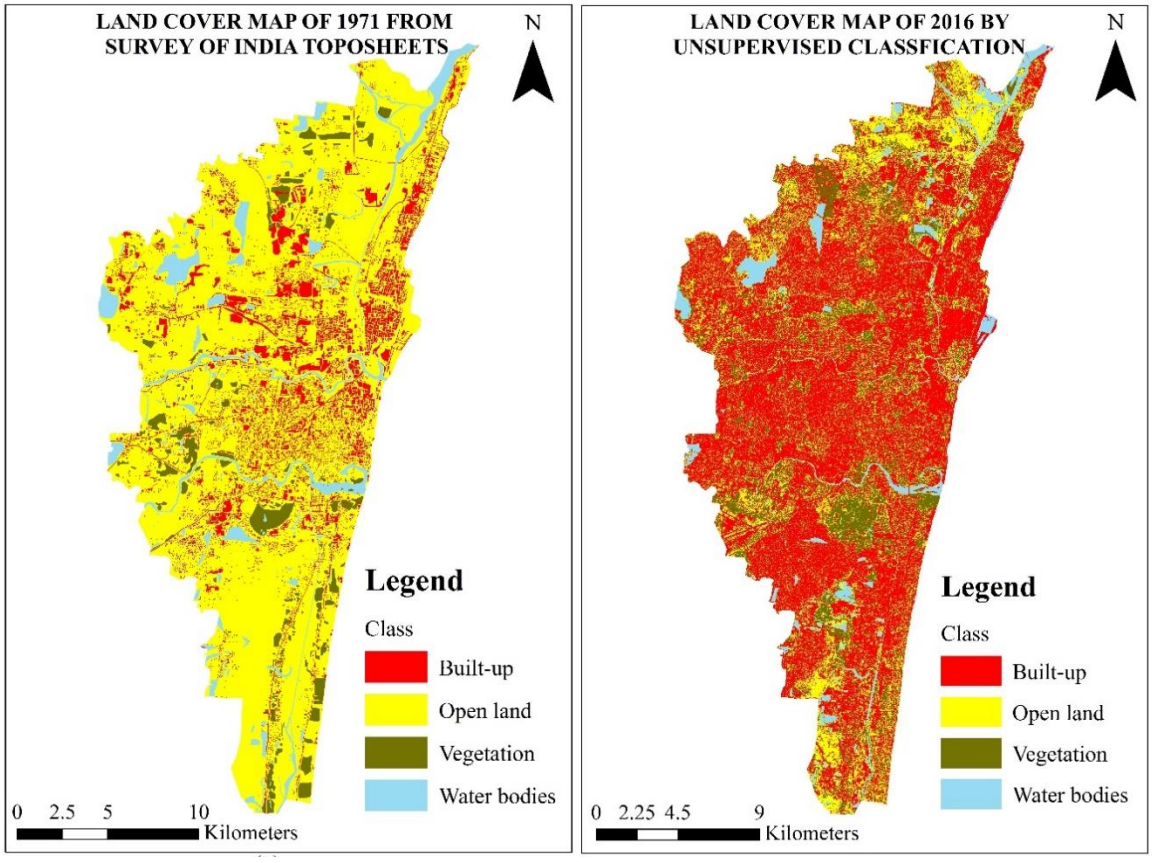

(a) (b)

Figure 2. Land cover map of (a) 1971 (b) 2016

Table 1. Accuracy assessment results

Class	Built-up	Water bodies	Open land	Vegetation	Total	User accuracy	Kappa
Built-up	50	1	2	1	54	0.93	0.00
Water bodies	0	10	0	0	10	1.00	0.00
Open land	0	0	24	0	24	1.00	0.00
Vegetation	0	0	0	12	12	1.00	0.00
Total	50	11	26	13	100	0.00	0.00
Producer accuracy	1.00	0.91	0.92	0.92	0.00	0.96	0.00
Kappa	0.00	0.00	0.00	0.00	0.00	0.00	0.94

It can be seen from Table 1 that the overall accuracy was found to be 96% and Kappa coefficient was calculated as 0.94. According to Congalton and Green (2009), an overall accuracy of 85% is the cut-off between acceptable and unacceptable results. As the overall accuracy is 96% in the present study, it indicates that the proposed approach of unsupervised classification using Google satellite images on the background is acceptable and well suited for classifying the land covers in Sentinel-2A data. A comparison with supervised and object based classification methods was also attempted. For supervised classification, Maximum Likelihood Method (MLM) was used by creating 50 training samples for each land cover category. The MLM method calculates the probability function for each land cover class using the training data given. It assumes Gaussian or normal distribution for the training dataset. Each unknown pixel in the image is assigned to a class that has the highest probability or maximum likelihood. For object based classification, image segmentation was carried out first by segmenting the original image into objects using IDRISI image processing software. Then the objects were used to create training samples for various land cover classes. Finally the MLM method of supervised classification was applied to prepare the land cover map. The results are shown in Figure 3. The accuracy assessment results are presented in Tables 2 and Table 3. An overall accuracy of 77% and 81% was obtained for supervised classification and object based classification respectively. Similarly the Kappa values are 0.65 and 0.70 for supervised and object based classification respectively. The result of accuracy assessment shows that the proposed method of unsupervised classification using Google satellite images on the background is superior to the supervised and object based methods as the overall accuracy of the proposed method is 96% with Kappa coefficient of 0.94.

Table 2. Accuracy assessment results of supervised classification

Class	Built-up	Water bodies	Open land	Vegetation	Total	User Accuracy	Kappa
Built-up	40	3	3	0	46	0.86	0
Water bodies	0	7	1	0	8	0.87	0
Open land	3	0	11	1	15	0.73	0
Vegetation	6	3	3	19	31	0.61	0
Total	49	13	18	20	100	0	0
Producer accuracy	0.81	0.53	0.61	0.95	0	0.77	0
Kappa	0	0	0	0	0	0	0.65

Table 3. Accuracy assessment results of object based classification

Class	Built-up	Water bodies	Open land	Vegetation	Total	User Accuracy	Kappa
Built-up	39	0	6	0	45	0.86	0
Water bodies	3	3	1	2	9	0.33	0

Table 3. Accuracy assessment results of object based classification (cont.)

Class	Built-up	Water bodies	Open land	Vegetation	Total	User Accuracy	Kappa
Open land	3	0	30	1	34	0.88	0
Vegetation	1	2	0	9	12	0.75	0
Total	46	5	37	12	100	0	0
Producer accuracy	0.84	0.6	0.81	0.75	0	0.81	0
Kappa	0	0	0	0	0	0	0.70

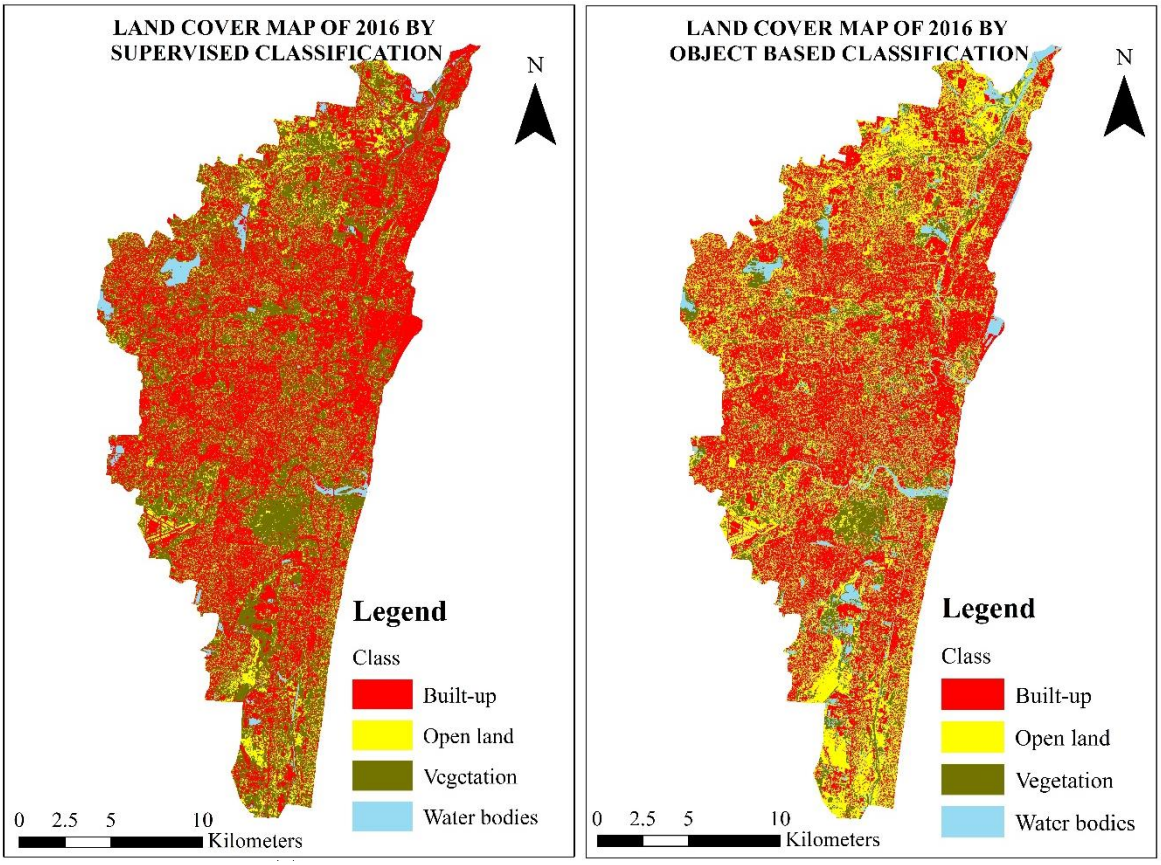

Figure 3. Land cover map by (a) supervised classification (b) object based classification

The overall accuracy of 96% as reported in the present study is more than what has been reported in the existing studies (Elhag and Boteva, 2016; Topaloglu et al., 2016; Clerici et al., 2017; Hansen et al., 2017; Marangoz et al., 2017; Mishra and Singh, 2017; Sekertekin et al., 2017; Schlaffer and Harutyunyan, 2018). Even the studies which combined the Sentinel-2A optical data with Sentinel-1A SAR data (Clerici et al., 2017; Schlaffer and Harutyunyan, 2018) reported a maximum overall accuracy of only 89%, whereas the present study which is purely based on optical data achieved a highest overall accuracy of 96%. Some studies have used both 20 m and 10 m bands of Sentinel-2A by resampling the 20 m band data to 10 m×10 m before they apply the classification (Topaloglu et al., 2016; Clerici et al., 2017). In such cases also, the reported accuracy were in the range of 76% to 89%. But in the present study, only three bands which are at 10 m resolution were considered and reported an overall accuracy of 96%. In existing studies using Sentinel-2A, the visual interpretation of the satellite image and training sample collection were done before digital image processing. This is one reason why the reported accuracy is less in existing studies because only representative samples for each land cover classes can be given during training sample collection. But in the present study, digital image processing using ISODATA unsupervised classification technique was applied first and then

visual interpretation using Google satellite images was carried out. By this way the entire classified output is thoroughly checked using the background Google images. As the present approach offers many advantages and yields high accuracy, the same can be used by researchers for urban land cover classification using Sentinel-2A data.

The area occupied by four land cover classes in 1971 and 2016 is shown in Figure 4. It can be seen from Figure 4 that in the year 2016, built-up land tops in the list with maximum area of 245 km^2 which accounts for about 57% of the total area. As Chennai is one of the well-developed metropolitan cities in the country, it is obvious that one could expect high proportion of built-up land compared to other classes as witnessed in Figure 4. It was found that between 1971 and 2016, there was a fourfold increase in built-up land, which is the highest recorded change when compared to other land covers. This fourfold rise in 45 years indicates that the built-up land has doubled in every decade. It can be seen from Figure 2 that in 1971, one could see built-up areas mainly in the eastern and northeastern side of Chennai in places like Mylapore, Triplicane, Nungambakkam, Theagaraya Nagar, George Town, Purasavakkam, Kilpauk and Alandur. While in 2016, except at a few places in the north and south, all of Chennai is occupied by mostly built-up land as shown by red colour in Figure 2.

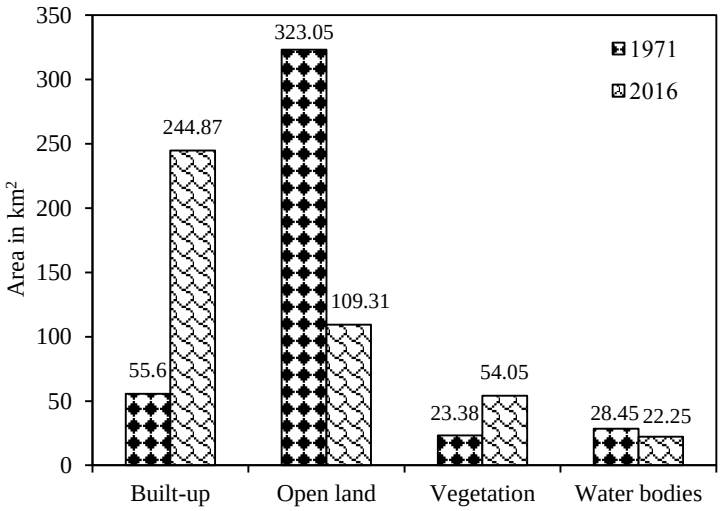

Figure 4. Area of various land cover types in 1971 and 2016

The land covered by vegetation in Chennai is only 13% of the total area in 2016. It was found that this 13% area is mostly reserved forests and parks without any agricultural land. Availability of green spaces is vital for any city as it forms the fundamental component of an urban ecosystem. They help to provide clean air and play a key role in reducing temperature in urban areas. Even though the green cover has increased from 23.38 km^2 to 54.05 km^2 (Figure 4) between 1971 and 2016, but still it is less than what is recommended by World Health Organization (WHO). According to WHO, a city should have a minimum of 9 m^2 of green space per person (WHO, 2010). The population of Chennai from census data is found to be 7.088 million in 2011. According to WHO standards, the total green space required is 63.792 km^2 in Chennai but the green space available is only 54.05 km^2 (Figure 4). That is, 7.626 m^2 of green space is available per person in Chennai which is less than the recommended value of 9 m^2 per person. This shows that more green spaces are required in Chennai to meet the WHO standards. This can be achieved by constructing more parks which not only provide recreational facilities for the public but also helps to maintain the ecological balance and supply quality oxygen.

From Figure 4, one can notice that the water bodies in Chennai have been reduced from 28.45 km^2 in 1971 to 22.25 km^2 in 2016. This shows that almost 6 km^2 of water bodies have disappeared over the study period of 45 years. The lack of maintenance and encroachment are the major reasons for the reduction in the proportion of water

bodies in Chennai. Figure 5 shows the past and present situation of tanks and lakes in Chennai. The land cover maps of 1971 and 2016 which are registered in the same datum (WGS84) and coordinate system (UTM Projection Zone 44N) were used to extract the past and present situation of water bodies. As seen in Figure 5, tanks and lakes, once waterbodies in the topographical map of 1971, were completely disappeared in 2016 and buildings were constructed over them. Some remains of the water bodies can be seen only in Konnur Tank and Velachery Lake, whereas all the remaining tanks and lakes were replaced by buildings and roads. This conversion of water bodies to built-up area is one of the major reasons for recent floods in Chennai as the buildings constructed on water bodies affect the natural flow of rain water and thus causes flooding and water logging. To avoid all these things, the civic authorities should take stringent action against encroachments on water bodies and should not grant permission for residential layouts or building plan approval on lands located on water bodies.

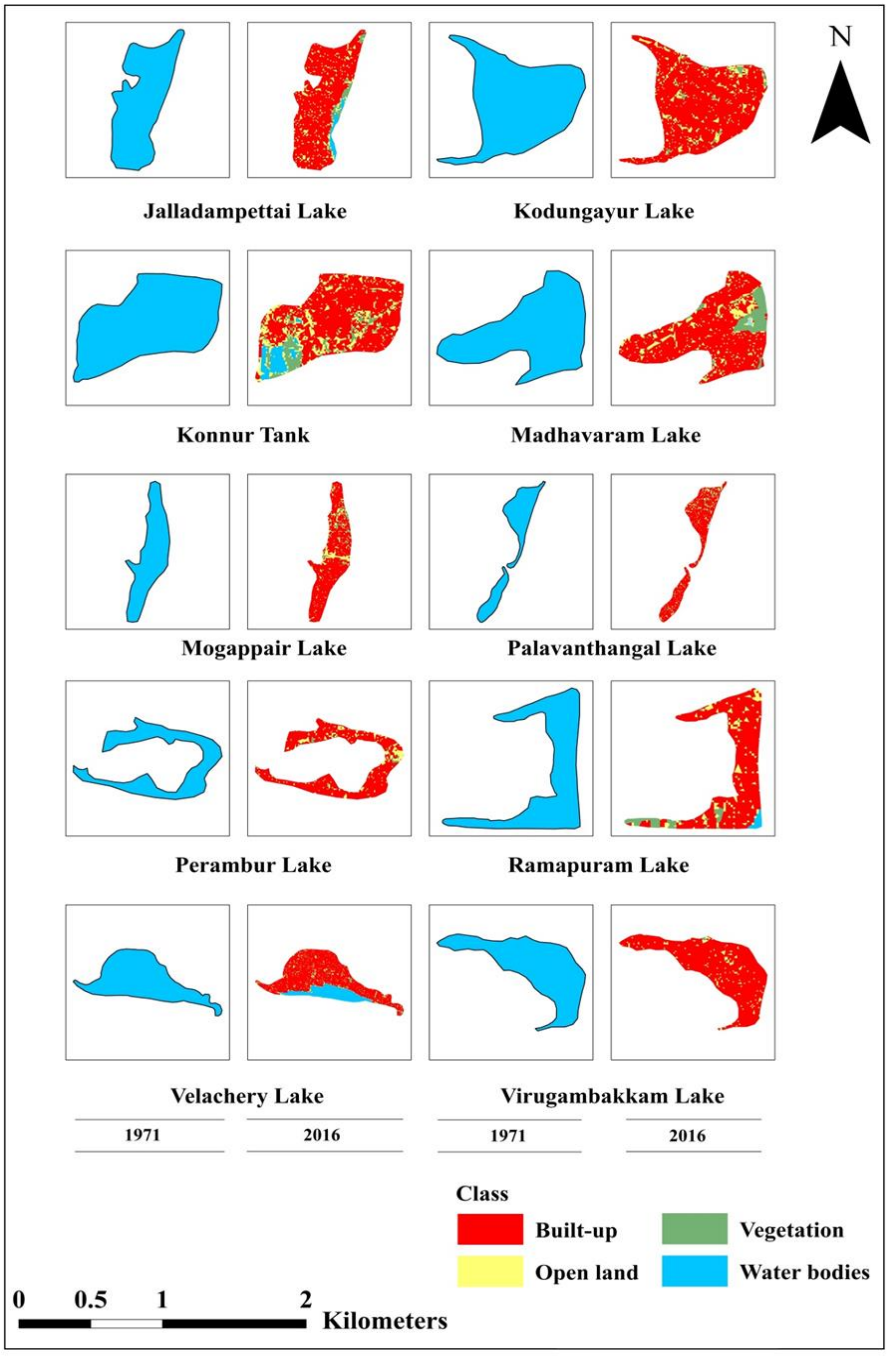

Figure 5. Past and present situation of water bodies in Chennai, India

In order to find the direction in which the urban growth has taken place, sixteen cardinal directions (N, NNE, NE, NEE, E, etc.) were plotted and placed over the built-up area map of 1971 and 2016 as shown in Figure 6. The originating point for the sixteen directions was located at Fort St. George because this is the place from where the Chennai city has grown over the years. The portion from NNE to S in clockwise direction (7 segments) was not considered as it's basically the coastal area (Bay of Bengal) and hence there is no built-up land as seen in Figure 6. The built-up area within the remaining 9 segments (N-NNE, S-SSW, SSW-SW, etc.) in 1971 and 2016 was extracted and shown in Figure 7.

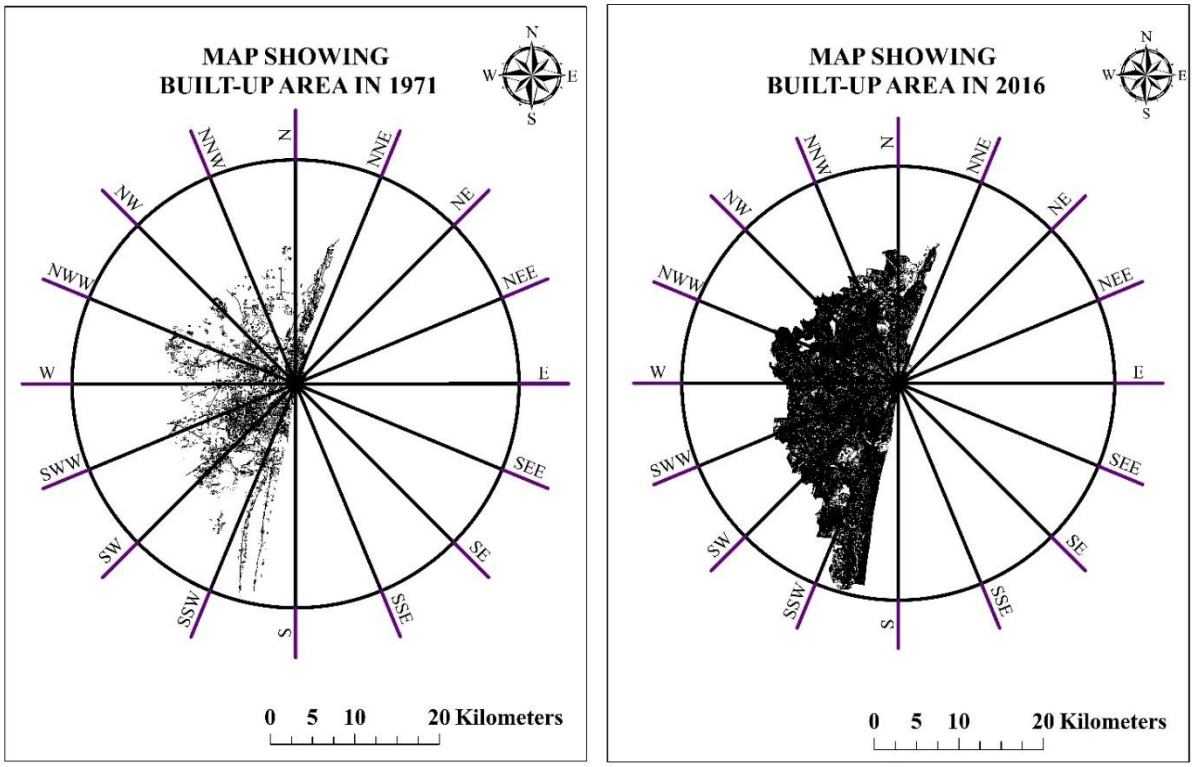

(a) (b)

Figure 6. Built-up area in (a) 1971 (b) 2016

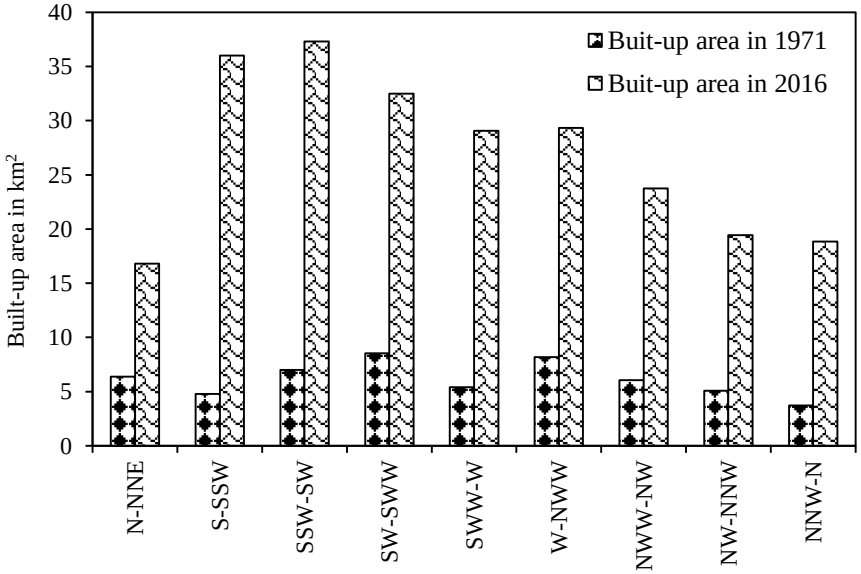

Figure 7. Direction-wise built-up area in 1971 and 2016

It was found that the direction SSW-SW experienced the maximum built-up area development with an enclosed area of 37.31 km^2 in 2016. Next to that, S-SSW and SW-SWW showed maximum growth with an area of 36.02 km^2 and 32.5 km^2 respectively. In terms of difference between the built-up areas of 1971 and 2016, the above said directions stands in the top with 31.25 km^2, 30.31 km^2, and 23.97 km^2 for S-SSW, SSW-SW and SW-SWW directions respectively. The reason for urban growth along these directions is that the major highways in Chennai, namely, Mount road, Grand Southern Trunk (GST) road, Old Mahabalipuram road, East Coast road, Velachery-Tambaram road and Mount Poonamallee road are all located along S-SSW, SSW-SW, SW-SWW directions. Proximity to the highway induced the built-up area to develop along these highways over the years. Such type of urban growth or sprawl is called ribbon sprawl or linear sprawl as sprawl takes place along the highways in outward direction from urban centre. As it was found that the urban growth in Chennai is influenced by major roads, there are more chances that if a new road is constructed, residential layouts, commercial establishments and industries may come up along the road which may lead to haphazard or uncontrolled urban growth with mixed land use and increase of land prices too. Hence the government should ensure proper land use planning and control built-up area development on both the sides of the proposed new roads in Chennai.

The land cover map prepared using Sentinel-2A in the present study can be used in urban heat island (UHI) studies as the land cover plays a dominant role in formation of heat islands in a city. The land surface temperature (LST) from the recently launched Sentinel-3 can be used to prepare UHI map and the UHI map can be correlated with the land cover map to identify the most influencing land cover type. Spatio-temporal variations of heat island and its relationship with land cover can also be done as both Sentinel-2A and 3 has very high revisit frequencies. Another area where there is a good scope for further research is the prediction of future urban sprawl using models like Cellular automata or Markov chains. The land cover maps of the past and present can be used to predict the areas of likely growth in the future. An in-depth investigation of various contributing factors of urban sprawl such as population, distance from roads, availability of basic amenities, infrastructure facilities, etc. and developing mathematical models to explain the urban sprawl phenomenon is another potential direction for further research.

4. CONCLUSIONS

Urbanization is a serious problem in most of the cities in developing countries and India is no exception to this. In order to have a control on urbanization and protect natural resources, it is essential for an urban planner to have accurate and up-to-date urban land cover information. As Sentinel-2A is providing high resolution satellite images free of cost to the public, it is now possible to prepare accurate and up-to-date land cover maps and the present study is an attempt in this direction. An approach based on unsupervised classification plus a post-classification editing (recoding) by referring to Google satellite images was proposed in this study for land cover map preparation using Sentinel-2A data. The proposed approach yielded accurate results and hence can be used by urban planners to prepare land cover maps using Sentinel-2A data and further use it for change detection analysis. The advantages of the proposed approach are simplicity, accuracy and it requires only open source data for preparation of the land cover map.

REFERENCES

Abdikan S, Sanli FB, Ustuner M, Calo F. Land cover mapping using Sentinel-1 SAR data. The International Archives of the Photogrammetry, Remote Sensing and Spatial Information Sciences 2016;41(7):757-61.

Akay SS, Sertel E. Urban land cover/use change detection using high resolution SPOT 5 and SPOT 6 images and urban atlas nomenclature. The International Archives of the Photogrammetry, Remote Sensing and Spatial Information Sciences 2016;XLI-B8:789-96.

Clerici N, Calderon CAV, Posada JM. Fusion of Sentinel-1A and Sentinel-2A data for land cover mapping: a case study in the lower Magdalena region, Colombia. Journal of Maps 2017;13(2):718-26.

Congalton RG, Green K. Assessing the Accuracy of Remotely Sensed Data: Principles and Practices. 2nd ed. CRC Press; 2009.

Djerriri K, Adjouj R, Attaf D. Convolutional neural networks for the extraction of built-up areas from Sentinel-2 images. Proceedings of the 20th AGILE Conference on Geographic Information Science; 2017 May 9-12; Wageningen, Netherlands; 2017.

Elhag M, Boteva S. Mediterranean land use and land cover classification assessment using high spatial

resolution data. IOP Conference Series: Earth and Environmental Science 2016;44:1-13.

Gaur MC, Moharana PC, Pandey CB, Chouhan JS, Goyal P. High resolution satellite data for land use/land cover mapping - a case study of Bilara Tehsil, Jodhpur district. Annals of Arid Zone 2015;54:125-32.

Goldblatt R, Deininger K, Hanson G. Utilizing publicly available satellite data for urban research: mapping built-up land cover and land use in Ho Chi Minh city, Vietnam. Development Engineering 2018;3:83-99.

Guan X, Liao S, Bai J, Wang F, Li Z, Wen Q, He J, Chen T. Urban land-use classification by combining high-resolution optical and long-wave infrared images. Geo-spatial Information Science 2017;20(4):299-308.

Hansen HS, Rosca V, Takacs M, Trock C, Vepstas A, Arsanjani JJ. The use of Sentinel 2 data for mapping European landscapes: the case of Denmark. Proceedings of the INSPIRE Conference 2017 on Infrastructure for Spatial Information in Europe; 2017 Sep 6-8; Strasbourg, France; 2017.

Malarvizhi K, Vasantha Kumar S, Porchelvan P. Use of high resolution Google Earth satellite imagery in landuse map preparation for urban related applications. Procedia Technology 2016;24:1835-42.

Marangoz AM, Sekertekin A, Akcin H. Analysis of land use land cover classification results derived from Sentinel-2 image. Proceedings of the 17th International Multidisciplinary Scientific Geo Conference; 2017 June 27-July 6; Albena, Bulgaria; 2017.

Mishra D, Singh BN. Classification and assessment of land use land cover in Bara Tahsil of Allahabad district using Sentinel-2 satellite imagery. Proceedings of the 38th Asian Conference on Remote Sensing; 2017 October 23; Delhi; 2017.

Mondal SH, Debnath P. Spatial and temporal changes of Sundarbans reserve forest in Bangladesh. Environment and Natural Resources Journal 2017;15(1):51-61.

Ongsomwang S, Dasananda S, Prasomsup W. Spatio-temporal urban heat island phenomena assessment using Landsat Imagery: a case study of Bangkok Metropolitan and its vicinity, Thailand. Environment and Natural Resources Journal 2018;16(2):29-44.

Salako G, Adebayo A, Sawyerr H, Adio A, Jambo U. Application of Remote Sensing/ GIS in monitoring *Typha* spp. invasion and challenges of wetland ecosystems services in dry environment of Hadejia Nguru wetland system Nigeria. Environment and Natural Resources Journal 2016;14(2):44-59.

Sekertekin A, Marangoz AM, Akcin H. Pixel-based classification analysis of land use land cover using Sentinel-2 and Landsat-8 data. The International Archives of the Photogrammetry, Remote Sensing and Spatial Information Sciences 2017;42(6):91-3.

Schlaffer S, Harutyunyan A. Remote Sensing of land cover/land use in the Voghji River Basin, Syunik Region, Armenia; Acopian Center for the Environment, American University of Armenia; 2018.

Thanvisitthpon N. Modeling of urban land use changes: a case study of communities near Rajamangala University of Technology Thanyaburi. Environment and Natural Resources Journal 2016;14(1):44-50.

Topaloglu RH, Sertel E, Musaoglu N. Assessment of classification accuracies of Sentinel-2 and Landsat-8 data for land cover/use mapping. The International Archives of the Photogrammetry, Remote Sensing and Spatial Information Sciences 2016;41(8):1055-9.

United States Geological Survey (USGS). Sentinel-2 (European Space Agency (ESA)) image courtesy of the U.S. Geological Survey [Internet]. 2018. Available from: https://earthexplorer.usgs.gov/

World Health Organization (WHO). Urban Planning, Environment and Health: From Evidence to Policy Action 2010; WHO, Denmark; 2010.

Benefits and Value of Big Trees in Urban Area: A Study in Bang Kachao Green Space, Thailand

Teeka Yotapakdee[1], Lamthai Asanok[2*], Torlarp Kamyo[2], Monton Norsangsri[3], Napak Karnasuta[4], Suwit Navakam[4] and Chidchai Kaewborisut[4]

[1]Economics Department, Maejo University Phrae Campus, Phrae 54140, Thailand
[2]Agroforestry Department, Maejo University Phrae Campus, Phrae 54140, Thailand
[3]Sciences Department, Maejo University Phrae Campus, Phrae 54140, Thailand
[4]PTT Public Company, Bangkok 10900, Thailand

ARTICLE INFO

Received: 24 May 2018
Received in revised:
2 Aug 2018
Accepted: 15 Aug 2018
Published online:
5 Oct 2018
DOI: 10.32526/ennrj.17.1.2019.04

Keywords:
Timber values/ Carbon credits/ Spiritual values/ Urban area/ Benefits

*** Corresponding author:**
E-mail:
lamthainii@gmail.com

ABSTRACT

Green Space is very important for the conservation of biodiversity in the urban areas of Thailand. In the case of Bang Kachao, Green Space has been improved by the development of gardens in the city. The objective of this study focused on an evaluation of the benefits of big trees in the urban area at Bang Kachao Green Space, Samutprakan province. Data was collected from six types of tree habitat classified as road side, abandoned area, public area, private area, temple area, and park located across six sub districts of Bang Kachao. Data were analyzed to evaluate the monetary value of big trees from direct and indirect benefits in three parts consisting of timber value, carbon credits value, and spiritual value. The results reveal that the most valuable big trees are in the parks, followed by temple area, road side, private area, abandoned area, and public area respectively. The total monetary value of big trees was 23,447 USD of which timber value was 13,844 USD, carbon credits value was 7,309 USD, and spiritual value was 2,294 USD. The evaluation suggests that management of high value big trees in park, temple, and road side areas is important from a stakeholder perspective. The recommendations based on this study will help develop appropriate policies for sustaining ecosystem services and contributions to human wellbeing.

1. INTRODUCTION

Ecosystem services (ES) are defined as services provided by the natural environment that benefit people. Some of these ecosystem services are well known including food, fiber and fuel provision and the cultural services that provide benefits to people through recreation and cultural appreciation of nature. Other services provided by ecosystems are not so well known. These include the regulation of the climate, purification of air and water, flood protection, soil formation and nutrient cycling (Department for Environment, Food and Rural Affairs, 2007). ES conception was based on an understanding of the critical relationship between ES and the community well-being, including security, basic material, health and good social relations (Millennium Ecosystem Assessment, 2005). Trees provide benefits from social, communal, environmental, and economic perspectives. Tree give shade to homes and buildings, lowering the inside temperatures and thus reducing demand for power to cool these buildings during hot times of the year (Pandit and Laband, 2010). Tree shade has the potential to reduce residential energy use for cooling from 10 to 50 percent (200 to 600 kWh, 30 to 110 USD) and peak electrical use up to 23% (0.7 kW) (Simpson and McPherson, 1996). Urban Green Spaces also reduce physiological equivalent temperature around 2°C (Sun et al., 2017). Trees reduce both air temperature and air pollution by absorbing carbon dioxide and other dangerous gases from the air (Nowak and Heisler, 2010) which means trees protect the urban climate from severe pollution and provide a climate buffering service (Mukherjee, 2015). Furthermore, trees provide many benefits and play an important role in urban environments and residents value the attractive scenery that trees provide (Dwyer et al., 1991). Meanwhile, areas planted with trees, including community parks and neighborhoods, provide opportunities for social interaction between neighbors. Moreover, trees offer a spiritual value and promote greater community cohesion (Cooper et al., 2016).

In addition, urban trees can provide socio-economics, environment, and ecological wealth, as the awareness of investment made in planting and caring for them (Food and Agriculture Organization, 2016) not only improves the urban areas but also improves the quality of life too. The awareness of planting and caring for trees in Thailand, Bang Kachao Green Space is a very important factor in creating the best urban oasis of Asia. Bang Kachao Green Space, which covers about 1,891 ha (Bang Kachao Subdistrict Administrative Organization, 2017), has been an important contributor to fresh air quality (Phetrut, 2016) as it purifies the air for Bangkok and Samutprakan province. Time Asia awarded this area "The best urban oasis of Asia" in 2006. This area has been under the care of the Royal Forest Department since 2005 (Royal Forest Department, 2017). The trees at Bang Kachao Green Space covers several functions to benefit the ecosystem such as supporting services, provisioning services, regulating services and cultural services. Direct benefits of trees include timber for building and indirect benefits of trees include carbon storage, spiritual, aesthetics, eco-learning, etc. In the recent years, Bang Kachao Green Space has become an ecotourism attraction famous for its garden in the city. An effect of this economic development was the risk of cutting big trees to make room for building structures. The objective of this study focused on the benefits of big trees and an evaluation of big trees in an urban area of Thailand at Bang Kachao Green Space, Samutprakan province. It was assumed that the existence of big trees in the case studied will be a model of urban area benefits from both the direct and indirect value of big trees. Not only will the study raise awareness of big tree values, but it also can help stakeholders decide to sustain and grow an urban Green Space.

2. METHODOLOGY

2.1 Study area

The study was undertaken on Bang Kachao Green Space, Samutprakan province, situated between 13°39'16" and 13°42'50" N and between 100°33'36" and 100°35'28" E. Bang Kachao Green Space (Figure 1) covers 6 sub districts: Thong-kanong, Bangyor, Bang Kachao, Bangnamphung, Bangkrasob and Bangkorbua, located in the estuary of the Chao Phraya River.

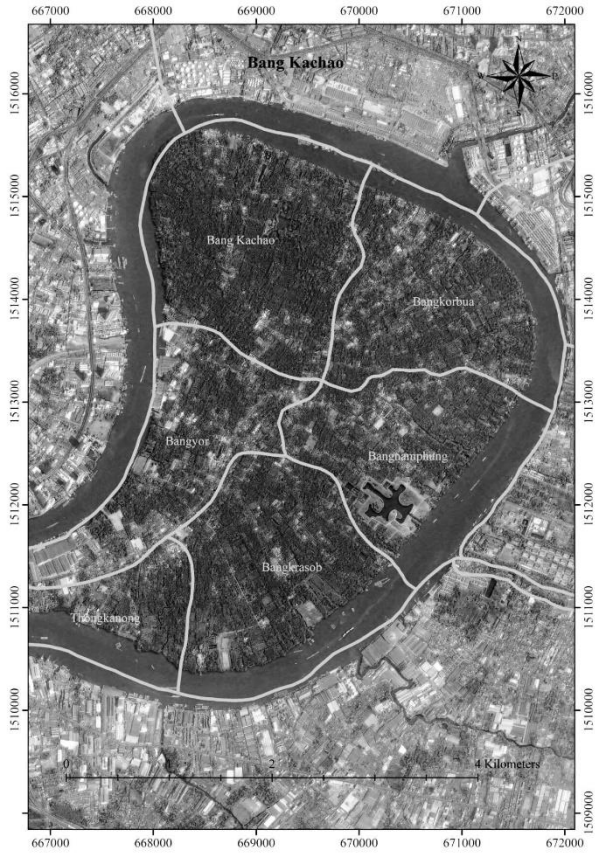

Figure 1. Study area

2.2 Data collection

Big tree samples were measured from six separate habitats composed of: Road side (the area is near the main road), Abandoned (areas without plants growing on them), Governance (public area of community), Private (private house or orchard), Temple (area of temple), and Park (public park). Trees were measured for their diameter at breast height (DBH refers to the tree diameter measured at 1.30 m above the ground), total height (H), and height branch (H_b). DBH can be measured with a specially calibrated diameter tape that displays the diameter measurement when wrapped around the circumference of a tree. Then, the number of big trees with a DBH≥50 cm was counted. All big trees were identified to the species level by collecting leaf specimens for comparison with standard specimens in the herbarium at Department of National Parks, Wildlife, and Plant Conservation. The cultural ecosystem services from big trees, connected to and resulted from their spiritual values, were measured by counting many types of things such as traditional Thai clothes, colorful cloths, ceramic animals, etc. left under the tree.

2.3 Data analysis

Data analysis of the direct and indirect benefits had three evaluation parts consisting of timber values, carbon credits values and spiritual values. Direct benefit was measured by calculating the market value of the available timber. Wood volume in the study areas was estimated using Huber's formula (Husch et al., 1982). Wood value was assigned with guidance of the market prices in October 2014 - January 2015 from Forest Industry Organization. The average price of softwood was 3.68 USD/ft^3 and hardwood was 13.20 USD/ft^3. However, we used a minimum market price of softwood and hardwood because we could not reference the real market price of each species. Thus, the half price for softwood was 1.84 USD/ft^3 and hardwood was 6.60 USD/ft^3. Timber value (USD)=wood volume x price.

The indirect benefit of carbon credit was evaluated from the W_T=Total biomass (kg) from each forest type such as mixed deciduous forest, dry evergreen forest and mangrove forest. Evaluation on the value of carbon stock in aboveground biomass and calculation for carbon sequestration came from the equations of mixed deciduous forest by Ogawa et al. (1965), dry evergreen forest by Tsutsumi et al. (1983), and mangrove forest by Sarayut and Rungsuriya (2011). The undergrowth biomass of big trees was calculated with an allometric equation from the Intergovernmental Panel on Climate Change (2006) . The value of carbon credits by carbon credit price was determined from the California Climate Action Registry (2017) which valued a carbon credit at 15.17 USD/ton CO_2e on 29th November 2017 (exchange rate 1 USD=32.577 baht) from Bank of Thailand (2017). The third part, spiritual value, was an indirect benefits evaluation obtained by surveying sacrifices at big trees and counting of sacred objects. Data for the spiritual cost of sacred objects by market price came from Varuwanshop (2017). Spiritual value (USD) =quantity x price.

3. RESULTS AND DISCUSSION

3.1 Evaluation of timber values

Direct benefit, timber evaluation of big trees at Bang Kachao Green Space was 120 tree samples and total volume 223.77 m^3 that show value 13,843.76 USD. A top ten high value were *Ficus microcarpa* L., *F. religiosa* Linn., *Sonneratia caseolaris* Engl., *Terminalia calamansanay* Rolfe., *Bruguiera gymnorrhiza* Savigny., *Terminalia catappa* L., *Hopea odorata* Roxb., *Ficus curtipes* Corner., *Cynometra ramiflora* Linn., and *Cerbera odollam* Gaertn. (Table 1). Timber price is one of the key elements in forest evaluation so the different prices of timber are unique to the factors of each timber tract: species, tree size, tree quality, volume of sale, distance to market, site accessibility, logging difficulty, market conditions etc. Kankam-Kwarteng et al. (2016) reported the types of wood have greater influence in determining pricing of wood products since they consider some wood to be of better quality than others. Cost of transportation also plays a significant role in the pricing of the wood product. On the other hand, the importance of timber production is more economical than eliminating consumption at the global level. Eliminating the production of illegal timber will result in uneven distribution of social wealth in the forest sector, and will pass the cost of reducing illegal logging onto developing countries (Zhang et al., 2016). The output in this study was not sale in the market, but measured the monetary value of direct benefit from big tree as means to preserving existing green space area. It can support the benefits nature provides to human wellbeing.

Table 1. Timber evaluation of big tree

Species	Common name	Sample (trees)	Volume (m^3)	Value (USD)
Soft wood				
[2]*Ficus microcarpa* L.f.	Curtain fig	13	44.49	1,881.65
[3]*Sonneratia caseolaris* Engl.	Crabapple mangrove	13	38.48	1,627.22
[2]*Ficus religiosa* Linn.	Bodhi	7	32.54	1,376.12
[2]*Terminalia catappa* L.	Bengal Almond	7	16.92	715.58
[2]*Ficus curtipes* Corner.	Ficus tree	2	12.12	512.54
[3]*Cerbera odollam* Gaertn.	Suicide tree	11	8.36	353.41

Table 1. Timber evaluation of big tree (cont.)

Species	Common name	Sample (trees)	Volume (m^3)	Value (USD)
Soft wood				
[2]*Ficus microcarpa* L.f.	Curtain fig	13	44.49	1,881.65
[3]*Sonneratia caseolaris* Engl.	Crabapple mangrove	13	38.48	1,627.22
[2]*Ficus religiosa* Linn.	Bodhi	7	32.54	1,376.12
[2]*Terminalia catappa* L.	Bengal Almond	7	16.92	715.58
[2]*Ficus curtipes* Corner.	Ficus tree	2	12.12	512.54
[3]*Cerbera odollam* Gaertn.	Suicide tree	11	8.36	353.41
[2]*Horsfieldia irya* Warb.	Kruai	5	7.66	324.16
[1]*Albizia lebbeck* Benth.	Indian Walnut	1	2.84	119.93
[2]*Parkia timoriana* Merr.	Nitta tree	1	2.04	86.47
[3]*Hibiscus tiliaceus* L.	Coast Cotton Tree	2	2.04	86.30
[1]*Dolichandrone serrulata* Seem.	D.longissima Schum	2	2.02	85.56
[1]*Mitragyna diversifolia* Havil.	Mitrayna Korth	2	1.9	80.14
[1]*Albizia procera* Benth.	White siris	2	1.7	71.72
[2]*Ficus rumphii* Blume.	Bodhi Tree	1	1.61	67.99
[1]*Albizia Odoratissima* Benth.	Black siris	2	1.58	66.78
[2]*Ficus benjamina* L.	Ficus tree	4	1.54	65.00
[2]*Cananga odorata* Hook.f. et Th.	Ylang-ylang Tree	1	1.37	58.08
[1]*Bombax ceiba* Linn.	Cotton tree	1	1.23	52.06
[1]*Artocarpus lacucha* Roxb.	Monkey jack	1	1.06	44.75
[1]*Limonia acidissima* L.	Wood Apple	1	0.69	29.37
[2]*Barringtonia acutangula* Gaertn.	Indian Oak	1	0.6	25.40
[1]*Crateva adansonii* DC.	Sacred barnar	1	0.44	18.79
[2]*Streblus asper* Lour.	Siamese rough bush	1	0.43	17.99
Hard wood				
[1]*Terminalia calamansanay* Rolfe.	Philippine almond	5	8.74	1,324.31
[3]*Bruguiera gymnorrhiza* Savigny.	Black Mangrove	6	6.85	1,037.75
[2]*Hopea odorata* Roxb.	Iron Wood	2	4.63	702.29
[2]*Cynometra ramiflora* Linn.	Cynometra	3	2.53	383.50
[2]*Dipterocarpus alatus* Roxb.	Yang	1	2.18	329.79
[1]*Terminalia chebula* Retz.	Myrabolan wood	2	1.93	292.72
[1]*Cassia fistula* L.	Indian laburnum	3	1.71	259.29
[2]*Diospyros castanea* Fletch.	Ebony	2	1.67	252.58
[1]*Schleichera oleosa (Lour.)* Merr	Ceylon Oak	1	1.61	243.63
[1]*Millettia leucantha* Kurz.	Yellow Millettia	2	1.45	219.36
[2]*Calophyllum inophyllum* L.	Alexandrian Laurel	2	1.4	211.51
[1]*Pterocarpus indicus* Willd.	Burmese Rosewood	1	1.32	200.75
[2]*Syzygium cumini* L.	Black Plum	2	1.24	188.39
[1]*Diospyros mollis* Griff.	Ebony tree	1	0.71	107.96
[1]*Antidesma ghaesembilla* Gaertn.	Wild black berry	2	0.68	103.10
[3]*Rhizophora mucronata* Poir.	Red Mangrove	1	0.64	96.36
[2]*Xanthophyllum lanceatum* J.J.Sm.	Chum Saeng	1	0.44	66.33
[1]*Millettia brandisiana* Kurz.	Millettia	1	0.38	57.13
Total		120	223.77	13,843.76

Forest type: [1]Mixed deciduous forest (31 trees and 18 species), [2]Dry evergreen forest (56 trees and 18 species) and [3]Mangrove forest (33 trees and 5 species)

Meanwhile the highest value came from big trees in the park area valued at 3,939.24 USD (28.46%), followed by the road side area at 3,099.86 USD (22.39%), and the temple area at 2,791.18 USD (20.16%) (Table 2), with each area having different management practices. Bang Kachao Green Space has two sites classified as park area: Srinakhon Khueankhan Park and Botanical Garden, managed by the Royal Forest Department. The tree management of road side area trees such as pruning for safety of residents and cars is done by the government sector. The temple area is responsible for the care and conservation of religious trees such as *Ficus microcarpa* and *F. religiosa*, and the house owners have to manage trees in their area. The benefits range from meeting basic human needs for food, shelter and firewood, to improved quality of life and health. Globally, over 1.5 billion people depend on forests for their livelihoods (World Wildlife Fund, 2016). Sustainability in this context refers to management practices which protect their rights and livelihoods. The benefits of tree shade on buildings comes from the lowering of inside temperatures and reducing the demand for power to cool these buildings during hot times of the year. One study reported the planting greenery or increasing albedo achieved temperature reductions of 0.6-1.0^{o}C and 0.1-0.5^{o}C, respectively, and energy savings of 40-80 and 70-90 kJ/m^2/day (per unit floor area) on a typical summer day at the city of Kawasaki, Japan (Hirano and Fujita, 2016). The urban greening or albedo increases achieved energy savings of up to 400 tCO_2/day in the entire target study region. In addition, the benefits of big trees from different habitats play an important role in the urban areas which manage their conservation.

Table 2. Timber evaluation by habitats of trees

Habitats of tree	Volume (m^3)	Total (USD)	Percent
Abandoned area	27.70	1,635.65	11.82
Government area	6.83	529.78	3.83
Park area	58.32	3,939.24	28.46
Private area	31.43	1,848.04	13.35
Road side area	49.27	3,099.86	22.39
Temple area	50.20	2,791.18	20.16
Total	223.75	13,843.76	100.00

3.2 Evaluation of carbon credit values

The total indirect benefit, evaluated as the carbon credit value from all habitats of tree, was 481.83 tonCO_2e of gas emissions and a total value 7,309.31 USD of carbon credit value from park, temple area, road side, private area, government area and abandoned area (Table 3). However, the indirect benefits from the state's street trees remove 567,748 tonCO_2 annually, equivalent to taking 120,000 cars off the road. Their asset value is 2.49 billion USD. The annual value of all ecosystem services is 1 billion USD or 110.63 USD/tree (Mc Pherson et al., 2016). The amount of carbon stored is different in the different types of forests and the carbon credit values can be estimated based on the forest type that conforms to Sutherland et al. (2016). Bang Kachao Green Space has three forest types consisting of dry evergreen forest (DY) (Figure 2 and Figure 3), mixed deciduous forest (MX) (Figure 4 and Figure 5) and mangrove forest (MG) (Figure 6 and Figure 7) with 83.36, 27.56, and 19.11 tonCO_2e carbon credit values, and monetary values of 1,264.59, 418.03, and 289.93 USD respectively. Likewise, trees at temple areas had a gas emission value of 123.65 tonCO_2e and a carbon credit value of 1,875.82 USD. The forest type in the temple area consisted of dry evergreen forest and mixed deciduous forest with gas emission values of 100.49 and 2 3 .1 6 tonCO_2e and carbon credit values of 1,524.52 and 351.29 USD, respectively. Meanwhile, road side trees total gas emission of 115.03 tonCO_2e means the total carbon credit value was 1,745.02 USD. The forest type in the road side area consisted of dry evergreen forest, mixed deciduous forest and mangrove forest with 80.28, 18.77, and 15.99 tonCO_2e and a carbon credit value of 1,217.78, 284.68, and 242.56 USD, respectively. The output was not sold in the carbon market, but measured the monetary value of indirect benefit. On the other case, the first carbon credit sale for Thailand and for

ASEAN countries occurred In-Pang community which covers five provinces: Kalasin, Mukdahan, Nakhonpanom, Sakonnakhon and Udonthani. A carbon credit can sell in the market for 4.25 USD and the farmer's network in In-Pang received 37,000 USD credit during the year 2009-2010 (Laosuwan et al., 2013). Meanwhile, the benefit value from urban trees, in all ten megacities (Endreny et al., 2017) such as Beijing (China), Buenos Aires (Argentina), Cairo (Egypt), Istanbul (Turkey), London (Great Britain), Los Angeles (United States), Mexico City (Mexico), Moscow (Russia), Mumbai (India) and Tokyo (Japan) can be estimated as 482 million USD/year due to reductions in CO_2, NO_2, SO_2, PM_{10}, and $PM_{2.5}$ and 8 million USD/year due to CO_2 sequestration. As the result, Bang Kachao Green Space has been an important part of fresh air quality, not only improving the urban areas but also improving the quality of life too.

Figure 2. DY: *Hopea odorata* Roxb.

Figure 3. DY: *Ficus curtipes* Corner.

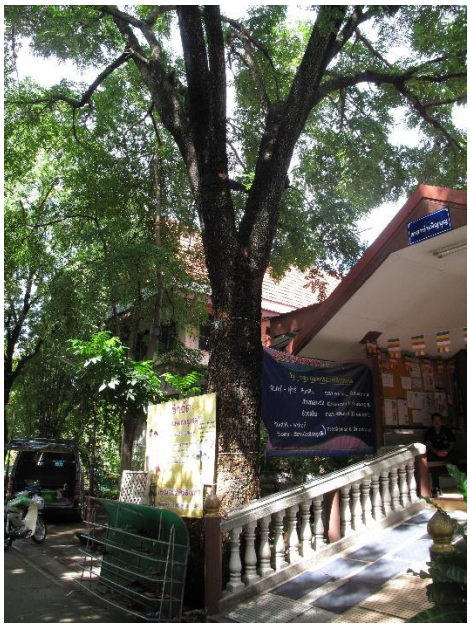

Figure 4. MX: *Albizia lebbeck* Benth.

Figure 5. MX: *Terminalia calamansanay* Rolfe.

Figure 6. MG: *Cerbera odollam* Gaertn.

Figure 7. MG: *Sonneratia caseolaris* Engl.

Table 3. Carbon credit evaluation by habitats of trees

Habitats of trees	Gas emission CO_2 (ton)	Valued carbon credit (USD)	Percent
Abandoned area total	50.25	762.31	10.43
Mixed deciduous forest	-	-	
Dry evergreen forest	9.43	143.02	
Mangrove forest	40.82	619.29	
Government area total	11.07	167.96	2.30
Mixed deciduous forest	-	-	
Dry evergreen forest	3.53	53.54	
Mangrove forest	7.54	114.42	
Park area total	130.03	1,972.55	26.99
Mixed deciduous forest	27.56	418.03	
Dry evergreen forest	83.36	1,264.59	
Mangrove forest	19.11	289.93	
Private area total	51.79	785.66	10.75
Mixed deciduous forest	0.68	10.34	
Dry evergreen forest	41.52	629.80	
Mangrove forest	9.59	145.51	
Road side area total	115.03	1,745.02	23.87
Mixed deciduous forest	18.77	284.68	
Dry evergreen forest	80.28	1,217.78	
Mangrove forest	15.99	242.56	
Temple area total	123.65	1,875.82	25.66
Mixed deciduous forest	23.16	351.29	
Dry evergreen forest	100.49	1,524.52	
Mangrove forest	-	-	
Total	481.83	7,309.31	100.00

3.3 Evaluation of spiritual values

Cultural ecosystem services is the nonmaterial benefits that people obtain from ecosystems through spiritual enrichment, cognitive development, reflection, recreation, and aesthetic experiences. Nature is a common element in most major religions. Natural heritage, traditional knowledge, and associated customs are important for creating a sense of belonging. The cost of spiritual enrichment evaluated from the sacred objects placed under trees totaled 2,293.95 USD (Table 4) from eight trees such as *Ficus religiosa* L., *Syzygium cumini* L., *F. microcarpa* L.f., *Hopea odorata* Roxb. (Table 5). The spiritual enrichment composed of small ceramic Buddhas totaling 807.32 USD, Thai dress totaling 675.32 USD, and other items totaling 811.31 USD such as colorful cloths, ceramic dolls, etc. However, aesthetic and spiritual understandings of the value of nature lead people to develop moral responsibilities towards nature and these are more significant than aesthetic and spiritual benefits from nature (Cooper et al., 2016). Assigning spiritual or religious significance to certain areas or species occurs in most societies (Daniel et al., 2012). However, how this significance is expressed varies across and within societies. Sacred areas are often marked by religious symbols (e.g., crosses or prayer flags on mountain summits, shrines along pilgrimage routes). Also, the spiritual values do not have to be solely individual preferences matters of artistic taste and freedom of religion. The output of spiritual value will be socially shared values that are independent of the spiritual dimension of nature.

Table 4. Evaluation of cost of spiritual enrichment

List	Quantity (unit)	Price (USD/unit)	Total (USD)
Small Buddha ceramic height 10 cm.	263	3.07	807.32
Monk cloth	8	3.68	29.47
Colorful cloth	154	0.31	47.27
Baby doll ceramic	75	1.84	138.13
Woman doll ceramic	145	1.84	267.06
Short flower steering wheel	84	0.61	51.57
Long plastic flower steering wheel	6	2.46	14.73
Small animal doll ceramic	124	1.84	228.38
Big animal doll ceramic	4	6.14	24.56
Thai dress	44	15.35	675.32
Drinking water	11	0.31	3.38
Snack	11	0.61	6.75
Total			2,293.95

In evaluating the spiritual value of habitat trees, *Ficus religiosa* Linn. (Bodhi) has great importance among Buddhists who regard Bodhi as the personification of Buddha. Lord Buddha attained enlightenment mediating under it. *Ficus religiosa* Linn. has its own symbolic meaning of enlightenment and peace. Nevertheless, *Hopea odorata* Roxb., in Thailand, is believed to be inhabited by a certain tree spirit known as a lady belonging to a type of ghost related to trees. The spiritual value of big trees in the temple habitat was estimated at 603.49 USD (26%). On the other hand, the spiritual value in park areas was *Hopea odorata* Roxb. 326 USD (14%) and private area was *Ficus microcarpa* L. f. 79.5 USD (4%) (Table 5). Indirect benefits of spiritual value can preserve big trees by participation of people in the religious community because most of the spiritual and belief trees are in the temple area. Therefore, community plays a role in conserving sustainable trees with spiritual value that help develop moral responsibilities towards nature.

Table 5. Evaluation of spiritual values by habitats of trees

Habitats of tree	Species	Quantity (tree)	Value of beliefs (USD)	Percent
Temple area	*Ficus religiosa* Linn.	4	962.64	56
	Syzygium cumini L.	1	322.31	
Private area	*Ficus microcarpa* L.f.	1	79.50	3.47
Road side	*Ficus microcarpa* L.f.	1	603.49	26.31
Park	*Hopea odorata* Roxb.	1	326.00	14.21
Total		8	2,293.95	100

3.5 Total values within habitats of trees

Total values of trees within habitats differed significantly (Table 6). The outstanding of habitat trees was private area where awareness of tree conservation by dwellers. In the same way, the habitats of tree in park area (Sri Nakhon Khuean Khan Park and Botanical Garden) was urban reforestation so support by Royal Forest Department as same as Singapore Botanic Gardens. Currently, the Gardens' mission includes providing botanical and horticultural support for the nation's greening plans, being a center for plant taxonomic and biodiversity research in the region, as well as a recreational and educational attraction (Singapore Botanic Gardens, 2017) . Bang Kachao community has the Sri Nakhon Khuean Khan Park and Botanical Garden where established for being the source production of fresh air, the public park for relaxing, education, biodiversity conservation and exercising for the people. Also, it is a place for ecosystem education on plant species and animals both local and within nearby area. Therefore, it compares as one of an oasis for the city people who want to experience nature, the local way of life and escaping Bangkok's chaos. Tree regeneration in urban habitats is typically achieved through planting initiatives and encouraging natural regeneration. However, in some urban greenspace, tree planting can be logistically challenging as practitioners need to balance multiple socio-economic and ecological factors (Le Roux et al., 2014) when implementing planting strategies, including: site location, public safety, aesthetics, land ownership, and existing vegetation. The value of urban forests for improving social health and equitable access to ecosystem services (Nesbitt et al., 2017). Although, quantifying cultural ecosystem services (Small et al., 2017) could be merit in discarding this term for the simpler non-material ecosystem services that the challenges in valuing the invaluable to focused on the beneficiary.

Table 6. Benefits and values of big tree by habitats of trees

Habitats of tree	Direct benefits of timber (USD)	Indirect benefits of carbon credit (USD)	Indirect benefits of spiritual (USD)	Total (USD)	Percent
Abandoned area	1,635.65	762.31	-	2,397.96	10.23
Government area	529.78	167.96	-	697.74	2.98
Park area	3,939.24	1,972.55	326.00	6,237.78	26.60
Private area	1,848.04	785.66	79.50	2,713.20	11.57
Road side area	3,099.86	1,745.02	603.49	5,448.37	23.24
Temple area	2,791.18	1,875.82	1,284.96	5,951.96	25.38
Total	13,843.76	7,309.31	2,293.95	23,447.01	100.00

4. CONCLUSIONS

Evaluation of habitats of trees at Bang Kachao Green Space estimated a high value for trees from parks, temple areas and the road side that suggests that management of this resource is meaningful from a stakeholder perspective at the community level. Benefits from big trees are not only important for social well-being in the area, but also could be an important starting point for management of big tree in other urban areas. Concerning direct benefits, timber value can preserve existing green space area that can support the benefits nature provides to

human wellbeing. On the other hand of indirect benefits, the carbon storage is important for fresh air quality which improves the urban areas and also the quality of life. In addition, the spirit value of trees can help preserve them by inspiring people to develop moral responsibilities towards nature. The outcome, the benefits, and value of big trees in urban areas will play an important role in the urban environment and dwellers which benefit from the values of big trees in providing attractive environments. The findings from this research support the development of appropriate policies for sustaining ecosystem services in urban area and document their contributions to human wellbeing.

ACKNOWLEDGEMENTS

We would like to thank PTT Public Company kindness support the foundation and thank Royal Forest Department, community and Maejo University Phrae Campus for supporting data and convenience of this project.

REFERENCES

Bang Kachao Subdistrict Administrative Organization. Information of Bang Kachao subdistrict. Information of Bang Kachao [Internet]. 2017 [cited 2017 Nov 2]. Available from: http://bangkachao.go.th/public/history/data/index/menu/22 (in Thai)

Bank of Thailand. Exchange rate [Internet]. 2017 [cited 2017 Nov 29]. Available from: https://www.bot.or.th/thai/_layouts/application/exchangerate/exchangerate.aspx (in Thai)

California Climate Action Registry. California carbon dashboard carbon credit price 2017 [Internet]. 2017 [cited 2017 Dec 1]. Available from: http://calcarbondash.org/

Cooper N, Brady E, Steen H, Bryce R. Aesthetic and spiritual values of ecosystems: recognising the ontological and axiological plurality of cultural ecosystem 'services'. Ecosystem Services 2016; 21:218-29.

Daniel TC, Muhar A, Arnberger A, Aznar O, Boyd JW, Chan KMA, Costanza R, Elmqvist E, Flint CG, Gobster PH, Gret-Regamey A, Lave R, Muhar S, Penker M, Ribe RG, Schauppenlehner T, Sikor T, Soloviy I, Spierenburg M, Taczanowska K, Tam J, Dunk Avd. Contributions of cultural services to the ecosystem services agenda. Proceedings of the National Academy of Sciences of the United States of America 2012;109(23):8812-9.

Department for Environment, Food and Rural Affairs. An introductory guide to valuing ecosystem services. London; 2007.

Dwyer JF, Schroeder HW, Gobster PH. The significance of urban trees and forests: toward a deeper understanding of values. Journal of Arboriculture 1991;17(10):276-84.

Endreny T, Santagata R, Perna A, Stefano CD, Rallo RF, Ulgiati S. Implementing and managing urban forests: A much needed conservation strategy to increase ecosystem services and urban wellbeing. Ecological Modelling 2017;360:328-35.

Food and Agriculture Organization. Building greener cities: nine benefits of urban trees [Internet]. 2016 [cited 2018 Apr 4]. Available from: http://www.fao.org/zhc/detail-events/en/c/454543/

Hirano Y, Fujita T. Simulating the CO_2 reduction caused by decreasing the air conditioning load in an urban area. Energy and Buildings 2016;114:87-95.

Husch B, Miller CI, Beers TW. Forest Mensuration. 3rd edition. John Wiley & Sons, New York; 1982.

Intergovernmental Panel on Climate Change. IPCC Guidelines for National Greenhouse Gas Inventories. International Panel on Climate Change. IGES, Japan; 2006.

Kankam-Kwarteng C, Donkor J, Acheampong S. Determinants of wood prices: analysis of wood retailers in Kumasi. Journal of Business and Management 2016;4:36-44.

Laosuwan T, Uttaruk P, Klinhom U, Navanugraha C. The achievement of Inpang community network under participation in global warming mitigation through forest sector. Thaksin Journal 2013;16(2):44-54.

Le Roux DS, Ikin K, Lindenmayer DB, Manning AD, Gibbons P. The future of large old trees in urban landscapes. PLoS ONE 2014;9(6):e99403.

Millennium Ecosystem Assessment. Ecosystems and human well-being: synthesis. Island Press, Washington DC, USA; 2005.

Mukherjee A. Importance of urban forestry with special reference to Kolkata. IOSR Journal Of Humanities And Social Science 2015;20(8):89-94.

Nesbitt L, Hotte N, Barron S, Cowan J, Sheppard S. The social and economic value of cultural ecosystem services provided by urban forests in North America: a review and suggestions for future research. Urban Forestry and Urban Greening 2017;25:103-11.

Nowak DJ, Heisler GM. Air quality effects of urban trees and parks. National Recreation and Park Association; 2010.

Ogawa H, Yoda K, Ogino K, Kira T. Comparative ecological studies on three main types of forest vegetation in Thailand II. Plant Biomass. Nature and Life in Southeast Asia 1965;4:49-80.

Pandit R, Laband DN. Energy saving from tree shade. Ecological Economics 2010;69(2010):1324-9.

Phetrut A. Willingness to Pay for the Benefits of Biodiversity and Ecosystem Services: A Case Study of Bang Ka Chao, Prapadang District, Samutprakarn Province. Report of the Royal Forest Department; 2016.

Royal Forest Department. Bang Krachao data 2017 [Internet]. 2017 [cited 2017 Sep 14]. Available from: https://www.forest.go.th/orip/index.php?option=com_conten&view=article&id=447 (in Thai)

Simpson JR, McPherson EG. Potential of tree shade for reducing residential energy use in California. Journal of Arboriculture 1996;22(1):10-8.

Singapore Botanic Gardens. History of Singapore botanic gardens [Internet]. 2017 [cited 2017 Dec 1]. Available from: https://www.sbg.org.sg

Small N, Munday M, Durance I. The challenge of valuing ecosystem services that have no material benefits. Global Environmental Change 2017;44:57-67.

Sun S, Xu X, Lao Z, Liu W, Li Z, Garcia EH, He L, Zhu J. Evaluating the impact of urban green space and landscape design parameters on thermal comfort in hot summer by numerical. Building and Environmental 2017;123:277-88.

Sutherland IJ, Gergel SE, Bennett EM. Seeing the forest for its multiple ecosystem services: indicators for cultural services in heterogeneous forests. Ecological Indicators 2016;71:123-33.

Tsutsumi T, Yoda K, Sahunalu P, Dhanmanonda P, Prachaiyo B. Forest: Felling, Burning and Regeneration. In: Kyuma K, Pairintra C, editors. Shifting Cultivation. Tokyo; 1983.

Varuwanshop. Price of cultural shopping 2017 [Internet]. 2017 [cited 2017 Nov 29]. Available from: http://www.varuwan.com/ (in Thai)

World Wildlife Fund. 100% sustainable timber markets the economic and business case. UK; 2016.

Zhang X, Xu B, Wang L, Yang A, Yang H. Eliminating illegal timber consumption or production: which is the more economical means to reduce illegal logging? Forests 2016;7(191):1-13.

Twelve-Year Monitoring Results of Radioactive Pollution in the Kazakh Part of the Syrdarya River Basin

Khairulla Zhanbekov[1*], Almaz Akhmetov[2] and Augusto Vundo[3,4]

[1]*Department of Academic Affairs, Abai Kazakh National Pedagogical University, Dostyk 13, Almaty 050010, Kazakhstan*
[2]*Orizon Consulting, 6841 Elm Street, McLean 22101, VA, USA*
[3]*Graduate School of Life and Environmental Sciences, University of Tsukuba, Tennoudai 1-1-1, Tsukuba 305-8577, Japan*
[4]*Pedagogical University, Nampula Branch, Av. Josina Machel 256, Nampula 544, Mozambique*

ARTICLE INFO

Received: 18 Apr 2018
Received in revised:
15 Aug 2018
Accepted: 15 Aug 2018
Published online:
8 Oct 2018
DOI: 10.32526/ennrj.17.1.2019.05

Keywords:
Syrdarya/ Kazakhstan/ River pollution/ Radioactive pollution/ Uranium industry

*** Corresponding author:**
E-mail: hairulla418@mail.ru

ABSTRACT

Assessment of radioactive pollution of the Syrdarya river was carried out. A large number of water samples were collected over a twelve-year period from three zones: upstream of uranium mines; around uranium mines; and downstream of the mines. Samples were analyzed for gross α-, β-activity and radionuclide concentrations. Gross α-activity exceeded the permissible level in almost every water sample. Both gross α- and β-activity in Baigekum village and PV-1 mine significantly exceeded safe levels throughout entire monitoring period. Concentrations of ^{230}Th and ^{210}Pb surpassed the national intervention levels in almost all water samples. In a number of samples from Baigekum village excessive concentration of ^{226}Ra was observed. Furthermore, water samples collected from Tabakbulak in the spring of 2009 had extremely high levels of radionuclides. In general, elevated levels of radionuclides had been observed around the uranium mines and down the stream of Syrdarya since 2008-2009 when industrial-level production started at Zarechnoye, Khorasan and Irkol uranium deposits. The results suggest that radioactive pollution of Syrdarya in Kazakhstan is primarily caused by uranium mining activities. It is likely that the Syrdarya waters are not only unpalatable for human, but it may also not be suitable for household and agricultural use due to radioactive pollution.

1. INTRODUCTION

Syrdarya is the longest river in Central Asia and its basin spreads across Tajikistan, Kyrgyzstan, Uzbekistan and Kazakhstan. It flows to the northern remnants of the Aral Sea through South Kazakhstan and Kyzylorda regions of Kazakhstan and plays a crucial role for regional economies. Heavy metal contamination of Syrdarya is of greatest emerging concern as contaminations in surface and groundwater exceed World Health Organization (WHO) drinking water guidelines (Kawabata et al., 2008; Friedrich, 2009). It was also determined that the Syrdarya waters could not be used for agriculture and household purposes (Besterekov, 2013). Furthermore, it was identified that health hazards are significantly higher in downstream surface waters in Central Asia (Törnqvist et al., 2011; Bekturganov et al., 2016). Particularly, water contamination caused by uranium mining poses health risks to the population around Syrdarya. The issue of surface water contamination by radionuclides is particularly important given notable cancer incidences and high maternal and child morbidity and mortality in South Kazakhstan and Kyzylorda regions (Igissinov et al., 2011; Zetterström, 1998; Turdybekova et al., 2015).

Currently, Kazakhstan is the world`s top uranium producer, with almost 40% of global production and as a result of a national program to become a world leader, production surged by more than 1000% during 2001-2013 (Kazatomprom, 2018). The share of uranium in total export increased from 1.6% in 2000 till 3.1% in 2012 and it was the 5th largest export commodity (Akhmetov, 2017). Kaztomprom is a national operator of the uranium market in Kazakhstan and it has subsoil use rights on uranium deposits (IAEA, 2016). The race to become the world's top uranium producer led to the environmental pollution (Arnoldy, 2013). Regional offices of the State Committee for Industrial and Mining Safety Supervision and the regional governments overlook adherence to the safety of the uranium mines (Conway, 2013; IAEA, 2016).

However, widespread corruption and rent-seeking undermine the integrity of environmental monitoring process (Conway, 2013).

Uranium mining in Kazakhstan is performed by in-situ leach (ISL), which is believed to be environmentally safe and cost effective method (Kazatomprom, 2018). However, it is known that ISL releases uranium, thorium, radium, radon and their respective progeny (Tweeton and Peterson, 1981; Kasper et al., 1979). The method also alters groundwater, causes spills of dangerous pollutants, contaminates aquifers and creates solid waste from excavations, injection and production wells (Fettus and McKinzie, 2012). Furthermore, surface pollution could be minimal, but underground impacts are significant (Mudd, 1998). ISL is employed in locations with different hydrochemical properties of groundwater. It has different effects on uranium compounds and they are not always advantageous for technological process.

Shu-Syrdarya uranium region, consisting of 15 deposits of commercial interest, has been the most important in Kazakhstan due to significant reserves (Fyodorov, 2000). Total reserves of Syrdarya uranium province consist of around 250 tons of uranium with the depth of uranium ore between 100-800 meters (World Nuclear Association, 2018; Fyodorov, 1997). The deposits are hosted by sandstones and characterized by high concentrations of rare and dispersed elements (Jaireth et al., 2008). It is possible that the ISL process could cause migration of radionuclides to the stem of Syrdarya (Kadyrzhanov et al., 2005).

It was identified that radioactivity levels in ground and wastewaters at the production sites exceed the national standards (Kayukov, 2008). Furthermore, it is likely that the uranium mining may have negative health effects on the nearby population (Bersimbaev and Bulgakova, 2015). Arnoldy (2013) and Conway (2013) suggested that Kazatomprom neglects environmental concerns related to ISL mining and considers investments in safety of operations as unnecessary capital costs and the operator also claims that nature will self-restore itself at the mining sites. Moreover, due to significant costs and low population density around mines, the need for treatment of contaminated waters has been considered unnecessary in the past (Fyodorov, 2000). Nevertheless, population density around Syrdarya is notable (CIESIN, 2016). On top of that, the river is the major source of irrigation in South Kazakhstan and Kyzylorda regions.

The regional economy of South Kazakhstan is primarily based on agriculture. Regional agricultural output contributes to 12% of the national agricultural production (Akhmetov, 2017). Almost 90% of rice in Kazakhstan is grown in Kyzylorda region. Hence, the quality of produced rice depends on pollution level of Syrdarya as the main source of water for rice farming. Moreover, acute and long-term health effects may occur due to water use for household purpose, drinking, boating, swimming, consumption of contaminated fish, etc.

The presence of radionuclides in Central Asian Rivers drew attention of scientists due to the history of radioecological problems in the former USSR. The three-year Navruz project was designed to bring together Kazakh, Uzbek, Tajik and Kyrgyz scientists to perform radioecological monitoring of Syrdarya and Amudarya rivers (Yuldashev et al., 2002; Yuldashev et al., 2005). The analysis of transboundary radionuclide contamination of Syrdarya was based on water samples from 60 monitoring sites (15 in each country) and analyzed for radiation readings, 71 radionuclides and heavy metals (Barber et al., 2005). The project concluded that radionuclide contamination of Syrdarya in Kazakhstan was caused by inflows from Uzbekistan, Keles and Arys river tributaries. Furthermore, the highest radionuclide concentrations were observed near Shieli uranium deposit in Kyzylorda region (Kadyrzhanov et al., 2005; Solodukhin et al., 2004).

Kawabata et al. (2008) investigated surface and drinking water at 21 sites in the Aral-Syrdarya area for uranium concentration during August, 2003. The results indicated that uranium concentration in drinking water samples from two sites with shallow wells exceeded WHO guidelines significantly (WHO, 2011), while the samples from deeper wells showed lower concentration of uranium. It was suggested that phosphate fertilizers and uranium mining were the sources of contamination.

Satybaldiyev et al. (2015) analyzed concentrations of ^{238}U, ^{234}U and ^{226}Ra radionuclides from 12 surface water samples collected along Syrdarya between the cities of Turkestan and Kyzylorda in May, 2013. Although all but one sample indicated uranium concentrations exceeding the WHO guideline level, it was concluded that they were within the level accepted for drinking water. It

was also suggested that the uranium mining does not affect the quality of Syrdarya waters.

Unfortunately, after management change at the national operator, independent research organizations were barred from collecting water and soil samples for investigation around active mines. Hence, no radioecological assessment studies after 2015 were carried out.

2. METHODOLOGY

Unlike previous studies, this analysis is based on longer period of sampling (2000-2012). Unfortunately, due to limited research budget, continual sampling could not be achieved and no samples were collected in 2010. The period after 2008-2009 is of particular interest due to commencement of production at Zarechnoye, Khorasan and Irkol uranium deposits. The objectives of this analysis are to assess the radioecological situation of Syrdarya, understand the migration and areas of accumulation of radionuclides. The samples are also analyzed for concentrations of 11 radionuclides. The research compares concentration of radionuclides and α- and β-radioactivity in samples with national norms of radiation safety. Given the national plans of uranium mining expansion, it is particularly important to understand the possible contribution of the existing uranium mines on radioactive pollution of Syradrya.

2.1 Study area

Zoning method in river water sampling is used to identify radionuclide contamination hazard prone areas (Salishev, 1987; Buksa and Myach, 1990). Following the stream of Syrdarya and location of uranium mines, three zones are defined:

1) Upstream of uranium producing mines (Chinaz and Shardara);

2) Near the mines (Tabakbulak, Shaulder, Tomenaryk, Rudoupravlenie-6 (RU-6) and Baigekum);

3) Settlements located after the mines, downstream of Syrdarya (Kyzylorda, Amangeldy and Amanotkel).

A total of 43 surface water samples were collected from Syrdarya at the following 13 sites from south to north-west: Chinaz, Shardara, Tabakbulak, Shaulder, Tomenaryk, Shieli, RU-6, PV-1, PV-2, Baigekum, Kyzylorda, Amangeldy, Amanotkel as seen in Figure 1.

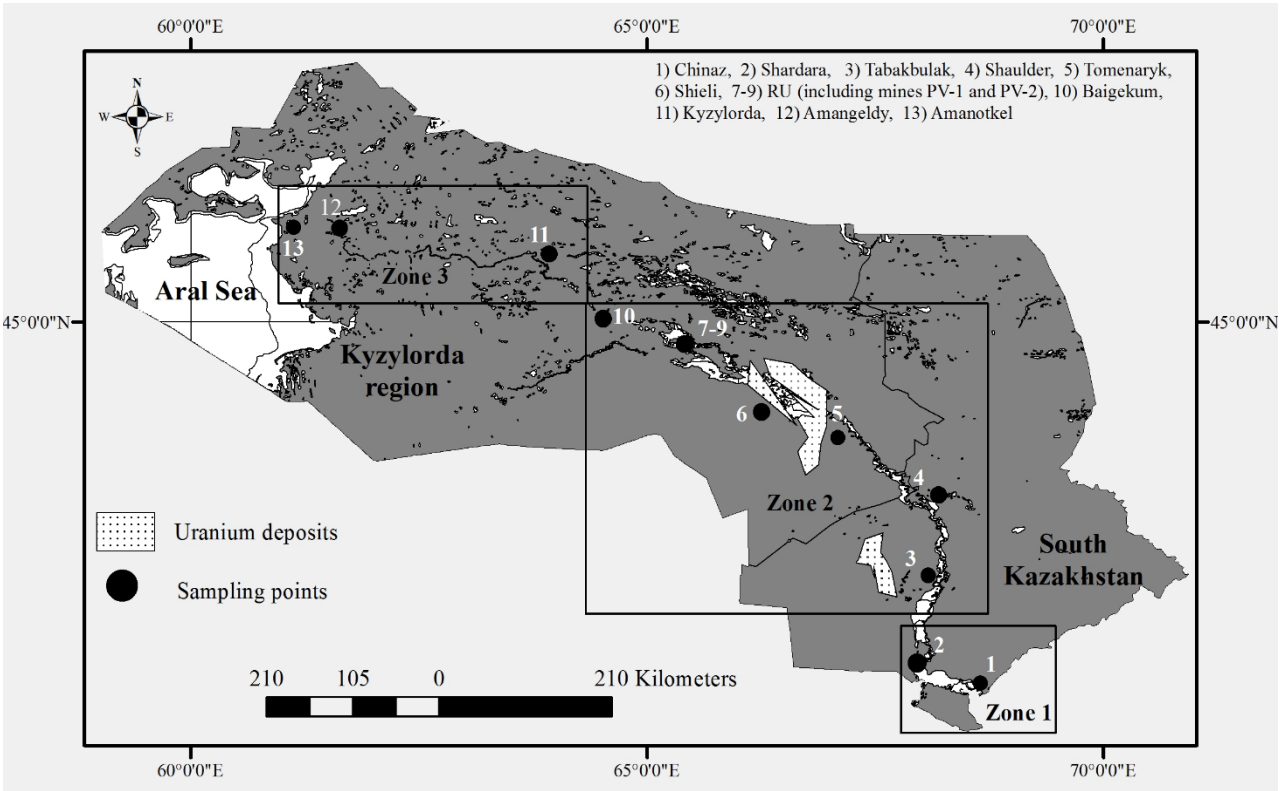

Figure 1. Idealized map of water sampling sites, location of zones and active uranium producing deposits

Chinaz is a town in Tashkent region of Uzbekistan, located on the confluence of Chirchiq and Syrdarya rivers. The reason for selecting this site is to analyze the Syrdarya water quality before the Shardara dam, while the samples from Shardara town in South Kazakhstan region aim to analyze water discharged from the reservoir. Shardara dam was constructed in the 1960s with the primary purpose of irrigation and hydropower production.

There are six main uranium producing deposits in the area. One is located in South Kazakhstan region, while others are in Kyzylorda region (World Nuclear Association, 2018). Zarechnoye uranium deposit is located in Otrar district of South Kazakhstan near Tabakbulak village, west of Syrdarya. Shaulder village is located 50 km east from the deposit on the banks of Syrdarya. Zarechnoye was prepared for industrial production in 1991. However, following the collapse of the USSR it was conserved. Preparation works to restart production started in 2006 and production reached 500 tons of uranium in 2009.

Northern and Southern Khorasan uranium deposits are located in Zhanakorgan district of Kyzylorda region, on the left bank of Syrdarya. Northern Khorasan is the largest uranium deposit in Kazakhstan, where test mining began in 2008 and commercial in 2013 Tomenaryk village is located north-east from this deposit on the banks of Syrdarya.

Irkol and Karamuryn uranium deposits are located in Shieli district of Kyzylorda region. RU-6, located in Shieli village, administers uranium production from Northern and Southern Karamuryn deposits. RU-6 is expected to sustain production of yellow cake at 1,000 tons/year for another 25 years. It is the oldest mine group of the uranium province, where production started in the 1980s, while mining at Irkol commenced in 2008. Baigekum village is located north-west from Shieli.

Kyzylorda city, Amangeldy and Amanotkel villages are located downstream of Syrdarya. Kyzylorda is a capital of Kyzylorda region with population of almost 200,000. Amangeldy and Amanotkel are the villages in Syrdarya district and Aral district respectively. Analysis in this area could help to understand the level of pollution downstream from uranium mines.

2.2 Sampling and analysis

Surface water samples were collected in accordance with the existing river water sampling method in Kazakhstan (VSEGINGEO, 1990). Samples were taken from the surface water layer (0.5-1 meter) of the river. The total volume of one sample comprised 20 liters. The samples were packed in polyethylene bottles and transported for analysis within 1-2 days to the certified laboratory at the Central Experience Methodical Expedition (CEME, 2018), where Total Dissolved Solids (TDS) in milligrams/liter (mg/L), gross α-, β-radioactivity and radionuclide concentrations were measured by UMF-2000 radiometer.

Then, the samples were evaporated to dryness and muffed for 1 hour at 350 ºC. Ethyl alcohol was added into porcelain dish as a solvent, residuals were removed from the walls of the cup and the solution was poured into a cuvette. The mixture was then dried under a lamp until homogeneous layer. An Ortec DSPEC LF spectrometer was used in accordance with the technique of measuring at the γ-spectrometer MI 2143-91 to determine radionuclide concentrations in the sample (VNNIIFTRI, 1991). Analyzed radionuclides are ^{226}Ra, ^{234Th}, ^{235}U, ^{227}Th, ^{223}Ra, ^{228}Th, ^{228}Ra, ^{40}K (Potassium-40), ^{210}Pb, ^{230}Th and ^{137}Cs. Gross α- and β-activity and radionuclide concentrations are compared with radiation safety norms in Kazakhstan presented in Table 1.

Table 1. Kazakh national intervention levels of radionuclides and permissible levels of gross α- and β-activity in water samples (Ministry of National Economy of Kazakhstan, 2015)

	Becquerel/liter (Bq/L)
^{226}Ra (Radium-226)	0.49
^{234}Th (Thorium-234)	40
^{235}U (Uranium-235)	2.9
^{227}Th (Thorium-227)	16
^{223}Ra (Radium-223)	1.4
^{228}Th (Thorium-228)	1.9
^{228}Ra (Radium-228)	0.2
^{210}Pb (Lead-210)	0.11
^{230}Th (Thorium-230)	0.65
^{137}Cs (Caesium-137)	11
Gross α-activity	0.2
Gross β-activity	1.0

3. RESULTS AND DISCUSSION

Results of this analysis indicate that TDS, gross α- and β-activity values are significantly high almost at every site as seen in Table 2. TDS tends to increase during ISL. Data indicates that average TDS is higher in spring and fall than in winter. It is lower upstream of the Shardara dam, increases when water is discharged from the reservoir, significantly higher around the mines and declines downstream. Extremely high values were observed at PV-1 and Tabakbulak in W2007 and S2009.

Overall gross α-radioactivity has declined over the years, but remained higher than the permissible level. Gross α-activity exceeds the permissible level in almost every sample, while gross β-activity exceeds in Baigekum (S2001, F2001, S2002), Kyzylorda (W2003), PV-1 (W2007) and Tabakbulak (S2009). Gross α- and β-activity is significantly high in the Baigekum and PV-1 mines throughout the entire observation period. The sample from Tabakbulak in S2009 exceeds safety norms for gross α- and β-activity 790 and 408 times respectively. Unlike TDS, gross α- and β-radioactivity do not follow seasonal variations. They have declined in Shardara, Tomenaryk, Shieli, RU-6, Baigekum and Kyzylorda, while the values have increased in Tabakbulak and PV-1 during the observation period. Moreover, in Shaulder gross α-activity has declined, while gross β-activity has increased.

Table 2. Gross α- and β-activity measurements (W-winter, S-spring and F-fall; samples exceeding intervention level are highlighted)

Season/year	Sample point	TDS (mg/L)	Gross α-activity (Bq/L)	Gross β-activity (Bq/L)
W2000	Shardara	1422	1.18±0.37	0.76±0.17
S2001	Chinaz	870	0.21±0.13	0.24±0.11
	Shardara	850	1.33±0.29	0.51±0.19
	Baigekum	1200	24.77	3.96
F2001	Baigekum	1600	20.59	3.51
W2002	PV-1	950	0.38	0.33
	RU-6	1740	0.76	0.68
S2002	Baigekum	2090	29.52	8.68
	Tomenaryk	420	1.58	0.52
	Kyzylorda	700	2.30	0.59
W2003	Kyzylorda	960	3.12	1.52
	PV-1	950	0.38	0.33
	RU-6	1740	0.76	0.68
S2003	Amanotkel	840	0.61	0.33
	Kyzylorda	950	0.46	0.33
W2004	PV-1	1950	0.39	0.45
	RU-6	950	0.20	0.54
S2005	Kyzylorda	940	0.17	0.38
	PV-1	1810	0.24	0.26
	PV-2	1770	0.31	0.26
W2006	Baigekum	590	0.08	0.25
S2006	Kyzylorda	910	0.29	0.57
	Tomenaryk	860	0.244	0.39
F2006	Baigekum	1450	0.50	0.57
W2007	RU-6	880	0.24	0.35
	PV-1	5330	1.39	2.11
	Tomenaryk	950	0.22	0.43

Table 2. Gross α- and β-activity measurements (W-winter, S-spring and F-fall; samples exceeding intervention level are highlighted) (cont.)

Season/year	Sample point	TDS (mg/L)	Gross α-activity (Bq/L)	Gross β-activity (Bq/L)
F2008	Baigekum	1910	0.222	0.104
	Shieli	1870	0.319	0.12
	Tabakbulak	2300	0.299	0.154
	Shaulder	2100	0.408	0.123
W2009	Baigekum	1620	0.63	0.249
	Shieli	1150	0.724	0.259
	Tabakbulak	2050	0.41	0.257
	Shaulder	2350	0.26	0.175
S2009	Tabakbulak	5230	158	408.1
	Baigekum	1680	1.69	0.706
	Shieli	2200	0.56	0.169
	Tomenaryk	1950	0.581	0.187
W2011	Shardara	1340	0.55	0.421
	Amangeldy	1069	0.54	0.482
W2012	Baigekum	860	0.47	0.182
	Shieli	1430	0.20	0.074

Radionuclide concentrations in samples are presented in Table 3. It is likely that the main contribution to radioactivity comes from the decay products of ^{238}U, ^{235}U and ^{232}Th. ^{226}Ra, ^{228}Ra ^{210}Pb and ^{234}Th are the decay products of the radionuclides. Decay chains of parent isotopes also contain radon gas and another contributing radionuclide is ^{40}K. Furthermore, ^{226}Ra, ^{234}Th and ^{40}K tend to migrate faster than others.

The results indicate that concentrations of ^{230}Th and ^{210}Pb significantly exceed the national intervention levels in almost all samples. Although ^{235}U concentration from Tabakbulak (S2009) was close to intervention level, concentrations of ^{235}U, ^{228}Th and ^{137}Cs have never exceeded safe levels. The concentration of ^{226}Ra significantly exceeded intervention levels in Baigekum (S2001, S2002, S2009) and Tabakbulak (S2009) by 4.7, 9.1, 1.3 and 108.6 times respectively. The latter sample also had excessive concentrations of ^{234}Th, ^{227}Th, ^{223}Ra, ^{228}Ra, ^{210}Pb and ^{230}Th. Samples from Shardara (W2011), Amangeldy (W2011), Baigekum (W2012) and Shieli (W2011) had excessive concentrations of ^{228}Ra.

In general, water inflows with elevated levels of radioactivity and radionuclide concentrations from Uzbekistan enters Shardara dam, where polluted water is accumulated and later discharged. Discharge of uranium mining effluents occurs further downstream around the mines. Polluted waters are observed downstream from the mines and eventually inflow into the Aral Sea. It should be noted that lack of continuous sampling is a major limitation of this study.

Radioecological monitoring of Syrdarya around uranium mines is currently performed by subsidiaries of the national operator, which undermines the integrity of the process. In the future, outside research organizations should be allowed to collect and analyze water and soil samples to verify independently the results of internal monitoring. Moreover, further research is needed to assess health impacts related to radiological pollution of Syrdarya.

Table 3. Radionuclide concentrations analysis (samples exceeding intervention level are highlighted)

		Radionuclide concentrations, Bq/L										
		^{226}Ra	^{234}Th	^{235}U	^{227}Th	^{223}Ra	^{228}Th	^{228}Ra	^{40}K	^{210}Pb	^{230}Th	^{137}Cs
W2000	Shardara	0.071	0.12	0.01	-	-	<0.008	<0.019	0.18	0.17	-	<0.006
S2001	Chinaz	<0.015	<0.08	<0.008	-	-	<0.01	<0.03	0.19	-	-	<0.08
	Shardara	0.13	<0.06	<0.013	-	-	<0.016	<0.05	0.18	-	-	<0.014
	Baigekum	2.29	1.49	0.014	-	-	<0.028	<0.06	0.18	-	-	0.016
F2001	Baigekum	0.021	-	-	<0.036	<0.02	0.009	0.02	0.26	-	-	<0.007
W2002	PV-1	0.047	-	-	-	-	<0.011	0.031	0.21	-	-	<0.009
	RU-6	0.062	-	-	-	-	<0.033	<0.041	<0.18	-	-	<0.02
S2002	Baigekum	4.47	0.94	0.08	0.09	0.24	0.06	0.012	0.4	1.17	<4.11	<0.031
	Tomenaryk	0.21	<0.05	<0.07	<0.06	<0.05	<0.018	<0.06	<0.23	<0.09	<1.39	<0.014
	Kyzylorda	0.19	0.168	0.016	<0.08	<0.07	0.023	<0.08	<0.20	<0.19	<2.3	<0.02
W2003	Kyzylorda	0.45	-	-	0.074	0.067	<0.032	<0.08	<0.27	-	-	<0.028
	PV-1	0.047	-	-	<0.001	<0.001	<0.011	0.031	0.21	-	-	<0.009
	RU-6	0.062	-	-	<0.002	<0.002	<0.033	<0.041	<0.18	-	-	<0.015
S2003	Amanotkel	<0.008	0.113	-	<0.032	<0.032	<0.01	0.028	0.14	<0.078	<0.83	-
	Kyzylorda	0.021	0.12	-	<0.025	<0.025	<0.008	<0.022	0.17	<0.062	<0.69	<0.006
W2004	PV-1	0.028	0.13	-	<0.047	<0.035	<0.013	0.047	0.14	<0.72	<1.8	<0.009
	RU-6	0.164	<0.09	-	<0.053	<0.04	<0.009	0.041	0.21	<0.81	<2.2	<0.01
S2005	Kyzylorda	<0.015	0.14	0.0083	-	-	<0.0101	<0.036	0.21	<0.058	<0.69	<0.008
	PV-1	<0.014	<0.058	<0.0066	-	-	<0.0071	<0.032	<0.13	<0.06	<0.73	<0.008
	PV-2	<0.014	0.065	0.0063	-	-	<0.0095	<0.024	<0.15	<0.061	<0.75	<0.008
W2006	Baigekum	0.011	0.057	<0.0085	-	-	0.013	<0.034	<0.13	<0.05	<0.58	0.008
S2006	Kyzylorda	0.019	0.109	<0.009	-	-	0.043	<0.049	0.2	<0.055	<0.87	<0.011
	Tomenaryk	0.024	0.072	0.0076	-	-	0.01	<0.049	<0.21	<0.062	<0.78	<0.013
F2006	Baigekum	<0.034	<0.14	<0.0121	-	-	<0.0265	<0.085	<0.37	<0.161	<1.7	<0.022
W2007	RU-6	0.017	0.122	0.0079	-	-	<0.0061	<0.024	<0.1	<0.038	<0.43	<0.006
	PV-1	0.062	0.191	<0.021	-	-	0.0279	<0.132	1.22	<0.228	<2.55	<0.034
	Tomenaryk	0.013	0.158	0.0013	-	-	0.009	<0.021	<0.09	<0.035	<0.39	<0.005
F2008	Baigekum	<0.06	0.17	<0.017	-	-	<0.03	<0.12	<6.0	<0.27	<2.2	<0.45
	Shieli	<0.05	0.16	0.016	-	-	<0.029	<0.11	<6.0	<0.26	<2.1	<0.4
	Tabakbulak	0.078	0.12	<0.015	-	-	<0.035	<0.13	<6.0	<0.23	<2.3	<0.4
	Shaulder	0.036	0.23	0.017	-	-	<0.023	<0.12	<5.0	<0.23	<2.3	<0.45

Table 3. Radionuclide concentrations analysis (samples exceeding intervention level are highlighted) (cont.)

		Radionuclide concentrations, Bq/L										
		^{226}Ra	^{234}Th	^{235}U	^{227}Th	^{223}Ra	^{228}Th	^{228}Ra	^{40}K	^{210}Pb	^{230}Th	^{137}Cs
W2009	Baigekum	0.039	0.25	0.0184	-	-	0.033	<0.06	<6.0	<0.14	<1.2	<0.45
	Shieli	0.05	0.23	0.019	-	-	0.021	<0.11	<6.0	<0.25	<2.1	<0.45
	Tabakbulak	0.046	0.18	<0.019	-	-	<0.024	<0.11	<6.0	<0.27	<2.3	<0.4
	Shaulder	0.054	<0.12	<0.018	-	-	<0.035	<0.11	<6.0	<0.18	<2.0	<0.45
S2009	Tabakbulak	53.2	67.9	1.19	30.6	25.3	0.93	<2.6	<7.0	124.0	372	<0.6
	Baigekum	0.638	0.27	<0.026	<0.12	<0.11	0.033	<0.12	<6.0	<0.29	<2.5	<0.4
	Shieli	0.045	0.26	0.015	<0.11	<0.1	0.033	<0.11	<6.0	<0.23	<2.2	<0.4
	Tomenaryk	<0.05	0.17	0.015	<0.11	<0.1	0.031	<0.11	<6.0	<0.26	<2.1	<0.4
W2011	Shardara	0.12	0.26	<0.04	<0.07	<0.022	-	<0.25	<6.0	<0.5	<4.0	<0.4
	Amangeldy	<0.10	0.25	<0.04	<0.06	<0.024	-	<0.24	<6.0	<0.5	<4.5	<0.4
W2012	Baigekum	<0.06	0.23	<0.023	<0.16	<0.16	<0.045	<0.25	<3.0	<0.4	<3.5	<0.19
	Shieli	0.07	0.25	<0.024	<0.06	<0.16	<0.06	<0.24	<4.0	<0.4	<3.5	<0.3

4. CONCLUSIONS

The uranium industry has become an important source of income for the resource-export oriented Kazakh economy. Expansion of production likely leads to radioactive pollution of Syrdarya. The results of this study indicate that both inflow and outflow water samples from Shardara dam contain elevated levels of radioactivity. However, it is likely that most radioactive water pollution of the Kazakh part of the Syrdarya river basin occurs around active uranium mines.

This twelve-year monitoring of Syrdarya indicates that gross α-activity exceeds permissible level in almost every water sample throughout the entire observation period. Gross β-activity is higher around the Karamuryn uranium deposit, while commencement of production at Zarechnoye likely caused extremely high gross α-, β-activity and radionuclide concentrations in water sample from Tabakbulak in 2009. In general, it is most likely that elevated levels of radionuclide concentrations in samples from sites around mines and downstream of the river in 2008-2009 and onwards are caused by expansion of uranium production.

Based on WHO drinking water guidelines (WHO, 2011), it could be said that water from Syradarya is unpalatable due to excessive TDS and dangerous radionuclide concentrations. Likewise, it is possible that the river water is not suitable for household and agriculture use. There is growing evidence that uranium production in the region causes radioactive pollution of Syrdarya. Hence, there is an urgent need to thoroughly assess the safety and environmental effects of ISL technology in Kazakhstan.

REFERENCES

Akhmetov A. Testing the presence of the Dutch disease in Kazakhstan. Munich Personal RePEc Archive (MPRA) Paper 77936; 2017.

All-Russian Research Institution of Physicotechnical and Radiotechnical Measurements (VNIIFTRI). Measurement procedure on gamma spectrometer. Moscow, USSR: VNNIIFTRI; 1991. (in Russian)

All-Union Research Institution of Hydrogeology and Geological Engineering (VSEGINGEO). Methodological recommendations on sampling, processing and storage of groundwater. Moscow, USSR: MinGeo USSR; 1990. (in Russian)

Arnoldy B. The cost of being the world's No. 1 uranium producer. The Christian Science Monitor [Internet]. 2013 [cited 2018 Apr]. Available from: https://www.csmonitor.com/World/Asia-South-Central/2013/0828/The-cost-of-being-the-world-s-No.1-uranium-producer.

Barber DS, Betsil JD, Mohagheghi AH, Passel HD, Yuldashev B, Salikhbaev U, Djuraev A, Vasiliev I, Solodukhin V. The Navruz experiment: cooperative monitoring for radionuclides and metals in Central Asia transboundary rivers. Journal of Radioanalytical and Nuclear Chemistry 2005;263(1):213-8.

Bekturganov Z, Tussupova K, Berndtsson R, Sharapatova N, Aryngazin K, Zhanasova M. Water related health problems in Central Asia: a review. Water 2016; 8(6):1-13.

Bersimbaev RI, Bulgakova O. The health effects of radon and uranium on the population of Kazakhstan. Genes and Environment 2015;37(18):1-10.

Besterekov U. Transboundary water pollution of the Syrdarya river by heavy metals. Proceedings of the Conference Dedicated to 70th Anniversary of South Kazakhstan State University named after M. Auezov; 2013 Oct 25-26; South Kazakhstan State University named after M. Auezov, Shymkent: Kazakhstan; 2013:190-5. (in Russian)

Buksa II, Myach, LT. Assessment of modern and future state of the environment. Moscow, USSR: Hydrometeoizdat; 1990. (in Russian)

Central Experience Methodical Expedition (CEME). Chemicoanalytical expedition [Internet]. 2018 [cited 2018 Apr]. Available from: http://www.come.kz/page/part/19. (in Russian)

Center for International Earth Science Information Network (CIESIN). Documentation for the Gridded Population of the World. Version 4 (GWP v4). Palisades, NY, USA: NASA-Socioeconomic Data and Applications Center; 2016.

Conway JE. The risk is in the relationship (not the country): political risk management in the uranium industry in Kazakhstan. Energy Policy 2013;56:201-9.

Fettus GH, McKinzie MG. Nuclear fuel's dirty beginnings: environmental damage and public health risks from uranium mining in the American West; Mar 2012; Natural Resources Defense Council; 2012.

Friedrich J. Uranium contamination of the Aral sea. Journal of Marine Systems 2009:76:322-35.

Fyodorov GV. Industrial types of uranium deposits in Kazakhstan. Proceeding of the IAEA-OECD Technical Committee Meeting on Assessment of Uranium Deposit Types and Resources - A Worldwide Perspective; 1997 Jun 10-13; IAEA-OECD, Vienna: Austria; 1997:77-83.

Fyodorov GV. Uranium production and the environment in Kazakhstan. Proceeding of the International Symposium on the Uranium Production Cycle and the Environment; 2000 Oct 2-6; IAEA-OECD, Vienna: Austria; 2000:191-8.

International Atomic Energy Agency (IAEA). In situ leach uranium mining: an overview of operations. Vienna, Austria: IAEA; 2016.

Igissinov N, Igissinov S, Moore MA, Shaidarov M, Tereshkevich D, Bilyalova Z, Igissinova G, Nuralina I, Kozhakhmetov S. Trends of prevalent cancer incidences in the Aral-Syr Darya ecological area of Kazakhstan. Asian Pacific Journal of Cancer Prevention 2011;12(9):2299-303.

Jaireth S, McKay A, Lambert I. Association of large sandstone uranium deposits with hydrocarbons: the geology of uranium deposits in Kazakhstan points to similar deposits in Australia. Australian Government Geoscience Australia 2008;89:1-6.

Kadyrzhanov KK, Barber DS, Solodukhin VP, Poznyak VL, Kazachevskiy IV, Knyazev BB, Lukashenko SN, Khazhekber S, Betsill JD, Passell HD. Radionuclide contamination in the Syrdarya river basin of Kazakhstan: results of the Navruz project. Journal of Radioanalytical and Nuclear Chemistry 2005; 263(1):197-205.

Kasper DR, Martin HW, Munsey LD, Bhappu RB, Chase CK. Environmental Assessment of In Situ Mining; Dec 1979; United States Department of the Interior Bureau of Mines; Open File Report 101-80;1979.

Kawabata Y, Aparin V, Nagai M, Yamamoto M, Shiraishi K, Katayama Y. Uranium and thorium isotopes from Kazakhstan. Journal of Radioanalytical and Nuclear Chemistry 2008;278(2):459-62.

Kayukov PG. Ecological considerations related to uranium exploration and production. In: Salbu B, Skipperud L, editors. Nuclear Risks in Central Asia. Dordrecht, Netherlands: Springer; 2008. p. 219-23.

Kazatomprom. National Atomic Company of the Republic of Kazakhstan [Internet]. 2018 [cited 2018 Apr]. Available from: http://www.kazatomprom.kz/en

Ministry of National Economy of Kazakhstan. Sanitary-epidemiological requirements for radiation safety assurance; 2015 Feb 27; Decree 155; 2015. (in Russian)

Mudd G. An environmental critique of in situ leach mining: the case against uranium solution mining; Jul 1998; A Research Report for Friends of the Earth (Fitzroy) with the Australian Conservation Foundation; 1998.

Salishev KA. Development of maps. Moscow, USSR: MGU; 1987. (in Russian)

Satybaldiyev B, Tuovinen H, Uralbekov B, Lehto J, Burkitbayev M. Heavy metals and natural radionuclides in the water of Syr Darya River, Kazakhstan. In: Merkel B, Arab A, editors. Uranium - Past and Future Challenges. Proceedings of the 7th International Conference on Uranium Mining and Hydrogeology. Cham, Germany: Springer; 2015. p. 155-60.

Solodukhin VP, Poznyak VL, Kazachevskiy IV, Knyazev BB, Lukashenko SN, Khazhekber S. Some peculiarities of the contamination with radionuclides and toxic elements of the Syrdarya river basin, Kazakhstan. Journal of Radioanalytical and Nuclear Chemistry 2004;259(2):245-50.

Törnqvist R, Jarsjö J, Karimov B. Health risks from large-scale water pollution: trends in Central Asia. Environment International 2011;37(2):435-42.

Turdybekova YG, Dosmagambetova RS, Zhanabayeva SU, Bublik GV, Kubayev AB, Ibraibekov ZG, Kopobayeva IL, Kultanov BZ. The health status of the reproductive system in women living in the Aral Sea region. Open Access Macedonian Journal of Medical Sciences 2015:3(3):474-7.

Tweeton DR, Peterson KA. Selection of lixiviants for in situ leach mining. In Situ Mining Research. Information Circular 8852. Bureau of Mines Technology Seminar; 1981 Aug 5; United States Department of the Interior, Bureau of Mines, Denver: USA; 1981.

World Health Organization (WHO). Guidelines for drinking-water quality, 4th edition. Geneva, Switzerland: WHO; 2011.

World Nuclear Association. Uranium and nuclear power in Kazakhstan (Updated February 2018) [Internet]. 2018 [cited 2018 Apr]. Available from: http://www.world-nuclear.org/information-library/country-profiles/countries-g-n/kazakhstan.aspx

Yuldashev B, Salikhbaev U, Radyuk R, Djuraev A, Djuraev A, Vasiliev I, Tolongutov B, Alekhina V, Solodukhin V, Pozniak V, Littlefield AC. The Navruz project: Monitoring for radionuclides and metals in Central Asia transboundary rivers. End of year one reports, 2002 Sep. New Mexico, USA: Sandia National Laboratories; 2002.

Yuldashev BS, Salikhbaev US, Kist AA, Radyuk RI, Barber DS, Passell HD, Betsill JD, Matthews R, Vdovina ED, Zhuk LI, Solodukhin VP, Poznyak VL, Vasiliev IA, Alekhina VM, Djuraev AA. Radioecological monitoring of transboundary rivers of the Central Asian region. Journal of Radioanalytical and Nuclear Chemistry 2005;263(1):219-28.

Zetterström R. Food pollutants and child health with special reference to the situation in the Aral Sea region in Kazakhstan. Näringsforskning 1998;42(1):130-5.

Activity of Carbon-Based Solid Acid Catalyst Derived from Palm Empty Fruit Bunch for Esterification of Palmitic Acid

Indika Thushari and Sandhya Babel*

Sirindhorn International Institute of Technology, Thammasat University, Pathum Thani 12120, Thailand

ARTICLE INFO

Received: 7 Jul 2018
Received in revised:
15 Aug 2018
Accepted: 24 Aug 2018
Published online:
8 Oct 2018
DOI: 10.32526/ennrj.17.1.2019.06

Keywords:
Carbon-based solid acid catalyst/ Direct sulfonation/ Esterification/ Palmitic acid/ Palm empty fruit bunch

*** Corresponding author:**
E-mail: sandhya@siit.tu.ac.th

ABSTRACT

The activity of a heterogeneous solid acid catalyst derived from palm empty fruit bunch, synthesized through the direct in-situ H_2SO_4 impregnation was investigated for the esterification of palmitic acid. The prepared catalyst was characterized by scanning electron microscopy (SEM), Nitrogen adsorption and desorption isotherm, Fourier transform infrared spectroscopy (FT-IR), X-ray photoelectron spectroscopy (XPS), and thermogravimetric analysis (TGA). It was also analyzed for acid density and elemental composition. The results revealed that the esterification efficiency increases with increasing reaction time, temperature, and methanol loading up to an optimum value. The catalyst showed an excellent activity resulting in >98% esterification efficiency using 5 wt% catalyst, a 6:1 methanol to palmitic acid molar ratio, at 80°C for 5 h in an open reflux reactor, for the reaction conditions. The catalyst was employed in three consecutive runs without considerable loss of the activity. The obtained high catalytic activity is attributed to the high acid density due to the presence of strong (SO_3H) and weak (COOH, OH) acid sites in the hydrophobic carbon structure.

1. INTRODUCTION

Biodiesel can be produced from the transesterification of triglycerides and esterification of fatty acids with alcohols using acid or alkaline catalysts. However, alkaline catalyzed trans-esterification is challenging in the presence of a high free fatty acids (FFA) content in feedstocks. An alkaline catalyst produces soap with FFA, making the biodiesel production more complex and expensive (Su and Guo, 2014). Therefore, it is necessary to neutralize the FFA in the acidic feedstocks for conventional biodiesel production.

Homogeneous acid catalysts have been widely used in acid catalyzed reactions, such as the esterification or pre-treatment of acidic feedstocks. However, difficulty in catalyst separation, recycling, and waste treatment has encouraged researchers to use solid acid catalysts (SACs) for the esterification or pre-treatment of acidic feedstocks (Su and Guo, 2014). Commercially available SACs, such as sulfated metal oxides (Zhang et al., 2017), ion exchange resin (Fu et al., 2015), and heteropolyacid (Han et al., 2016) are favorable for biodiesel production. However, the activity of these SACs is very low compared to the homogeneous acid catalysts. In addition, low stability, high cost, and the possible environmental damage make their use less popular in biodiesel production (Dehkhoda, 2010). Therefore, the demand for the development of novel, economical, and sustainable SACs with high activity and stability is increasing. Carbon-based SACs have gained much interest in esterification due to various advantages; they can eliminate further washing and neutralization steps while increasing the catalyst reusability (Nakajima et al., 2007; Su and Guo, 2014). Also, they can be derived from various types of low-cost carbon precursors, such as agricultural and industrial wastes (Bennett et al., 2016; Fu et al., 2013; Konwar et al., 2014; Ngaosuwan et al., 2016; Savaliya and Dholakiya, 2015) via economical and sustainable methods. Various types of carbon-based SACs have been developed and successfully employed for esterification. A coffee residue based SAC was used by Ngaosuwan et al. (2016) for the esterification of caprylic acid. Bamboo (Zhou et al., 2016), banana peel (Liu et al., 2015), rice husk (Zeng et al., 2016) derived SACs were used for the esterification of oleic acid. Thailand produces an extensive amount of agricultural waste biomass (Visvanathan and Chiemchaisri, 2008). Therefore, this study attempts to develop a promising SAC from the abundant agricultural waste biomass in Thailand for the esterification of palmitic acid.

Palm empty fruit bunch (PEFB), which is an easily obtainable agricultural waste biomass in Thailand, was used for the preparation of a SAC via a simple and economical method (Thushari and Babel, 2018). In this study, the activity of the prepared PEFB-based SAC was investigated for the esterification of palmitic acid. The effects of reaction time, temperature, and methanol loading on the esterification efficiency and the reusability of the catalyst were explored.

2. METHODOLOGY

2.1 Materials

All chemicals were of analytical grade. Ethanol (C_2H_6O, Wako), methanol (CH_4OH, Wako), palmitic acid (CH_3 $(CH_2)_{14}COOH$, Wako), potassium hydroxide (KOH, Wako), and sulfuric acid (H_2SO_4, Wako) were used as received.

2.2 Preparation of PEFB-DS-SO_3H catalyst

The PEFB-based SAC was prepared by the direct in-situ concentrated H_2SO_4 acid impregnation method, as reported in Thushari and Babel (2018). In a typical procedure, the ground PEFB powder (average particle size <500 microns) was dried in an oven (FED 115, BINDER) at 110°C for 5 h. The oven dried PEFB powder (10 g) and concentrated H_2SO_4 acid (50 g) were then mixed in a flat glass beaker on a hot plate (C-MAG HS7, IKA) at 100°C for 1 h to facilitate in-situ incomplete sulfuric carbonization. After 24 h following the sulfuric carbonization, the reaction mixture was diluted, filtered, and repeatedly washed with hot distilled water using vacuum filtration until the pH of the filtrate was neutral. Then, the obtained black residue was dried in an oven at 120°C for 2 h and denoted as PEFB-DS-SO_3H. The prepared PEFB-DS-SO_3H catalyst was stored in an airtight container before using for esterification.

2.3 Characterization of PEFB-DS-SO_3H catalyst

Properties of the prepared catalyst were investigated using the standard methods, as reported in Thushari and Babel (2018). The total acid density was measured by standard acid-base back titration, following Dehkhoda (2010). The elemental composition of the catalyst was determined by energy dispersive X-ray spectroscopy (EDS) (S-3400 N, HITACHI) using EDAX Genesis software and a CHNS/O analyzer (628 series, Leco Corporation). N_2 adsorption and desorption isotherm data at -196°C (BELSORP miniII, Japan) were used to investigate the surface area, pore volume, and pore size distribution of the catalyst. Surface morphology of the PEFB-DS-SO_3H catalyst was examined by a scanning electron microscope (SEM) (VE-8800, Keyence, Japan). Fourier transform infrared spectroscopy (FT-IR) (610, Jasco) with attenuated total reflectance technique was used to investigate the functional groups present on the surface of the catalyst. The chemical states of the functional groups were analyzed by X-ray photoelectron spectroscopy (XPS) (PH15000 Versa Probe II @ Ulvac- PHI Inc, Japan) with Al Ka radiation. The thermal stability of the catalyst was analyzed by thermogravimetric analysis (TGA/DSC3 +HT/1600/219) under an N_2 flow (25 mL/min) at 25-900°C.

2.4 Evaluation of catalytic activity

The activity of the PEFB-DS-SO_3H was investigated for the esterification of palmitic acid with methanol, in a 250-mL round bottom flask equipped with a reflux condenser and a thermometer on a hot plate with a magnetic stirrer. Palmitic acid (10 g), PEFB-DS-SO_3H catalyst (0.5 g), and methanol were loaded into the reactor. The esterification efficiency was investigated using a different reaction temperature (40, 60, and 80°C), time (1, 2, 3, 4, and 5 h), and methanol:palmitic acid molar ratio (2:1, 4:1, 6:1, and 8:1). Upon completion of the reaction after the desired time, used catalysts were separated for reuse by vacuum filtration using a suction filtration kit, washed with ethanol, and oven dried for 2 h at 105°C. Excess methanol in the final product was removed by evaporation at 80°C in a water bath. All of the experiments were conducted in duplicate, and the average values were reported and discussed.

The esterification efficiency of the catalysts was determined using the following equation:

$$\text{Esterification efficiency (\%)} = \frac{(AV_0 - AV_1)}{AV_1} \times 100 \quad (1)$$

Where, AV_0 and AV_1 are the acid values (mg KOH/g) of the feedstock and the final product, respectively.

The acid value of the reaction medium was measured by titration following the Guabiao (GB) standard test method (The National Standard of the

People's Republic of China, 2005). In a typical procedure, about 0.5 g of the sample was vigorously dissolved in 50 mL of ethanol by heating the mixture for 10 min. Then, the resultant mixture was titrated against 0.1 M KOH solution.

3. RESULTS AND DISCUSSION

3.1 Characterization of PEFB-DS-SO_3H catalyst

As found from the CHNS/O analyzer, the elemental analysis reveals the presence of carbon, hydrogen, nitrogen, oxygen, and sulfur in the PEFB-DS-SO_3H catalyst (Table 1). Results showed that the elemental composition changes in the catalyst, compared to the original PEFB. Carbonization and activation of biomass in the presence of concentrated H_2SO_4 increase the carbon and sulfur content of the catalyst. Dehydration and de-oxygenation during carbonization decrease the hydrogen and oxygen contents of the catalyst. Similar phenomena are reported by Zhou et al. (2016) and Malins et al. (2016) during the preparation of a carbon-based SAC using bamboo and cellulose.

Table 1. Elemental composition of PEFB-DS-SO_3H catalyst

	C (wt%)	H (wt%)	N (wt%)	O (wt%)	S (wt%)	O:C
Raw PEFB	44.18	5.08	0.58	39.75	0.21	0.89
PEFB-DS-SO_3H	58.20	2.23	0.37	31.02	1.10	0.53

The total acid density of the PEFB-DS-SO_3H catalyst was found to be 5.4 mmol/g (Thushari and Babel, 2018). Three acid groups, SO_3H, COOH, and OH, contributed to the total acid density of the biomass-derived SACs (Nakajima et al., 2007; Su and Guo, 2014). The presence of a large amount of sulfonic acid groups is important as they are directly involved in catalyzing the esterification. As mentioned by Hara (2010), the hydrophilic COOH and OH groups present in the carbon framework enhance the catalytic activity by acting as the anchoring sites for the reactants. Therefore, the presence of a high density of both strong (SO_3H) and weak (COOH and OH) acid groups promotes the catalytic activity.

Figure 1 shows the FT-IR spectra of raw PEFB, PEFB-DS-SO_3H, and the used catalyst after the first run. The presence of functional groups (on the surface of the catalyst), which are responsible for esterification, was confirmed by FT-IR analysis (Thushari and Babel, 2018). As shown in Figure 1, the strong and broad peak at 3,600-2,800 cm^{-1} is attributed to the alcoholic or phenolic OH (Coates, 2000) in the raw PEFB, PEFB-DS-SO_3H, and the used catalyst. FT-IR spectra showed that the intensity of the peak decreases with the activation of biomass due to deoxygenation and dehydration. The decrease of the peak intensity after the first run may be due to the hydration of the catalyst. The peak present at around 1,800-1,500 cm^{-1} is attributed to the carbonyl/carboxyl region of COOH (Allen et al., 2007). According to Coates (2000), the peak at around 1,700 cm^{-1} may be assigned to SO_3H (1712 cm^{-1}). As can be seen in Figure 1, this peak is only conspicuous in the catalysts, confirming the presence of SO_3H after the activation. The intensity of the peak at around 1,700 cm^{-1} remains unchanged after the first run, showing the stability of the active SO_3H groups in the catalyst. The sharp and strong stretching peak at around 1,230-1,120 cm^{-1} is attributed to the S=O group which is from the sulfonic acid or sulfonate ion or O=S=O symmetric and asymmetric stretching vibrations of SO_3H, which is conspicuous in the catalysts produced after the sulfonation of incompletely carbonized biomass (Fu et al., 2012).

The XPS of PEFB-DS-SO_3H clearly reveals the peaks corresponding to the S2p, C1s, and O1s at 168 eV, 284 eV, and 530 eV binding energy, respectively (Russo et al., 2014; Thushari and Babel, 2018), confirming the presence of chemically bound SO_3H, COOH, and OH functional groups in line with the FT-IR results.

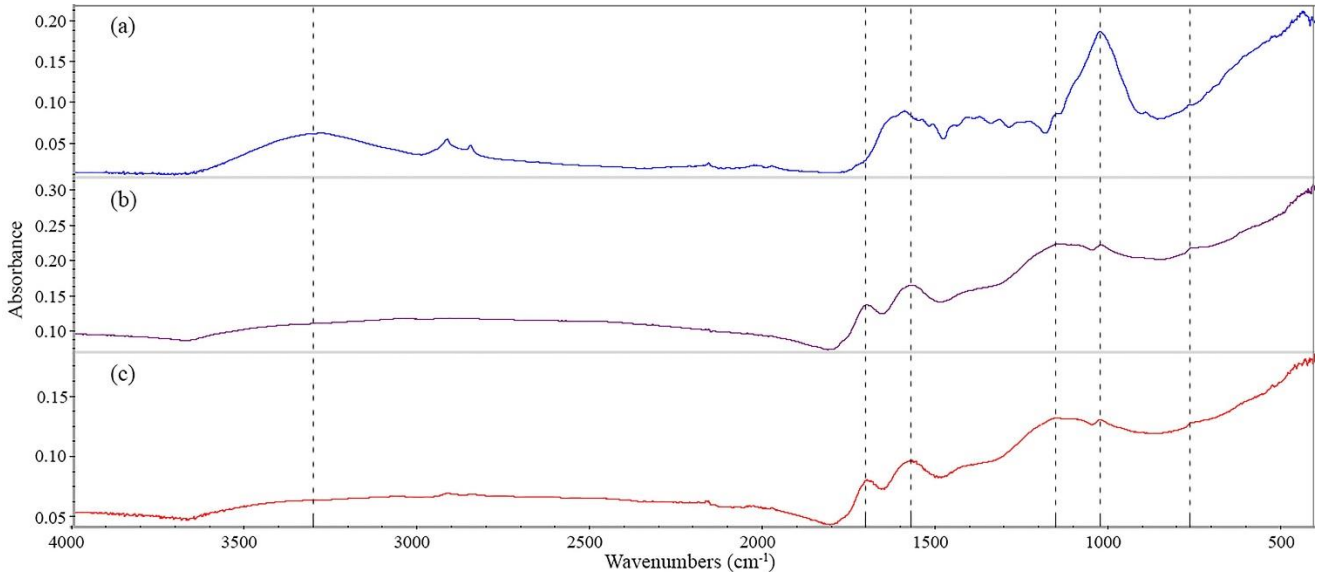

Figure 1. FT-IR spectrum of (a) Raw PEFB, (b) PEFB-DS-SO_3H catalyst, and (c) used catalyst after the 1st run (remark: (a) and (b) were taken from Thushari and Babel (2018))

Table 2 shows the surface area, pore volume, and diameter of the fresh catalyst and used catalyst after the third run. Results showed that the surface area of the catalyst decreases from 5.5 to 3.0 m^2/g after the third run. The relatively small surface area and pore volume of PEFB-DS-SO_3H catalysts may be due to the accumulation of SO_3H groups. Accumulation of products, by-products, and intermediates in the pores decreases the surface area and volume in the reused catalysts.

Table 2. Microstructural properties of PEFB-DS-SO_3H

	Surface area (m^2/g)	Mean pore volume (cm^3/g)	Pore diameter (nm)
PEFB-DS-SO_3H catalyst	5.5	0.13	17.0
Used catalyst (after 3rd run)	3.0	0.07	17.5

The nitrogen adsorption and desorption isotherms of the catalyst were found to be type III and/or type IV. This indicates the presence of nonporous and mesoporous phases of the catalyst, as confirmed by SEM (Brunauer et al., 1938; Thushari and Babel, 2018).

The TGA spectrum of PEFB-DS-SO_3H is shown in Figure 2. The low-temperature weight loss is below 200°C and the high-temperature weight loss is from 200 to 900°C. The small weight loss in the low-temperature range is due to the evaporation of absorbed water from the catalyst (Fu et al., 2012). Since the thermal degradation of the catalyst starts after 200°C, the reaction temperature should be below 200°C to achieve a maximum catalytic activity.

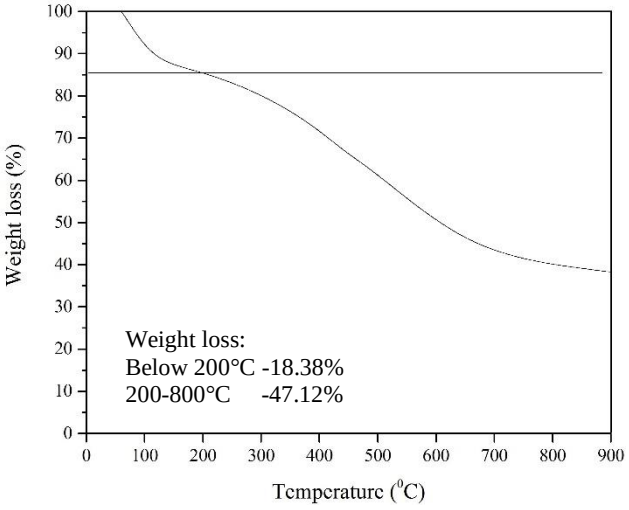

Figure 2. TGA of PEFB-DS-SO_3H catalyst

3.2 Evaluation of catalytic activity

The activity of the PEFB-DS-SO_3H catalyst for esterification is shown by a decrease in the acid value of the palmitic acid feedstock. The reaction scheme of the esterification of palmitic acid with methanol is depicted in Figure 3.

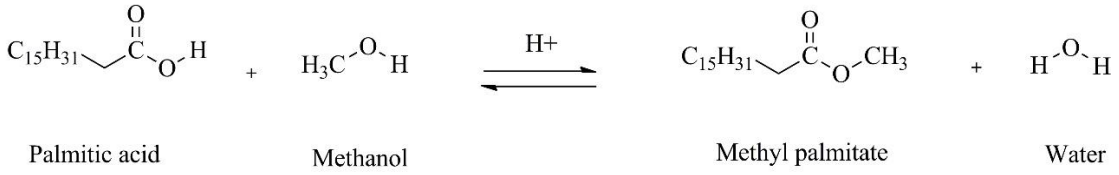

Figure 3. Acid-catalyzed esterification of palmitic acid

3.2.1 Effect of reaction time and temperature on catalytic activity

The reaction medium for the esterification of palmitic acid with methanol using PEFB-DS-SO_3H is a heterogeneous system. It is necessary to have sufficient time to complete the esterification reaction. Therefore, the effect of reaction time on esterification efficiency was investigated. Since the esterification of palmitic acid is an endothermic reaction, high temperatures shift the reaction equilibrium towards methyl palmitate formation. Therefore, the effect of temperature on the palmitic acid esterification efficiency was investigated. The results are shown in Figure 4. It is found that the catalytic activity increases with increasing reaction time and temperature up to an optimum value. The highest esterification efficiency of 98.5% was obtained using 5 wt% of catalyst, a 6:1 methanol to palmitic acid molar ratio, at 80°C after 5 h. Among the three selected reaction temperatures used in this study, more than 70% esterification efficiency is obtained at both 60°C and 80°C after 3 h. An increase of reaction temperature increases the solubility of palmitic acid in methanol and promotes the rapid diffusion of catalyst and reactants in the liquid mixture. In addition, an increase of molecular motion due to the increased temperature increases the mass transfer, increasing the catalytic activity (Zhou et al., 2016). Also, methanol starts to boil and the methanol vapor can effectively contact with the palmitic acid, providing higher esterification efficiency at 80°C. However, Saravanan et al. (2016) reported a 90% yield of methyl palmitate at 60°C while Zhou et al. (2016) reported 98.4% oleic acid esterification efficiency at 90°C.

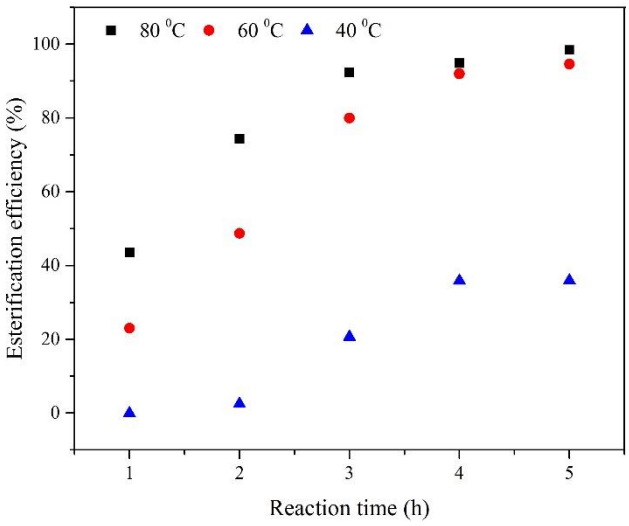

Figure 4. Effect of reaction time and temperature on esterification efficiency of palmitic acid with 5 wt% PEFB-DS-SO_3H and 6:1 methanol to palmitic acid molar ratio.

3.2.2 Effect of methanol loading on catalytic activity

The effect of methanol loading on the esterification of palmitic acid is shown in Figure 5. The esterification reaction stoichiometrically requires a 1:1 methanol:fatty acid molar ratio. It is found that the esterification efficiency increases with increasing methanol:palmitic acid molar ratio up to an optimum value. Esterification is a reversible reaction, and thus, it requires more methanol than the theoretical amount to shift the reaction equilibrium towards product formation. Nevertheless, the presence of excess methanol can deactivate the catalyst by inundating the active acid sites (Saravanan et al., 2016), decreasing the esterification efficiency.

However, a further increase of the methanol: palmitic acid molar ratio beyond 6:1 did not significantly affect the esterification efficiency. Saravanan et al. (2016), reported an increase of the methyl palmitate yield from 32% to 60% when increasing the methanol:palmitic acid molar ratio from 5:1 to 20:1 using 1 wt% of sulfated zirconia catalyst, at 60°C for 7 h.

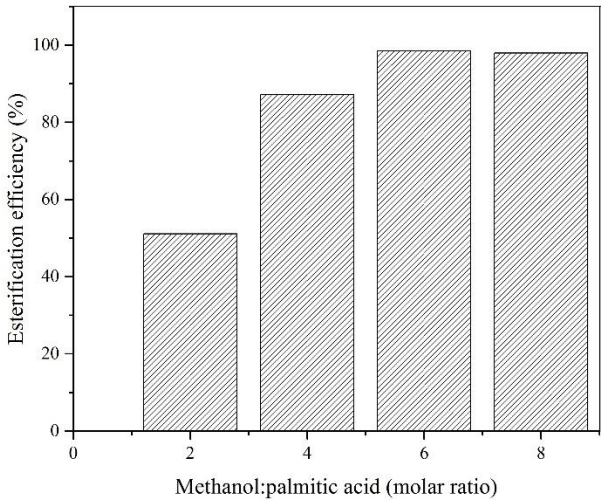

Figure 5. Effect of methanol loading on esterification efficiency of palmitic acid using 5 wt% PEFB-DS-SO_3H at 80°C for 5 h

3.2.3 Reusability of PEFB-DS-SO_3H catalyst

Reusability is important in measuring the performance of a SAC. The used catalyst after each run was easily recovered by vacuum filtration. Results showed that the esterification efficiency of the PEFB-DS-SO_3H catalyst decreases from 98.5% to 90.8% after the third run (Figure 6). This decrease of esterification efficiency during reuse is due to various reasons. Deactivation of catalyst active sites, such as SO_3H, due to the accumulated water and methanol decreases the esterification efficiency (Fraile et al., 2012). Deposition of reactants, intermediates, and products on the surface and the pores of the catalyst also decreases the activity due to the hindrance of actives sites (Ngaosuwan et al., 2016).

This study reveals the capability of using PEFB as an abundant lignocellulose waste biomass for SAC preparation through a simple and one-step protocol for the esterification of palmitic acids. Table 3 shows that the esterification efficiency of a SAC varies according to the type and amount of catalyst used. This variation is also due to the other conditions, such as reaction temperature, time, methanol loading, and the reactor type. However, as can be seen in Table 3, it can be concluded that the PEFB-DS-SO_3H catalyst shows appreciable activity, compared to the reported carbon-based SACs in the literature for esterification. Since the PEFB-DS-SO_3H can be reused, it is an environmentally friendly catalyst and is a promising alternative for a homogeneous acid catalyst.

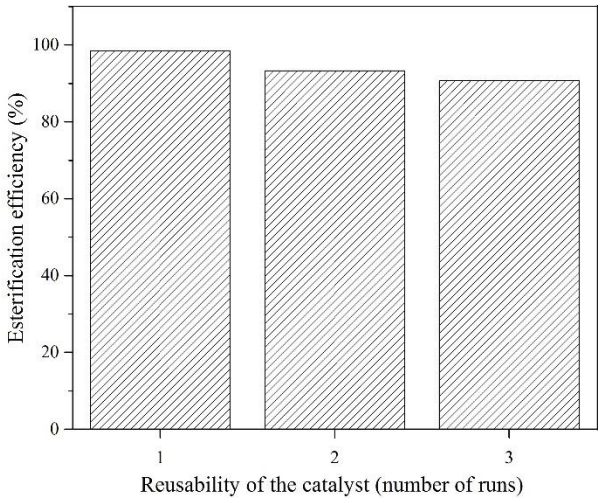

Figure 6. Reusability of PEFB-DS-SO_3H for esterification of palmitic acid using 5 wt% catalyst and 6:1 methanol to oil molar ratio at 80°C for 5 h

4 Conclusions

The PEFB derived SAC, prepared through the one-step concentrated sulfuric acid impregnation, was successfully used for the esterification of palmitic acid with methanol. XPS and FT-IR analysis confirmed the activation of the PEFB-DS-SO_3H catalyst. As found from TGA, the catalyst can be employed at temperatures of up to 200°C without decomposition of the active functional groups. The high acid density, despite a relatively small surface area, may be attributed to the obtained high catalytic activity. A maximum esterification efficiency of 98.5% was achieved using 5 wt% catalyst, a 6:1 methanol to palmitic acid molar ratio, at 80°C for 5 h, for the reaction conditions. The catalyst had good stability and was used for three consecutive runs without considerable loss of the activity. In addition to the high activity, facile and economical synthesis using waste biomass makes the PEFB-DS-SO_3H a promising catalyst for esterification. However, a further improvement of the porous structure and the stability of the functional groups will increase the activity and the reusability of the catalyst.

Table 3. Comparison on usage of carbon-based SAC for esterification

Catalyst	Catalyst preparation	Catalyst characterization	Catalytic activity		Reference
		Total acid density (mmol/g)/ sulfonic acid density (mmol/g or wt%)/surface area (m^2/g) /pore size (nm)/pore volume (cm^3)	Feedstock/methanol loading (molar ratio)/catalyst loading (wt%)/reaction temperature (°C)/reaction time (h)	Conversion or yield (%)/ reusability	
PEFB based SAC	Simultaneous carbonization and sulfonation: Conc. H_2SO_4 (1:5 wt%), 100°C, 1 h	5.4/1.1/5.5/17/0.13	Palmitic acid/6:1/5/80/5 in a reflux reactor	98.5/2 cycles	This study
Glycerol based SAC	Simultaneous carbonization and sulfonation: Conc. H_2SO_4 (1:4 wt%), 180°C, 20 min	1.6/-/1.0 /-/-	Palmitic acid/25 mL for 2.56 g/10/65/4 in a reflux reactor	99%/8 cycles	Devi et al. (2009)
Banana peel derived SAC	Activation:Fragments of banana peel (1.2 kg) submerged in an aqueous $FeCl_3$ (1.8 L, 80°C, 1 week) Carbonization: 650°C, 3 h under N_2 environment	1.43-2.68/0.9-4.8%/156-1097/6.1-11.4/0.17-0.74	Oleic acid/150 mg: 5 g/150 mg/80/2 in a reflux reactor	63-94%/4 cycles	Liu et al. (2015)
Bagasse based SAC	Simultaneous carbonization and sulfonation: Conc. H_2SO_4 (5 g:30 mL), 180°C, 10 h	1.9/-/1.27/-/0.003	Soap stock oil/15:1/5/65/11 in a reflux reactor	97.2%/3 cycles	Savaliya and Dholakiya (2015)
Rice husk derived SAC	Activation: calcined for 450°C, 15 h under N_2 environment (leaching with NaOH, 100°C, 5 h) Sulfonation: Conc. H_2SO_4 (98%), 150°C, 12 h under N_2 environment	5.25/-/1233/38.9/0.74	Oleic acid/5:1/0.015 g catalyst (20 mmol oleic acid)/80/9 in a reflux reactor	91%/10 cycles	Zeng et al. (2016)
Coffee residue derived SAC	Activation:mixed with $ZnCl_2$ (1:3 wt/wt) at 110°C for 12 h Carbonization: 600°C, 4 h under CO_2 atmosphere Sulfonation: Conc. H_2SO_4 (1 g: 20 mL), 200°C for 18 h	0.99/0.45/1091/3.5/3.5	Caprylic acid/3:1/5/60/4 in an autoclave reactor	71.4%/4 cycles (very low reusability)	Ngaosuwan et al. (2016)

ACKNOWLEDGEMENTS

The authors gratefully acknowledge the partial financial support provided by the Thammasat University, Thailand Research Fund under the TU research scholar contract No. 1/2559.

REFERENCES

Allen A, Foulk J, Gamble G. Preliminary Fourier-transform infrared spectroscopy analysis of cotton trash. The Journal of Cotton Science 2007;11(1):68-74.

Bennett JA, Wilson K, Lee AF. Catalytic applications of waste derived materials. Journal of Materials Chemistry A 2016;4(10):3617-37.

Brunauer S, Emmett PH, Teller E. Adsorption of gases in multimolecular layers. Journal of the American Chemical Society 1938;60(2):309-19.

Coates J. Interpretation of infrared spectra: a practical approach. In: Meyers RA, editor. John Wiley & Sons Ltd, Chichester; 2000.

Dehkhoda AM. Developing biochar-based catalyst for biodiesel production [dissertation]. Vancouver, Canada: University of British Columbia; 2010.

Devi PBL, Gangadhar KN, Sai Prasad PS, Jagannadh B, Prasad RB. A glycerol-based carbon catalyst for the preparation of biodiesel. ChemSusChem 2009; 2(7):617-20.

Fraile JM, García-Bordejé E, Roldán L. Deactivation of sulfonated hydrothermal carbons in the presence of alcohols: evidences for sulfonic esters formation. Journal of Catalysis 2012;289:73-9.

Fu J, Chen L, Lv P, Yang L, Yuan Z. Free fatty acids esterification for biodiesel production using self-synthesized macroporous cation exchange resin as solid acid catalyst. Fuel 2015;154:1-8.

Fu X, Li D, Chen J, Zhang Y, Huang W, Zhu Y, Yang J, Zhang C. A microalgae residue based carbon solid acid catalyst for biodiesel production. Bioresource Technology 2013;146:767-70.

Fu Z, Wan H, Hu X, Cui Q, Guan G. Preparation and catalytic performance of a carbon-based solid acid catalyst with high specific surface area. Reaction Kinetics, Mechanisms and Catalysis 2012;107(1): 203-13.

Han X-X, Chen K-K, Yan W, Hung C-T, Liu L-L, Wu P-H, Lin K-C, Liu S-B. Amino acid-functionalized heteropolyacids as efficient and recyclable catalysts for esterification of palmitic acid to biodiesel. Fuel 2016;165:115-22.

Hara M. Biomass conversion by a solid acid catalyst. Energy and Environmental Science 2010;3(5):601-7.

Konwar LJ, Das R, Thakur AJ, Salminen E, Mäki-Arvela P, Kumar N, Mikkola J-P, Deka D. Biodiesel production from acid oils using sulfonated carbon catalyst derived from oil-cake waste. Journal of Molecular Catalysis A: Chemical 2014;388:167-76.

Liu R-L, Gao X-Y, An L, Ma J, Zhang J-F, Zhang Z-Q. Fabrication of magnetic carbonaceous solid acids from banana peel for the esterification of oleic acid. RSC Advances 2015;5(114):93858-66.

Malins K, Brinks J, Kampars V, Malina I. Esterification of rapeseed oil fatty acids using a carbon-based heterogeneous acid catalyst derived from cellulose. Applied Catalysis A: General 2016;519:99-106.

Nakajima K, Hara M, Hayashi S. Environmentally benign production of chemicals and energy using a carbon-based strong solid acid. Journal of the American Ceramic Society 2007;90(12):3725-34.

Ngaosuwan K, Goodwin JG, Prasertdham P. A green sulfonated carbon-based catalyst derived from coffee residue for esterification. Renewable Energy 2016;86:262-9.

Russo PA, Antunes MM, Neves P, Wiper PV, Fazio E, Neri F, Barreca F, Mafra L, Pillinger M, Pinna N, Valente AA. Solid acids with SO_3H groups and tunable surface properties: versatile catalysts for biomass conversion. Journal of Materials Chemistry A 2014;2(30):11813-24.

Saravanan K, Tyagi B, Shukla RS, Bajaj HC. Solvent free synthesis of methyl palmitate over sulfated zirconia solid acid catalyst. Fuel 2016;165:298-305.

Savaliya ML, Dholakiya BZ. A simpler and highly efficient protocol for the preparation of biodiesel from soap stock oil using a BBSA catalyst. RSC Advances 2015;5(91):74416-24.

Su F, Guo Y. Advancements in solid acid catalysts for biodiesel production. Green Chemistry 2014;16(6): 2934-57.

The National Standard of the People's Republic of China. GB/T 5530: Animal and vegetable fats and oils determination of acid value. Standard Press of China: Beijing; 2005.

Thushari P, Babel S. Biodiesel production from waste palm oil using palm empty fruit bunch-derived novel carbon acid catalyst. Journal of Energy Resources Technology 2018;140(3):032204.

Visvanathan C, Chiemchaisri C. Management of Agricultural Wastes and Residues in Thailand: Wastes to Energy Approach. Asian Institute of Technology: Thailand; 2008.

Zeng D, Zhang Q, Chen S, Liu S, Wang G. Synthesis of porous carbon-based solid acid from rice husk for esterification of fatty acids. Microporous and Mesoporous Materials 2016;219:54-8.

Zhang Z, Huang H, Ma X, Li G, Wang Y, Sun G, Teng Y, Yan R, Zhang N, Li A. Production of diacylglycerols by esterification of oleic acid with glycerol catalyzed by diatomite loaded SO_4^{2-}/TiO_2. Journal of Industrial and Engineering Chemistry 2017;53:307-16.

Zhou Y, Niu S, Li J. Activity of the carbon-based heterogeneous acid catalyst derived from bamboo in esterification of oleic acid with ethanol. Energy Conversion and Management 2016;114:188-96.

Environmental Changes in the Hindu Raj Mountains, Pakistan

Fazlul Haq[1], Liaqat Ali Waseem[1*], Fazlur-Rahman[2], Ihsan Ullah[2], Iffat Tabassum[2] and Saima Siddiqui[3]

[1]Department of Geography, Government College University Faisalabad, Punjab 38000, Pakistan
[2]Department of Geography, University of Peshawar, Khyber Pakhtunkhwa 25000, Pakistan
[3]Department of Geography, University of the Punjab, Lahore 54000, Pakistan

ARTICLE INFO

Received: 24 Jun 2018
Received in revised:
5 Sep 2018
Accepted: 7 Sep 2018
Published online:
8 Oct 2018
DOI: 10.32526/ennrj.17.1.2019.07

Keywords:
Global environmental change/ Mountain environment/ Resource degradation/ Natural resource base/ Deforestation

*** Corresponding author:**
E-mail:
ch.lqtwaseem@gmail.com

ABSTRACT

Global Environmental Change among the world's mountains has become a field of interest for researchers and this issue has been widely studied in many parts of the world. This exploratory research aims to study the changes that have occurred and are still occurring in the Hindu Raj Mountains of northern Pakistan, which is an unexplored region with a wide potential for research. To study the changes in various aspects of physical and social setup, five villages/sub-valleys were selected at varying altitudes above mean sea level. Changes in the bio-physical environment were explored using remote sensing technology. It was found that drastic changes have taken place and are still going on in the natural environment as well as the socio-economic setup of the study area since 1970. The population of the study area has increased by manifold resulting in changes in the household and family structure. Moreover, the land use land cover of the study area has changed considerably. Forest cover has decreased drastically with an increase in both the built up and barren land areas.

1. INTRODUCTION

The northern mountainous belt of Pakistan has witnessed substantial changes in the biophysical and socio-economic setup during the last four to five decades. Changes can be observed in every aspect of the biophysical environment whether it is climatic pattern and behavior of weather elements, productivity and regeneration capacity of natural resources, availability and distribution of irrigation and domestic water, biodiversity, forest cover and the intensity and frequency of flooding events. Natural springs - the main water supplier for both irrigation and domestic use - have been drying out gradually resulting into an alarming situation. In many areas, the centuries' old and productive springs have died out completely. In most parts of this diverse mountainous belt, irrigated agriculture has become a myth and the lands, once producing paddies, are now cultivated with barley and other rain-fed crops. While having a look at the history of these changes, it can be observed that these have occurred in a short period of time and governed by complex natural and human factors (Flint, 1994; Gautam et al., 2003; Ali et al., 2006; Fazlur-Rahman, 2007a; Fazlur-Rahman, 2007b; Rahman et al., 2014).

However, the above mentioned changes are not occurring independently, and neither their effects remain confined to the same setup. These anomalies are driven by various other factors mostly related to human activities and in turn these changes initiate and drive transformations in the socio-economic setup of the region and the process is going on in a cyclic manner (Jodha et al., 1992). Out-migration both on national and international scale is a recurrent phenomenon amongst several other changes in the socio-economic setup. The out-migration is mainly an indicator of deficient local natural resource base, high dependency on exogenous food supplies, insufficient local food supplies and declining agricultural productivity (Ehlers and Kreutzmann, 2000; Grotzbach, 1984; Kreutzmann, 1992; Ehlers, 1996; Ehlers, 1997). Fazlur-Rahman (2007b) argues that the traditional social setup throughout the mountainous region of Pakistan has been affected by the ongoing process of changes. Accessibility improvement has connected these remote communities to the lowlands and plain areas.

Improved transportation network has become an important factor of changes in the mountainous areas as stated by Ali et al. (2005). This study claims that about half of the natural vegetation cover has been cleared during the last thirty years, mainly as a result of the development of transportation network and improved accessibility to the natural forests.

The coupling effects of the biophysical and socio-economic changes result into the transformation of the traditional and historical natural resource management systems and affected the performance of local social institutions such as reciprocal activities and collective actions (Jodha, 2007). Continuously growing population, changes in household and family systems, economic transformations and changes in livelihood strategies are among the major factors of increase in stress on the fragile environment and diverse mountains' resources (Rahman et al., 2014). As a result, the natural resources are degraded and the sustainability of the fragile mountain environment is threatened. In this situation, the traditional and historical indigenous social institutions and mechanisms for natural resource management are losing their effectiveness and going through the process of transformation (Somanathan, 1991). The key question addressed in this study is: What factors drive the current and unprecedented changes in every aspect of the natural and social environment and effects do these changes have on the natural resource base of the mountainous areas? This research is basically exploratory in nature with the main goal to explore the process of change and the governing factors in the northern mountainous belt of Pakistan. Moreover, the study aims to establish a link between the changes in the biophysical environment and socio-economic setup.

2. METHODOLOGY

2.1 Characteristics of the study area

The present study has been conducted in the Dir Valley (Dir Valley refers to the entire valley formed by River Panjkora covering the Upper and the Lower Dir districts), which is located in the northwestern frontier region of the Khyber Pakhtunkhwa province between Latitude 34°45′ N to 35°45′ N and Longitude 71°30′ E to 72°30′ E. Geographically, the study area is an intermountain valley of the Hindu Raj spurs of the great Hindukush Mountain Ranges of Pakistan. The elevation of the study area ranges from 1,400 m above mean sea level up to around 5,000 m above mean sea level in the northern and northwestern part (Figure 1). The physiographic setup of the area is modified into deeply cut valleys by River Panjkora and its major and minor tributaries originating from mountains all around. These valleys provide flat surface for the construction of dwellings as well as agriculture. The relatively gentler slopes, alluvial fans and terraces near the valley bottom up to an altitude of 3,000 m above mean sea level are used for the construction of permanent human dwellings. On the other hand, temporary seasonal summer houses and animal huts can be found in the mountains above 3,000 m elevation. The summer houses are constructed for pastoralism and seasonal movements in the summer months.

The study area is inhabited by the Yousafzai Pathan Tribe with some other small tribes and non-bona-fide migrated people. All the natural resources in the jurisdiction of the valley are owned by the bona-fide inhabitants, managed and utilized under an indigenously devised land tenure system. Up to 1969, the study area was a princely state ruled by various dynasties and feudal rulers. In 1970, it was given the status of settled district and in 1996; it was divided into two districts, i.e., Dir Upper and Dir Lower. The merger of the State in Pakistan and its declaration as a settled district was the arrival of a new era in the dark feudal history of the valley. This administrative shift triggered changes in every aspect of the socio-economic environment of the valley.

2.2 Methods and sources of data collection

2.2.1 Timeframe

This research is mostly based on primary information collected through field survey. To have an insight into the ongoing process of change and transformation, five villages were selected for the study from different sub-valleys with varying elevation above mean sea level. Khall was selected from the lowermost altitudinal zone which is the most easily accessible area. Three villages, namely Balkore, Daskore and Jabar were selected from intermediate altitudinal zones, while Thal was selected from the Kohistan Sub-valley with an altitude above 3,000 m above mean sea level (Figure 1). These villages are characterized by diverse physical socio-economic conditions. To discover temporal variations in environmental and socio-

economic setup, two data points were selected. The first data point was 1970, which can be termed as the beginning of a new era in the history of the study area, while 2014 was taken as the last data point on the basis of data availability.

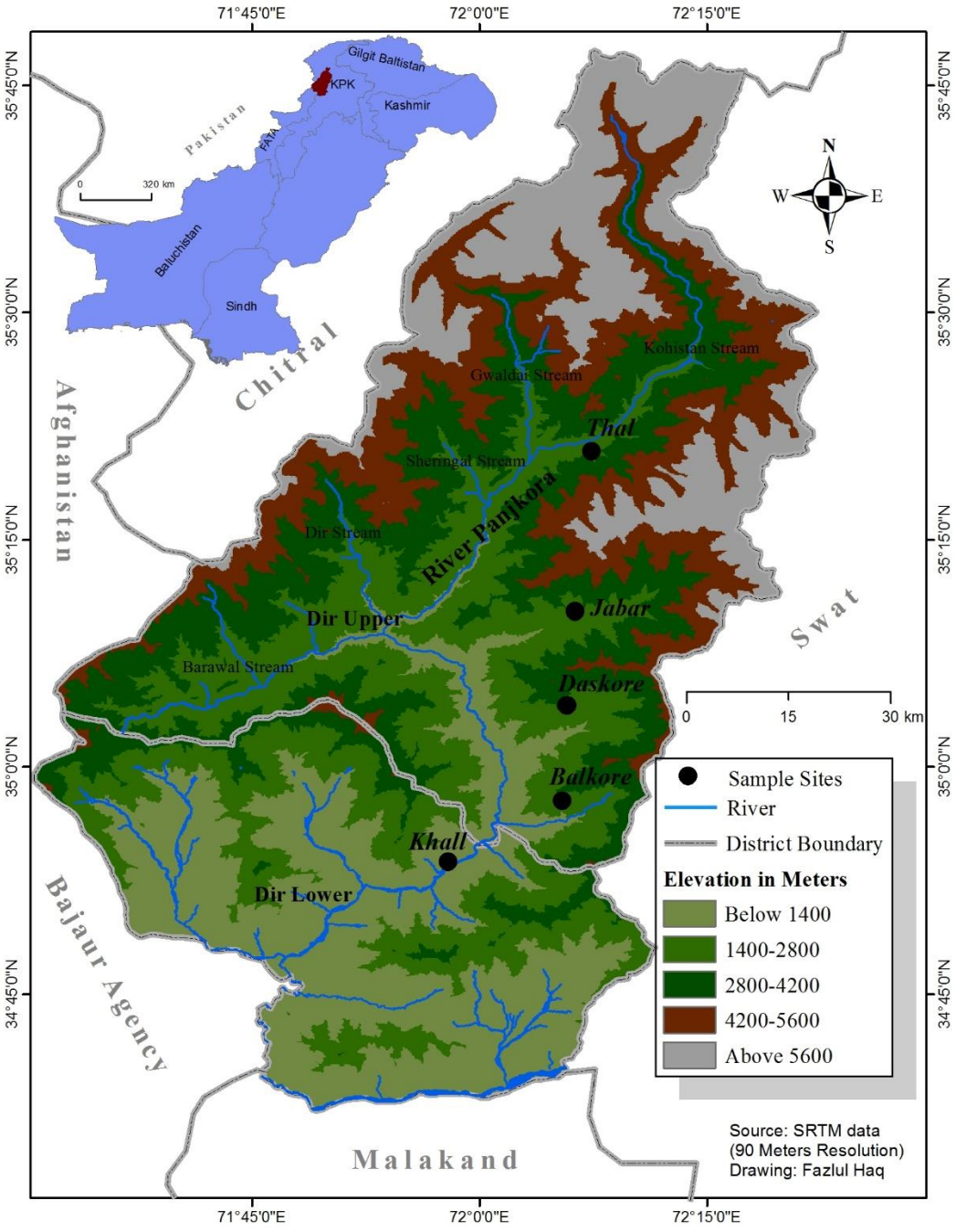

Figure 1. Study area: location, drainage pattern and physiography

2.2.2 Questionnaire survey and sampling

Questionnaire survey and geographical information system (GIS) were used to discover and quantify the changes. The major variables covered through the questionnaire were; economic transformations, modernization of agriculture and irrigation, animal husbandry and migration. A total of 500 respondents were interviewed from the selected villages. The respondents were selected on the basis of birth year to be earlier than 1960 who could perceive the changes during the last four decades. The purpose of the questionnaire survey was to determine the socio-economic changes occurred during 1970 to 2014. Therefore,

comparative statistical charts were prepared for the two data points using MS Excel

2.2.3 Geo-spatial techniques

GIS was used to determine the spatial and temporal variations in the biophysical environment utilizing the land cover maps of 1970 and 2014 (GoNWFP, 1975; GoKPK, 2014), which were scanned and imported in ArcMap package of ArcGIS 10.3. The rectified raster maps were processed for the preparation of land use land cover maps for 1970 and 2014. The main objective of this step was to quantify the dynamics of forest resources and agricultural land during the study period.

3. RESULTS AND DISCUSSION

3.1 Population and household dynamics

Population growth and the related household dynamics are one of the important elements of socio-economic transformations. While having a look at the figures, it can be observed that the population of the study area has grown from 5,100 in 1972 to 23,110 in 1998 revealing an increase of about five times (Figure 2). Population growth affects almost every sector of life and environment and this issue has been studied extensively worldwide (United Nations, 1973; United Nations, 2001; Repetto, 1986; World Bank, 1992; FAO, 1994; Templeton and Scherr, 1997; Sati, 2009; Gracheva et al., 2012). It has played the pivotal role in the process of environmental changes in the study directly and by triggering household dynamics.

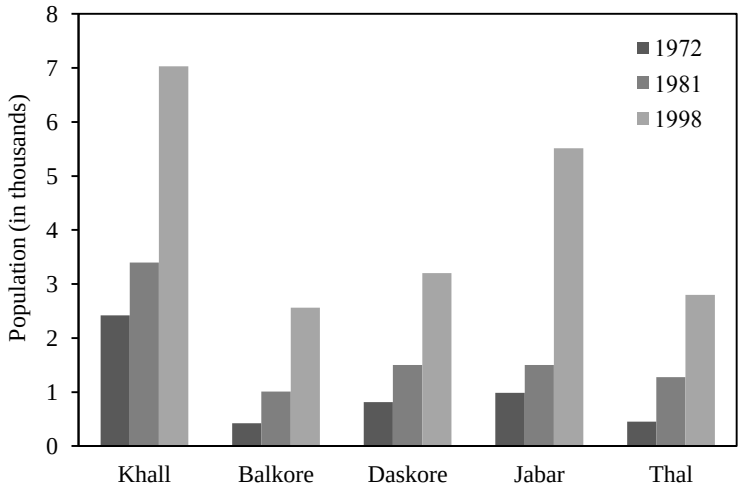

Figure 2. Population growth in the study area (1972-1998) (GoP, 1961; GoP, 1972; GoP, 2000)

Traditionally, the inhabitants of the study area used to live in the form of joint family system as it was an important integrating factor keeping all the relatives together, and also a strategy to cope with issues like conflicts, food insecurity, natural hazards and economic problems. However, during recent decades, the joint family system has decreased significantly and the same trend has been observed in other areas as well (Liu et al., 2003; Knight and Rosa, 2012). Results reveal that during 1970s, 65% families were living in joint and extended family systems and only 35% were nuclear families. During the last four decades, the number of nuclear families has increased to 64% (Figure 3).

As a result of joint family disintegration, the average household size has significantly decreased during 1970-2014. The proportion of larger families (10 members and above) was 53% in 1970, which decreased to 10% in 2014 replaced by smaller families with 5 or fewer members (Figure 3). Keilman (2003) also concluded the same findings that the household size in most of the developing countries has declined (from 5.1 to 4.4) during 1970-2000, while it fell from 3.2 to 2.5 in the developed countries.

The forces driving household dynamics are numerous. Continuously growing household size makes it hard for the joint family to handle space sharing and the allocation of domestic chores and responsibilities. Therefore, separation becomes necessary resulting in disintegration. Several joint families disintegrated because of the internal

conflicts created as a result of competition for space and allocation of duties as also reported by Goode (1963). Additionally, there are other socio-cultural forces, as identified by the demographic behavior theories (Verdon, 1998), which play a role in the disintegration of joint families. According to Keilman (2003), these factors include less tolerance to cultural norms; less religion tendency and increased freedom; women education and economic independence; emphasis on gender equity and residential autonomy.

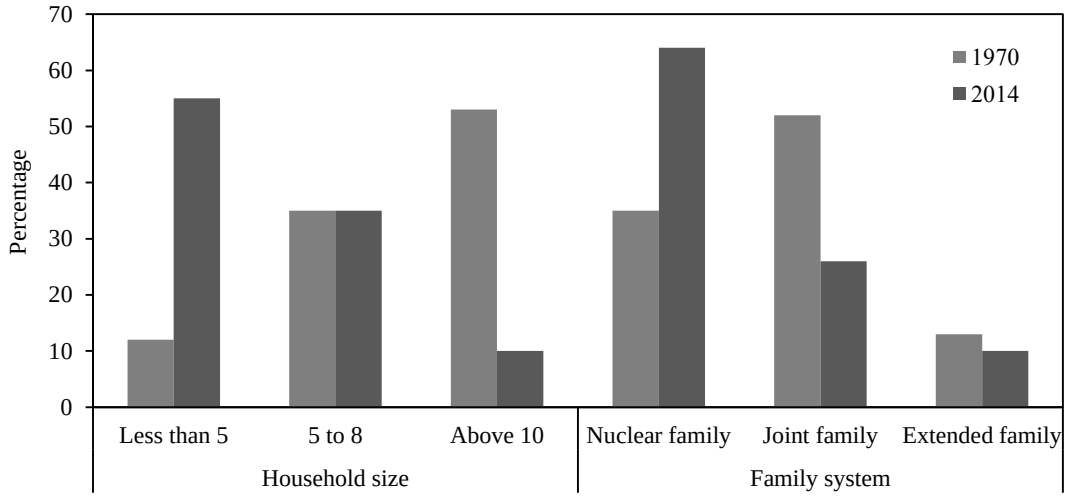

Figure 3. Dynamics of household size and family system (1970-2014)

As families disintegrate, the house design and layout are considerably changed. Most of the structural changes in house construction and designs started after the political change of 1970s'. During the reign of the feudal ruler Shah Jehan, construction of big houses was forbidden in the jurisdiction of the state. However, after the merger of the Dir State in Pakistan, the inhabitants started to modify and construct settlements without such restrictions. Based on building material, the houses are of three types in the study area. 1) Kaccha house which is made up of stones, mud and wood. 2) Pakka houses which are fully concrete structures with doors and windows, usually but not exclusively, metal made. 3) Semi-pakka houses, when cement and corrugated sheets are used along with wood and stones. Results reveal that during 1970-2014, kaccha houses have considerably decreased and pakka houses have increased throughout the study area with slight local variations (Table 1). This shift from traditional and local building material is mainly because of "motorized access to the regional center and availability of money" (Fazlur-Rahman, 2007b), along with the political change and population dynamics.

Another major change is the addition of facilities and rooms to the traditional single room houses. Historically, in the mountainous areas of Pakistan, the houses were in the form of single room, "…without any windows or ventilation, with animal sheds, hay stores, a byre and a storeroom attached to it on one end. All the facilities were under the single roof, ranging from kitchen and sleeping area to wood storage and the storage of agricultural implements" (Fazlur-Rahman, 2007b). The local inhabitants used to build separate rooms with the passage of time in order to accommodate new family members and their spouses, while the rest of the family sharing the main room. More and more innovations were added to the traditional houses from time to time. Separate bedrooms, guestrooms (The guestrooms are not only used for the purpose of serving guests, but also used as bedrooms by the unmarried males of the family who in the past used to sleep on the roofs and open spaces), animal-sheds and kitchens became common after 1970. In addition, the trend of using open-air toilets declined and attach toilets became one of the basic components of the house structure because of several cultural factors. The proportion of households with attached toilets has increased considerably during 1970-2014 (Table 1).

Table 1. Change in house construction, layout, facilities and design in the study area

	Change in house construction, layout and design: % increase or decrease in number from 1970 to 2014									
Study area	Kaccha houses	Semi-pakka houses	Pakka houses	Single room houses	Double room houses	Multiple room houses	Kitchen	Guestroom	Toilet	Animal shed
Khall (N=100)	-48	-17	65	-69	12	57	69	62	80	70
Balkore (N=100)	-39	11	28	-61	23	38	58	84	76	76
Daskore (N=100)	-31	-15	46	-65	39	26	58	86	72	76
Jabbar (N=100)	-45	-13	58	-44	-8	52	69	61	66	56
Thal (N=100)	-27	-17	10	-52	22	30	62	67	60	70

3.2 Agricultural transformations

Mixed mountain agriculture, i.e., cultivation of crops and domestication of livestock have played a major role in food security and livelihood sustenance of the inhabitants. Both these pillars of mixed mountain agriculture have gone through several changes and transformations. The major aspects of change are; land use, productivity and per unit yield, agricultural inputs and output, labor engagement and distribution, cropping pattern, irrigation sources and methods, landholding size and farming methods. Population growth and increasing demands for food and fodder have resulted in innovations and the land is now utilized more intensively as compared to the past by introducing modern inputs such as genetic seeds and fertilizers, labor intensification, mechanization and multiple cropping techniques. Innovations in agriculture can also be observed in the surrounding mountainous areas as according to Fazlur-Rahman (2007b) "many modern innovations have been grafted onto the traditional agricultural system, such as new seed varieties and chemical fertilizers". Although due to certain physical constraints, agriculture cannot be mechanized fully; however, mechanization has partially replaced the old sowing and threshing methods. The traditional bull tilling is still important as tractor tilling is not possible everywhere due to inaccessibility, thin soil layer and steep slopes of the terrace fields.

Availability of suitable land for agriculture is limited due to rough topography. The available agricultural land is extensively fragmented resulting into small landholdings per household. The trend of fragmentation of arable land is not confined to the study area, but common in the neighboring mountainous regions of Pakistan, driven by inheritance and increasing number of households (Fazlur-Rahman, 2007b). Data reveals that 89% of the households own less than 0.5 acres arable land. The percentage of small landholdings was 56% in 1970 and the rest of the households owned more than 0.5 acres land. Presently, bigger landholdings belong only to 11% of the households (Figure 4). As a result agriculture is becoming an activity of secondary importance and off-farm sources of earning are opted.

Changes in cropping pattern and crop rotation are an important strategy to get more yield as the areas where only one crop per annum was grown are now cultivated with multiple crops. The climatic conditions of the lower and middle altitudes favor different crops and enjoy two distinct cropping seasons. Results reveal that the percentage of the respondents growing multiple crops has increased from 13% to 39% during 1970-2014. On the other hand, the percentage of double and single cropping systems decreased from 31% and 56% to 20% and 41% respectively during 1970-2014 (Figure 4). It implies that 80% of the respondents harvest two or more crops per annum while single cropping is practiced only by 20% of the respondents.

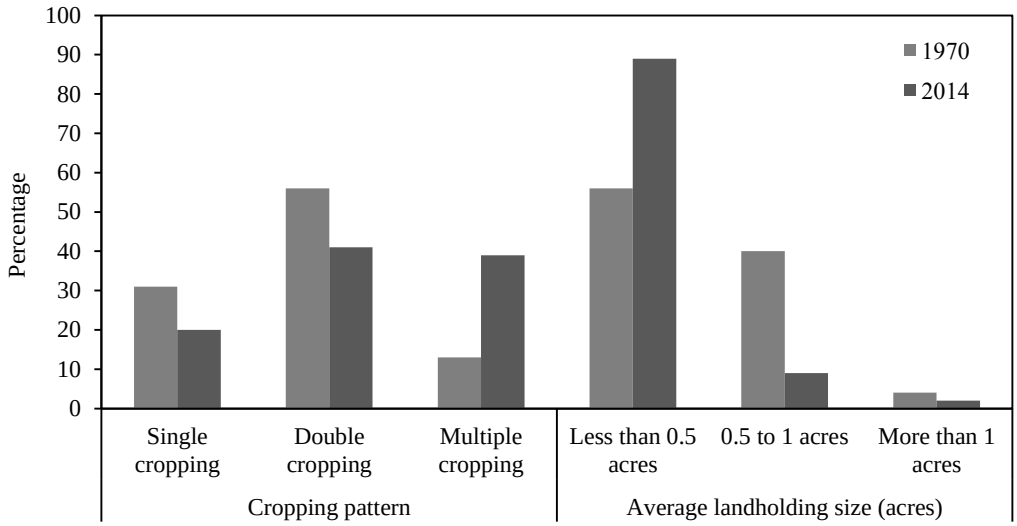

Figure 4. Changes in agricultural landholdings per household and cropping pattern (1970-2014)

In addition to crop intensification, considerable improvements can also be observed in irrigation infrastructure. The canal taken off from Ushiri Stream in the 1970s is a good example, which has brought most of the cultivated land of the Jabar village under irrigation. Moreover, a number of minor water courses have been taken off from the local streams. As a result, the proportion of irrigated and semi-irrigated land has increased considerably, particularly in Jabar where the number of respondents having land under irrigation has increased from 52% in 1970 to 88% in 2014 (Table 2). The overall proportion of irrigated landowners has increased from 44% to 65%, while the rain-fed landholdings have decreased from 42% to 15%. Irrigation infrastructure has been improved which is another factor of increase in irrigated land. Small water reservoirs are constructed to store the water diverted from seasonal torrents and springs (Figure 5). The stored water is released to the fields through narrow water courses and managed under complex appropriation systems. The decrease in irrigated landholdings in Thal is because of the expansion of un-irrigated land to the pastures and poorly suitable areas (Figure 6).

Table 2. Proportion of agricultural landholdings under irrigation

Study area	Proportion of landowners by irrigation (%age)					
	Irrigated		Semi-irrigated		Rain-fed	
	1970	2014	1970	2014	1970	2014
Khall	42	64	2	30	56	6
Balkore	54	42	22	35	24	23
Daskore	62	50	18	14	20	36
Jabar	52	88	20	7	20	5
Thal	92	81	4	13	4	6
%age	44	65	13	20	42	15

3.3 Dynamics of land use land cover

Land use land cover of the study area has considerably changed during the study period, driven mainly by the socio-economic transformations. Land cover of the study area is dominated by natural vegetation including alpine forests dominated by deodar; coniferous forests; rangelands in the proximal hills of the residential areas and high altitude pastures.

Figure 5. Reservoir for the storage of surplus water discharge from springs

Figure 6. Poorly structured high altitude cultivated fields in the village Thal

Results reveal that in 1970 natural vegetation cover constituted 73% of the land cover - 57% forests and 16% rangelands and pastures - distributed throughout the valley (Table 3 and Figure 7). Agricultural area covered 17% of the land of the study area. Barren rock outcrops and permanent snow cover was 9% of the total land area and only 1% was covered by built up area. Considerable change can be observed in the land use land cover pattern of the study area during 1970-2014. Natural

vegetation has decreased to 54% of the total land area where forests have recorded a decrease of 17%, while rangelands and pastures have decreased by 2%. Agricultural land has increased to 22% and built up area has recorded 5 times increase from 1% to 5%, while the barren land has increased from 9% to 19% during 1970-2014 (Table 3).

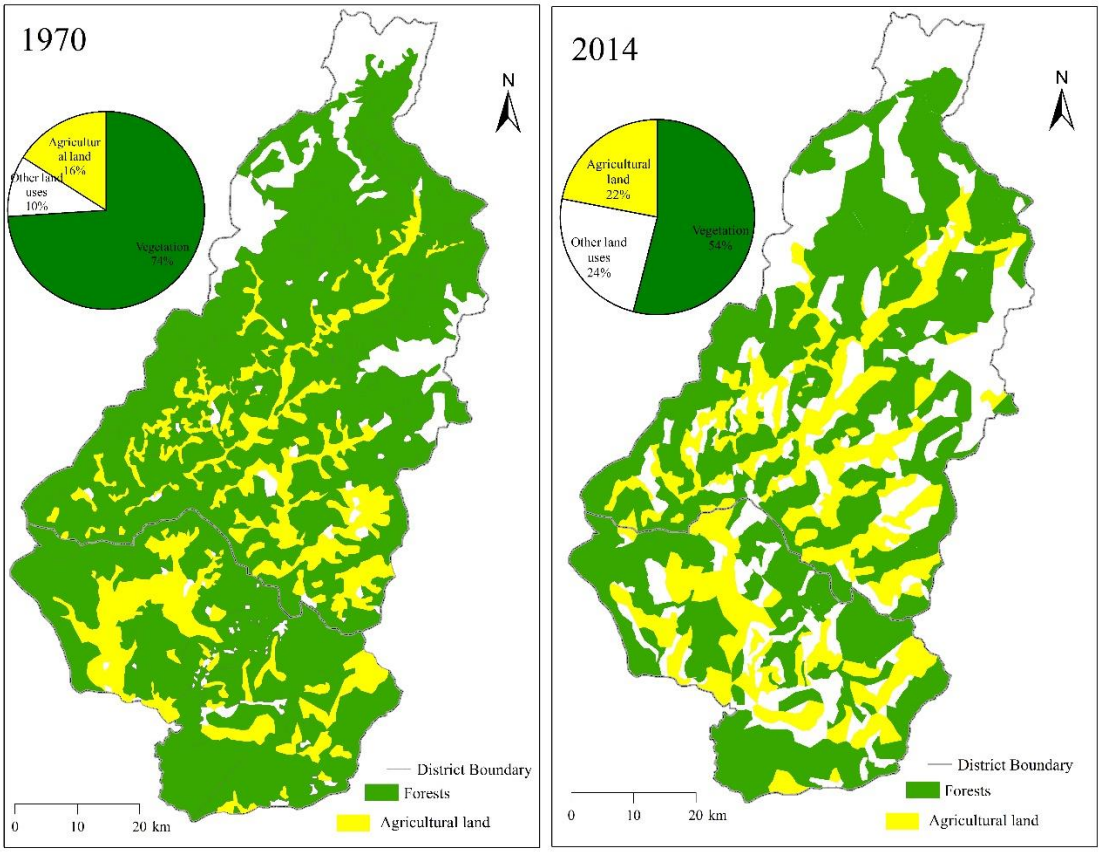

Figure 7. Dynamics of agricultural land and forest cover (GoNWFP, 1975; GoKPK, 2014)

Table 3. Land use land cover dynamics in the study area (1970 to 2014)

Land cover	Area/percentage (1970)		Area/percentage (2014)	
	Area (000 Hectare)	Percentage	Area (000 Hectare)	Percentage
Forests	305.8	57	210.5	40
Rangelands/pastures	84.3	16	74.8	14
Agricultural land	89.3	17	115.4	22
Built up area	6.4	1	28.6	5
Barren land	45.5	9	103	19
Total	532	100	532	100

Agricultural land has expanded in all directions but mainly onto the grazing lands and lower altitude forests. The rangelands and forests are cleared and the slopes are modified into terrace fields known as Karin (Figure 8). The less favorable hill slopes around the villages at high altitude, are brought under cultivation through introducing fast ripening seed varieties of barley, maize and potato. Built up area has also expanded substantially mainly because of population growth and the associated household dynamics. The existing residential areas are not capable to accommodate more settlements. To acquire space, the nearby forests and rangelands are cleared and in certain areas, the built up areas expand onto the agricultural lands.

Figure 8. Rain-fed cultivated terraces on hill slopes

Rapid expansion of residential areas has recently become one of the important aspects of change threatening the sustainability of natural resource base. The major impact of this expansion is deforestation and destruction of natural ecosystems. The increasing number of households has affected the forest cover in two ways: first by the expansion of built up areas and secondly, the pressure on forests for the collection of timber as well as non-timber forest products (NTFPs) has increased. In the villages where the surrounding vegetation cover areas are too steep to be used for settlements, the built up areas have expanded to the cultivated land and isolated dwellings can be seen in the fields (Figure 9). However, if suitable land is available and accessibility does not obstruct, settlements are constructed in the nearby forest areas and rangelands (Figure 10). Clearing of forest areas for the construction of dwellings has become a common practice. A study conducted in the village Ambodiaviavy in Madagascar (Harrison, 1992) explains the relationship of household dynamics and deforestation as, in 1947; a total of 32 people in eight families came and settled over in this forest cover area. Until 1990s, the valley bottom lands filled up completely and the new couples started to clear forest on the valley slopes. As a result of this expansion, in a period of about four decades, two third of the forests of the valley were cleared.

Due to a smaller number of households in the past, the use of timber and fuel wood was negligible compared to the regeneration capacity of the natural vegetation cover. At maximum, a few standing trees were cut once in several years for the construction and repair of houses and livestock shelters, if the dry fallen wood didn't meet the needs. The situation changed after the drastic socio-economic changes, and raised living standards of people during 1970s and 1980s. During the 1980s and 1990s, the increasing trend of constructing big houses with multiple rooms multiplied the consumption of timber. Presently, even the smallest house consists of at least four rooms: a living room, a guestroom, a kitchen and an animal shed. The abandonment of single room houses and the transformation of joint families increased the consumption of firewood and timber causing high rate of deforestation.

Figure 9. Expansion of settlements to the agricultural land

Figure 10. Construction of settlements in rangelands and forest cover areas

3.4 Development of accessibility/road networks

The construction of roads in the mountainous areas in general and the study area in particular is one of the important elements of change. In the past, the area was isolated and away from the development activities and socio-economic changes occurring in the adjacent plain areas. However, the past few decades have witnessed considerable development in infrastructure and transportation networks which have linked these communities to the rest of the world. These developments have opened the way for several changes and transformations in every sector of life (also see Cook and Butz, 2011).

Before the political change of 1970, the Nawab of Dir deliberately kept the then State isolated through restricting the means of transport inside and outside the State jurisdiction. It was a strategy to keep people dispersed not to unite against his ruthless rule and also to restrict the movement of British Officials. The highway running from Chakdara (the southernmost part of the valley) to the

present day Dir city (the capital of the then state) was the only transportation route. This route was strictly monitored by the Nawab's authorities and was mainly used by the state's vehicles. This route was also used by the British Officials once or twice a year moving to Chitral under an agreement between the state ruler and the British.

Presently every village is connected to the markets and the low lying plain areas (Figure 11). The important positive effect of the improved accessibility is the betterment in material circumstances of the inhabitants by increasing monetary wealth particularly in the far-off villages of the study area. The construction of roads brought the markets closer resulting into the modernization of agriculture and exogenous food to supplement the local production. However, unfortunately, the improved access to the remote mountains played a key role in deforestation in the study area as in other mountainous regions (Allen and Barnes, 1985; Kreutzmann, 1991; Kreutzmann, 1993; Uhlig and Kreutzmann, 1995; Allan, 1985; Allan, 1986; Allan, 1989). In the past, the forests of the upper parts of the study area were protected as it was very difficult to transport wood in bulk. Presently the high altitude forests and pastures are linked to the lowlands. The route constructed to the Kumrat forests of the Thal village has exposed the forests to commercial harvesting. Even heavy vehicles can reach the high altitude forests of Kumrat (above 3,000 m) and the bulk of timber and fuel wood is transported down (Figure 12).

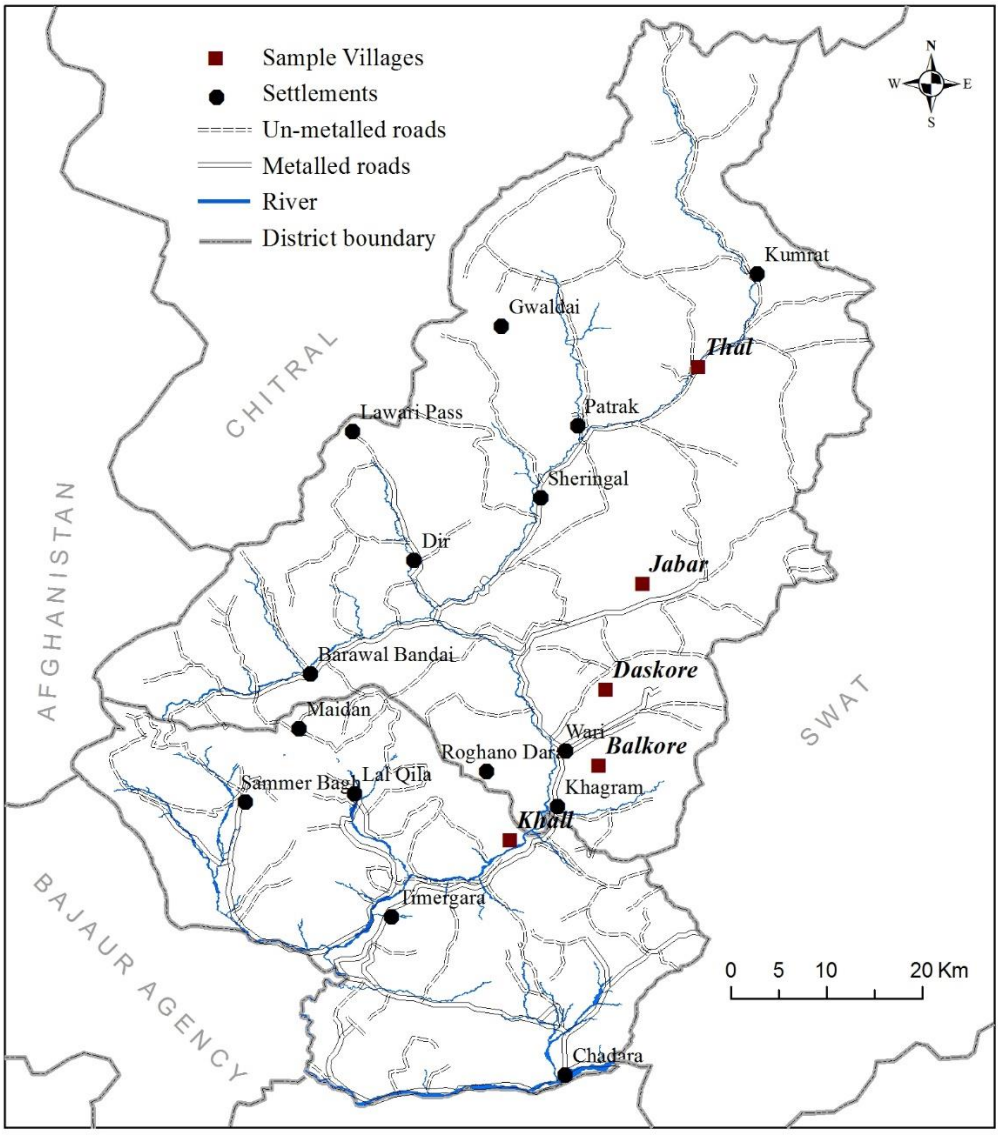

Figure 11. Study area: road network

Figure 12. Truck route in the high mountains forests of Thal

4. CONCLUSIONS

The past few decades have witnessed considerable changes in the socio-economic conditions of the communities inhabiting the Hindu Raj Mountains. The major changes in the socio-economic environment include population growth, increase in the number of household and decrease in the average household size, agricultural transformations, economic changes and improvements in accessibility. The socio-economic transformations triggered a number of changes in various aspects of the biophysical environment particularly land use land cover pattern and natural resource base. Researchers have identified a number of causes and driving forces behind land use changes. Population and household dynamics along with other factors are the main driving forces resulting into substantial changes in the land use pattern and leading towards environmental degradation. Growing population and increasing number of households need more space and thus resulting into the expansion of built up areas, which engulf other land use categories.

The built up areas have expanded towards both the agricultural land and vegetation cover. In the villages with limited suitable residential land, built up areas have expanded towards the agricultural land. The expansion of built up areas towards the vegetation cover has affected the forests and rangelands both directly and indirectly. In the former case, vegetation cover areas are cleared for acquiring space for the construction of new houses. In the latter case, people who inhabit those areas harvest the forests for fuel wood and timber resulting in the conversion of vegetation cover into barren land. A total of 17% decrease has been observed in forest cover areas during the study period. Hence, barren lands have expanded considerably along with the settlements expansion.

REFERENCES

Ali J, Benjaminsen TA, Kammad AA, Dick BQ. The road to deforestation: an assessment of forest loss and its causes in Basho Valley, Northern Pakistan. Global Environmental Change 2005;15:370-80.

Ali T, Shabaz B, Suleri A. Analysis of myths and realities of deforestation in Northwest Pakistan: implications for forestry extension. International Journal of Agriculture and Biology 2006;107:110-8.

Allan N. Periodic and daily markets in the highland-lowland interaction systems: Hindukush-Western

Himalaya. In: Singh TV, Kaur J, editors. Integrated Mountain Development. New Delhi, India: Himalayan Books; 1985.

Allan N. Accessibility and altitudinal zonation models of mountains. Mountain Research and Development 1986;185:194-6.

Allan N. Kashgar to Islamabad: the impact of the Karakoram Highway on mountain society and habitat. Scottish Geographical Magazine 1989;105:130-41.

Allen JC, Barnes DF. The causes of deforestation in developing countries. Annals of the Association of American Geographers 1985;75(2):163-84.

Cook N, Butz D. Narratives of accessibility and social change in Shimshal, Northern Pakistan. Mountain Research and Development 2011;31(1):27-34.

Ehlers E. Population growth, resource management and well adapted land-use in the Bagrot/Karakoram. Applied Geography and Development 1996;48:7-28.

Ehlers E. Traditional environmental knowledge and consciousness and the problem of sustained agricultural development. Applied Geography and Development 1997;49:79-95.

Ehlers E, Kreutzmann H. High mountain ecology and economy potential and constraints. In: Ehlers E, Kreutzmann H, editors. High Mountain Pastoralism in Northern Pakistan. Stuttgart: Erdkundliches Wissen; 2002.

Food and Agriculture Organization (FAO). Land degradation in South Asia: its severity, causes and effects upon the people. World Soil Resources Reports No. 78. Rome: Food and Agriculture Organization of the United Nations; 1994.

Fazlur-Rahman. Agro-pastoral economy, property rights and locally formulated resource management mechanisms in Astor valley, northern areas of Pakistan. Pakistan Journal of Geography 2007a;17(1-2):55-75.

Fazlur-Rahman. Persistence and Transformation in the Eastern Hindu Kush: A Study of Resource Management Systems in Mehlp Valley, Chitral, North Pakistan. St. Augustin, Germany: Bonner Geographische Abhandlungen 118; 2007b.

Flint EP. Changes in land use in South and Southeast Asia from 1880 to 1980: a data base prepared as part of a coordinated research program on carbon fluxes in the tropics. Chemosphere 1994;29(5):1015-62.

Gautam AP, Webb EL, Shivakoti GP, Zoebisch MA. Land use dynamics and landscape change pattern in a mountain watershed in Nepal. Agriculture, Ecosystems and Environment 2003;99(1-3):83-96.

Government of Khyber Pakhtunkhwa (GoKPK). Land cover Atlas of Pakistan. Peshawar: Pakistan Forest Institute; 2014.

Goode W. World Revolution and Family Patterns. New York, USA: Free Press; 1963.

Government of North West Frontier Province (GoNWFP). Land use survey of North West Frontier Province Part I. Peshawar, Pakistan: Peshawar and Malakand Division; 1975.

Government of Pakistan (GoP). District Census Report of Dir District, 1972. Islamabad: Population census organization of Pakistan; 1972.

Government of Pakistan (GoP). District Census Report of Dir District, 1981. Islamabad: Population census organization of Pakistan; 1981.

Government of Pakistan (GoP). District Census Report of Dir Lower District, 1998. Islamabad: Population census organization of Pakistan; 2002.

Gracheva R, Kohle RT, Tadelbauer J, Meessen H. Population dynamics, changes in land management, and the future of mountain areas in Northern Caucasus: The example of North Ossetia. Erdkundi 2012;66(3):179-219.

Grotzbach E. Mobility of labor in high mountains and socio-economic integration of peripheral areas. Mountain Research and Development 1984;4(3):229-35.

Harrison P. The Third Revolution: Environment, Population and a Sustainable World. London and New York: Tauris and Co. Ltd; 1992.

Jodha NS. Mountain commons: changing space and status at community levels in the Himalayas. Journal of Mountain Science 2007;4(2):124-35.

Jodha NS, Banskota M, Partap T. Strategies for the Sustainable Development of Mountain Agriculture: An Overview. India: Oxford and IBH; 1992.

Keilman N. The threat of small households. Nature 2003;421:489-90.

Knight KW, Rosa EA. Household dynamics and fuel wood consumption in developing countries: a cross-national analysis. Population and Environment 2012;33(4):365-78.

Kreutzmann H. The Karakoram Highway. Modern Asian Studies 1991;25:711-36.

Kreutzmann H. Development processes in the Hunza Valley, a case study from the Karakoram Mountains. Pakistan Journal of Geography 1992;1:1-17.

Kreutzmann H. Challenge and response in the Karakoram: socioeconomic transformation in Hunza, Northern areas, Pakistan. Mountain Research and Development 1993;13(1):19-39.

Liu J, Daily G, Ehrlich P, Luck G. Effects of household dynamics on resource consumption and biodiversity. Nature 2003;421:530-3.

Rahman F, Haq F, Tabassum I, Ullah I. Socio-economic drivers of deforestation in Roghani Valley, Hindu-Raj Mountains, Northern Pakistan. Journal of Mountain Science 2014;11:167-79.

Repetto R. Soil loss and population pressure on Java. Ambio 1986;15(1):14-8.

Sati PV. Population and sustainability issues in mountains: a case for the Uttaranchal Himalaya. ENVIS Bulletin 2009;14(2):1-8.

Somanathan E. Deforestation, Property Rights and Incentives in Central Himalaya. Economic and Political Weekly 1991;26(4):37-46.

Templeton SR, Scherr SJ. Population pressure and the micro-economy of land management in hills and mountains of developing countries. Washington, USA: International Food Policy Research Institute; 1997.

Uhlig H, Kreutzmann H. Persistence and change in high mountain agricultural systems. Mountain Research and Development 1995;15(3):199-212.

United Nations. The Determinants and Consequences of Population Trends: New Summary of Findings on Interaction of Demographic, Economic and Social Factors. Population Studies, Vol. I. New York, USA: United Nations; 1973.

United Nations. Population, environment and development. The concise report. New York, USA: United Nations; 2001.

Verdon M. Rethinking Households. London: Routledge; 1998.

World Bank. World Development Report 1992: Development and the Environment. New York: Oxford University Press; 1992.

Comparison of Carbon Footprint of Organic and Conventional Farming of Chinese Kale

Monthira Yuttitham*

Faculty of Environment and Resource Studies, Mahidol University, Nakhon Pathom 73170, Thailand

ARTICLE INFO

Received: 20 Jul 2018
Received in revised:
7 Sep 2018
Accepted: 11 Sep 2018
Published online:
8 Oct 2018
DOI: 10.32526/ennrj.17.1.2019.08

Keywords:
Chinese kale/ Carbon footprint/ Organic farming/ Conventional farming/ Greenhouse gas emission

*** Corresponding author:**
E-mail:
monthira.yut@mahidol.edu

ABSTRACT

This study compared the carbon footprint (CF) of organic agriculture with that of conventional agriculture in the cultivation of Chinese kale. The farm management data collected included the use of chemical and organic fertilizers, and fossil fuel for tillage, irrigation and transportation. Greenhouse gas emissions (GHG) were calculated and added to the CF. The results showed that conventional agriculture had a CF of 0.402±0.47 kg CO_2e/kg Chinese kale. Proportion of CFs from: chemical fertilizer (51%), transportation (21%), irrigation (19%), tillage (5%), organic fertilizer (2%), herbicide (1%) and insecticide (1%), and organic agriculture had a CF of 0.195±0.122 kg carbon dioxide CO_2e/kg Chinese kale (proportion of CFs from: transportation (81%) organic fertilizer (12%) and fossil fuel for irrigation (7%). The CFs differed, depending on farm management, and that of conventional agriculture was almost double that of organic agriculture because of the higher emissions from use of chemical fertilizers and of fossil fuel for tillage, herbicide and insecticide applications. The conventional farm management led to higher production per unit of planted area. Thus, it seems that conventional farming has relatively higher CF than organic farming. There is still room for both management practices to reduce their GHG emissions and their CFs by reduce chemical fertilizer and fossil fuel use in conventional farming. The promotion of organic farming practices will help to improve sustainable, environmentally friendly agricultural production of Chinese kale in Thailand.

1. INTRODUCTION

Agriculture has a complex relationship with global warming, by theses; Chinese kale is one of the important food crops in Thailand. Thailand is an agricultural-based country and agriculture contributed about 21% of its total greenhouse gas (GHG) emissions in 2000 (51 Mt carbon dioxide (CO_2e) (The Joint Graduated School of Energy and Environment, 2009). Emissions are influenced by cultivation practices and processes throughout agricultural production and product use. Organic farming began in Thailand to lower the high production costs for agriculture (chemical fertilizers, herbicides, insecticides) and reduce the chemical residues in products that caused problems for the food web and human health. To reduce production costs and maintain a good environment, the Thai government aimed to promote organic farming with a "Sufficiency Economy Concept" (SE), a philosophy initiated by King Bhumipol Adulyadej (King Rama IV of Thailand) that advocates moderation, self-sufficiency and reasonable consumption patterns to Thai farmers and the general populous". This involved the government transferring knowledge to and supporting a philosopher who was known to practice good organic farming and acted as a role model, motivating other farmers and interested members of the general public. Thus, it could improve conservation by applying this knowledge to sustainable agriculture (Ministry of Agriculture and Cooperatives, 2010). In addition, a philosopher knowledgeable about organic farming could extend that knowledge to other communities. Thus, organic farming could reduce production costs in general, while also being environmentally friendly in terms of carbon footprint (CF) by reducing GHG emissions.

For example, a previous study reported sustainable agriculture methods in the sustainable cultivation of Thai Hom Mali (Jasmine) rice in Thailand. The study had statistical samples from the most intensive cultivation provinces, such as Phayao (Northern region), Sisaket (Northeastern), Chachoengsao (Central region) and Nakhonsi-thammarat (Southern region). Two indicators were

assigned to assess the sustainable cultivation of Thai farmers, designated as Sustainability in Cultivation Practices (SCP), and the Composite Sustainability Indicators (CSI). The findings revealed that the northeastern region had the highest values of SCP and a higher level of CSI than other regions of Thailand. Besides the independent variables of SCP, in particularly production costs, chemical and fertilizer utilization, the risk of weeds and pests were found to be the significantly common variables in most of the regions of Thai Hom Mali (Jasmine) rice cultivation environment. A sustainability Index and some indicators were adopted for SA (Sustainable agriculture), such as the Framework for the Evaluation of Sustainable Land Management, Land Quality Indicators, and Environmental Sustainability Index for agricultural systems. There are additional indicators for sustainable cultivation designated non chemical fungicide use, non-chemical insecticide use and non–chemical herbicide use. These are promoted options to farmers to have sustainable cultivation in Thailand by organic farming (Chaimanuskul et al., 2011).

In addition, several studies have reported and linked to sustainable agriculture in Thailand. In one organic farmers program, non-governmental organizations have assisted farmers. This research examined the socio-ecological benefits of organic production to rice farmers by using semi-structured interviews with 50 farmers in northeastern Thailand. These Thai organic farmers shed light on shared values, perceptions, and actions towards nature. In another study, 75 members of organic farmer groups investigated the ways that informants improved soil fertility. Organic farmers perceived bountiful rice and good health as externalities of nurturing the soil. By engaging in organic fertilizer practices respondents came to see themselves as part of an extended community of life. Data analysis reveals that participation in fertilizer groups contributes to improved health, wellbeing, and the long-term sustainability of organic farms. A better environment and good health are given by organic farming (Kaufman et al., 2011). The development of organic rice as a niche experiment was partly due to landscape changes but also due to NGOs, farmers and academic leaders, often as a reaction to the negative impacts of agrochemical-based commercial rice. A previously reported in-depth study found that if intensive promotion is applied, organic rice could become quite successful in terms of production and marketing (Kerdnoi et al., 2014).

A previous study reported that the concept of organic farming and sufficiency economy can help to reduce GHG emissions from agricultural activities and improve soil fertility and the soil carbon stock (Chaimanuskul et al., 2011; Kaufman et al., 2011; Thailand Research Fund, 2010). The latter study also reported the CF of organic and conventional farming and showed that organic farming had a lower CF than conventional farming. The comparisons between GHG emissions from coffee cultivation in Costa Rica show that the reported organic farming CF was 0.12-0.52 kg CO_2e/kg fresh coffee and the reported conventional farming CF was 0.26-0.67 kg CO_2e/kg fresh coffee. The difference in CF between these two systems was represented by nitrogen chemical fertilizer use. Energy use from organic farming was lower than in conventional farming (Dalgaard et al., 2001; Meisterling et al., 2009; Kaltasas et al., 2007). Moreover the life cycle assessment (LCA) and CF concept was a good concept for response to consumers who are environmental friendly. Estimates of CF is not only useful for agriculture products but also other products, for example; aquatic product (shrimp), green logistic systems, biodiesel etc. (Mungkung et al., 2012; Prapaspongsa et al., 2012; Rewlay-Ngoen et al., 2013). Levels of GHG emissions in terms of CF can be estimated from such crop systems, but emissions from organic farming in Thailand are less well known.

In this study, the CF of Chinese kale was chosen because of increasing demand and more widespread use of this product as food. Normal cultivation practice for Chinese kale involves large amounts of chemical fertilizer, herbicide and insecticide to control weeds and pests. This paper presents the findings of a study whose objective was to evaluate the CF of organic and conventional farming of Chinese kale. We expect that the results of this study can be used to promote the policy of organic farming in other areas of Thailand. Organic production allows farmers to be more competitive and market-oriented, to keep their land in good agricultural and environmental condition, and to ensure food safety and animal health and welfare. The life cycle assessment (LCA) concept can be the basis for assessing the environmental sustainability of organic agriculture, and for identifying options

aimed at improving the global environmental performance of agricultural products.

2. METHODOLOGY

2.1 Description of sites and data collection

This study estimated emissions from conventional and organic farming of Chinese kale. The study site was located on an experimental farm in Kamphaeng Saen, Mueang and Don Tum district, Nakhon Pathom province, Thailand (Figure 1). Chinese kale in all areas of Thailand covered 5,134.88 ha; production was 1,900 tons; and the average yield was 10.08 kg/ha (Office of Agricultural Economics, 2015). Statistics show that western Thailand had the highest production. In addition, Nakhon Pathom province had the highest number of households that planted Chinese kale.

Data were collected from 518.08 ha of Chinese kale planting area in the 2015 production year, or about 10.09% of the total planting area in Thailand (Figure 1).

The following are the cultivation practices commonly applied to the Chinese kale field in this region, which served as the basis for estimating CFP in this study: Chinese kale is planted 2-3 times per year and the harvest takes place 45-55 days after planting. Plowing of the fields are carried out. Organic fertilizer is usually applied before planting. Chemical fertilizer is applied only once as a composite fertilizer and urea (chemical fertilizer was applied in conventional farming). In addition, if irrigation water is needed, it is usually pumped from nearby ponds just prior to planting and 2-3 days after planting periods. Herbicide and insecticide are usually applied to control weeds and insects (Table 1 and Table 2).

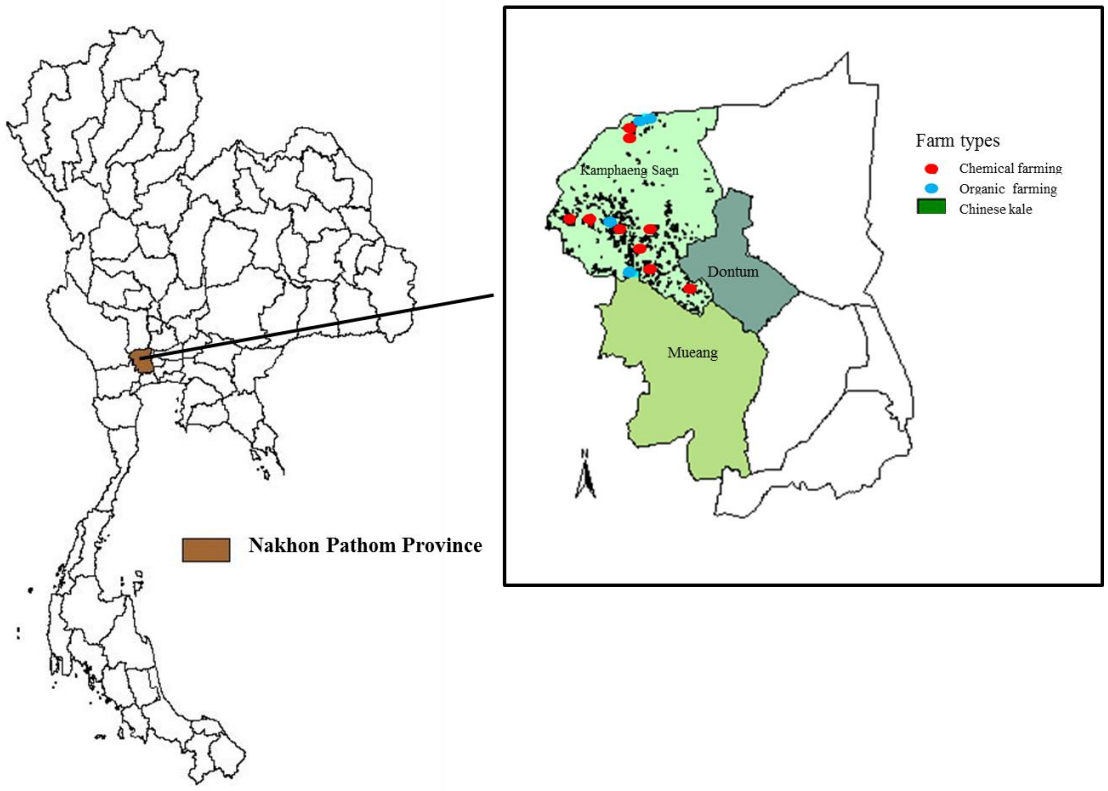

Figure 1. Chinese kale area located in Nakhon Pathom province, Thailand

2.2 LCA approach

2.2.1 System boundaries

We analyzed the global warming potential (GWP) from the CF of two different boundaries: organic and conventional farming practice. The CF was estimated following the life cycle assessment (LCA) concept and Publicly Available Specification (PAS) 2050 method (The British Standards Institution, 2008; Sinden, 2009). Four stages of the life cycle of Chinese kale (cultivation, production, processing and transportation) were considered. The systems boundary covered GHG emissions from raw materials used in Chinese kale cultivation (Figure 2). The system boundaries were used in a Business-to-

Business (B2B) or Cradle to Gate approach and covered GHG emissions from raw material use for cultivation and production (Figure 2 and Figure 3). The study boundaries of both systems included all production steps from field to farm gate including machinery production and use, fossil fuel use for farm operations, inputs (fertilizers, herbicides, insecticides and seed), water use and transportation of the produce to the central market.

In general, the system boundary of organic farming included irrigation, application of bio-active herbicides and insecticides, the production process and organic fertilizer application (Figure 2). Organic farming processes try to reduce the use of chemical substrates. Conventional farming is different: most conventional farming uses chemical substances including fertilizer, herbicide and insecticide. The system boundary of conventional farming includes tillage, irrigation, herbicide and insecticide application, chemical fertilizer and organic fertilizer use (Figure 3).

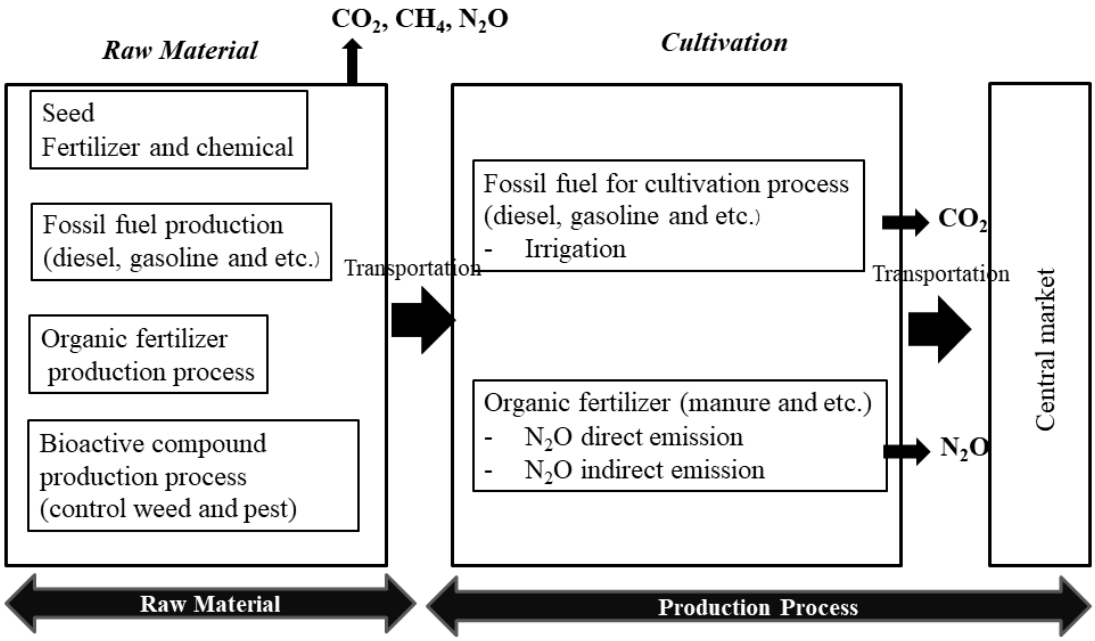

Figure 2. System boundary of organic farming

2.2.2 Functional unit

The functional unit (FU) was defined as kg CO_2e/kg of Chinese kale. These were compared between two system boundary from organic and conventional as mentioned above. The scope and goals were defined to record the data from the input and output of the cultivation process, estimating the CF from fresh Chinese kale. It assumed that the boundary of production extended from the farm to the central market. The GHGs to be estimated were CO_2, methane (CH_4) and nitrous oxide (N_2O). Each gas was converted into its CO_2 equivalent by use of GWP equivalent factors. CO_2, CH_4 and N_2O have a GWP of 1, 25 and 298, respectively. These values came from the latest IPCC 100-year time horizon of GWP equivalent factors (IPCC, 2007).

2.2.3 Life cycle inventory

The inventory analysis quantified the environmentally significant inputs and outputs of the systems examined, by means of the mass and energy balances of the selected FU of the study. The main energy and materials input and output of the Chinese kale supply chain were collected from the experimental farm (Figure 1) according to the information provided by farmers collected by using questionnaires. The data show the main inputs and outputs involved in organic (Table 1) and conventional farming (Table 2).

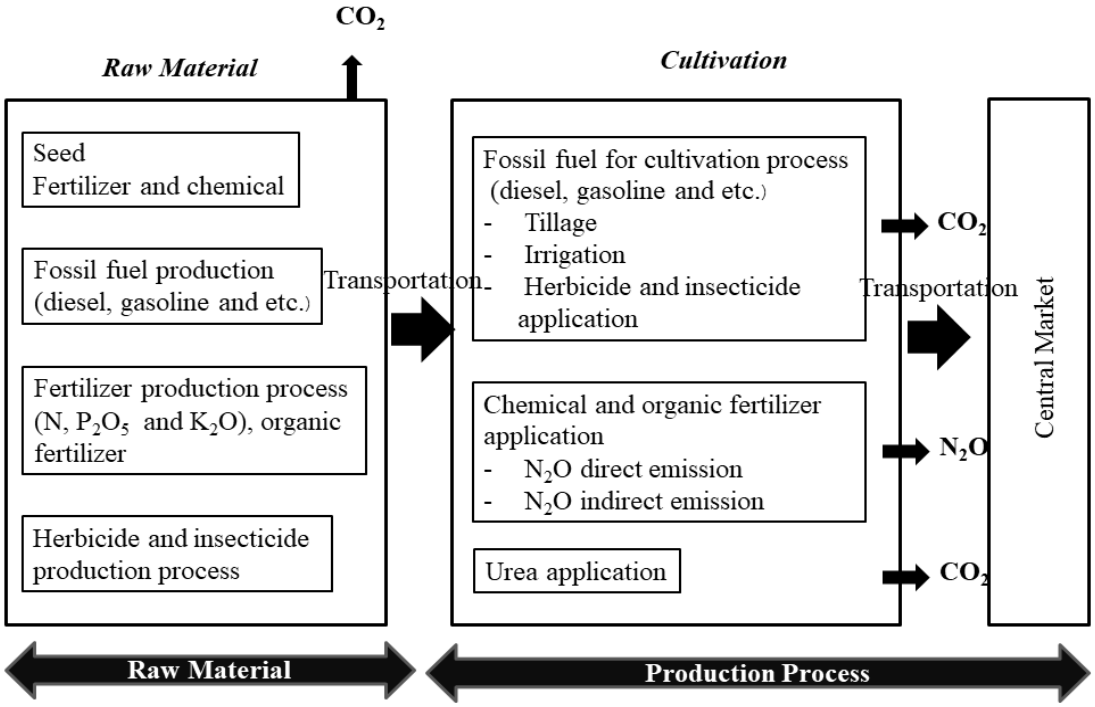

Figure 3. System boundary of conventional farming

Table 1. Data input; planted area, yield, the quantity of fertilizer application, fossil fuel use, seed, cultivation method from organic farming

Details	Organic farming
Harvested time (day)	45-55
Seed (kg/ha)	3.13
Planted area (ha)	12.5-31.25
Planted period in this area (year)	1-2
Crop rotation (crop/year)	2
Yield (ton/ha)	10
Product price (USD/kg)[b]	0.43-0.57
Diesel for tillage practice (L/ha)	–
Tillage time (time/crop)	–
Number of fertilizer application	1-2
Quantity of nitrogen in chemical fertilizer (kg/ha)	–
Quantity of nitrogen in organic fertilizer (kg/ha)	4.75
Urea (46-0-0) (kg/ha)	–
Organic fertilizer (kg/ha)	625-3,125
Type of bioactive compound to control weed and pest	Pyroligneous acid, Buvaria, Effective microorganisms(EM)
Quantity of herbicide and insecticide (cc/ha)	–
Type of weed control	Man power
Quantity of weed control (cc/ha)	–
Gasoline for machinery to spray herbicide and insecticide (L/ha)	–
Gasoline for machinery to spray chemical to control weed (L/ha)	–
Diesel for irrigation system (L/ha)	–
Price of electricity for irrigation system (USD/ha)[b]	35.71
Water resource	Natural pond

Table 1. Data input; planted area, yield, the quantity of fertilizer application, fossil fuel use, seed, cultivation method from organic farming (cont.)

Details	Organic farming
Quantity of nitrogen in organic fertilizer (chicken manure) (%/W)[a]	1.2-4.9
Quantity of nitrogen in organic fertilizer (cow manure) (%/W)[a]	0.32-1.2
Distance to central market (two way) (km)	24-30 Mueang district, Nakhon Pathom province
Fossil fuel use for transportation (L/km)	24

[a]Suwannarit, 2010
[b]Exchange rate: 1 USD ~ 35 baht

Table 2. Data input; planted area, yield, the quantity of fertilizer application, fossil fuel use, seed, cultivation method from conventional farming

Details	Conventional farming
Harvested time (day)	45-55
Seed (kg/ha)	3.13
Planted area (ha)	12.5-62.5
Planted period in this area (year)	3-30
Crop rotation (crop/year)	2-5
Yield (ton/ha)	12.5-31.25
Product price (USD/kg)[b]	0.057-0.114
Diesel for tillage practice (L/ha)	50-93.75
Tillage time (time/crop)	1-3
Number of fertilizer application	1-3
Quantity of nitrogen in chemical fertilizer (kg/ha)	250-625
Quantity of nitrogen in organic fertilizer (kg/ha)	
Urea (46-0-0) (kg/ha)	62.5-1,250
Organic fertilizer (kg/ha)	312.5-1,875
Type of bioactive compound or chemical compound to control weed and pest	Buakum, Hachi Hachi, Simtrack, Abamethene
Quantity of herbicide and insecticide (cc/ha)	3,125-6,250
Type of weed control	Gramoxone, Rampat, Glyphosate
Quantity of weed control (cc/ha)	3,750-6,250
Gasoline for machinery to spray herbicide and insecticide (L/ha)	3.13-62.5
Gasoline for machinery to spray chemical to control weed (L/ha)	3.13-25
Diesel for irrigation system (L/ha)	143.75-518.75
Price of electricity for irrigation system (USD/ha)[b]	35.71
Water resource	Natural pond
Quantity of nitrogen in organic fertilizer (chicken manure) (%/W)[a]	1.2-4.9
Quantity of nitrogen in organic fertilizer (cow manure) (%/W)[a]	032-1.2
Distance to central market (two way) (km)	200 Talad Thai market, Patum Thani province
Fossil fuel use for transportation (L/km)	68

[a]Suwannarit, 2010
[b]Exchange rate: 1 USD ~ 35 baht

2.2.4 Estimation of CF from organic and conventional farming

GHG emissions were calculated from the production and application of fertilizers, herbicides and insecticides, and of fossil fuel use, during the two methods of cultivation. This study aimed to compare emissions from different farming methods (organic and conventional farming). The system boundaries were drawn at the farm gate and included raw materials used in cultivation (Figure 2 and Figure 3). Information was obtained from the interviews of Chinese kale farmers (4 farms of organic farming and 11 farms of conventional farming). The study site was located on an experimental farm in Kamphaeng Saen, Mueang and Don Tum district, Nakhon Pathom province, Thailand as mention above. The distance between farms was approximated 1-30 kilometers (Figure 1). Moreover, both chemical and organic fertilizers were applied. The application amount was obtained from interviews of Chinese kale farmers for the whole period of Chinese kale planting. We used 0.01 kg-N N_2O/kg N applied to estimate N_2O from direct nitrogen fertilizer application. Indirect N_2O emissions from atmospheric deposition, leaching and runoff were also estimated. CO_2 emissions from the use of urea were accounted for using the emission Intergovernmental Panel on Climate Change (IPCC) factors (IPCC, 2006). Information on energy use for farm operations and management was obtained from the questionnaires. The energy types included gasoline and diesel for herbicide and insecticide application, tillage, irrigation and transportation of product to the central market. The emissions were estimated from the amount of fuel used and the emission factors listed in Table 3. Finally, the calculation was based on the IPCC method (IPCC, 2006).

Table 3. Emission factors use for calculation of greenhouse gases emissions from Chinese kale cultivation from organic and conventional farming

Activity	Emission factors	Unit
Production (Raw material)		
Production of diesel[c]	0.3282	kg CO_2e/kg
Production of gasoline[c]	0.7069	kg CO_2e/kg
Production of diesel (low S)[a]	0.4293	kg CO_2e/L
Production of gasoline (unleaded)[a]	0.5093	kg CO_2e/L
Production of N[c]	3.3036	kg CO_2e/kg
Production of P_2O_5[c]	1.5716	kg CO_2e/kg
Production of K_2O[c]	0.4974	kg CO_2e/kg
Production of Urea-Production[c]	3.2826	kg CO_2e/kg
Urea (include N_2O) (production + utilization)[c]	5.5300	kg CO_2e/kg
Organic fertilizer (dry chicken manure)-production[c]	0.1097	kg CO_2e/kg
Electricity, grid mix (electricity)[c]	0.6093	kg CO_2e/kWh
Natural gas[c]	0.1515	kg CO_2e/kg
LPG[c]	0.4232	kg CO_2e/kg
Glyphosate[c]	16.000	kg CO_2e/kg
Atrazine[c]	5.0100	kg CO_2e/kg
Alachlor[c]	8.0900	kg CO_2e/kg
Paraquat[c]	3.2300	kg CO_2e/kg
Bromacil[c]	5.2500	kg CO_2e/kg
Diuron[c]	7.0400	kg CO_2e/kg
Ametine[c]	8.5100	kg CO_2e/kg
Utilization (Emission from utilization)		
Diesel-combustion[b]	2.7080	kg CO_2e/L
Gasoline-combustion[b]	2.1896	kg CO_2e/L

Table 3. Emission factors use for calculation of greenhouse gases emissions from Chinese kale cultivation from organic and conventional farming (cont.)

Activity	Emission factors	Unit
Electricity utilization[d]: CO_2	0.0564	kg CO_2e/MJ
CH_4	1	kg CH_4/TJ
N_2O	0.1	kg N_2O/TJ
N_2O direct emission from fertilizer use[d]	0.01	kg N_2O-N/ kg N-input
N_2O direct emission from fertilizer after N leaching and runoff[d]	0.0075	kg N_2O-N (kg leaching per runoff)
N_2O indirect emission after emission of fertilizer N as NO_x and NH_3[d]	0.01	kg N_2O-N (kg of N applied per kg NH_3-N + NO_x-N)
Urea [c]	2.2474	kg CO_2e/kg
The nutrient from organic fertilizer (cow manure)[e] % by Weight;		
N	0.32-1.2	%/W
P	0.21-0.39	%/W
K	0.16-3.10	%/W
The nutrient from organic fertilizer (chicken manure)[e] % by Weight;		
N	1.2-4.9	%/W
P	0.7-4.1	%/W
K	0.47-3.50	%/W

[a]Thailand National Technical Committee on Product Carbon Footprint, 2009
[b]Thailand National Technical Committee on Product Carbon Footprint, 2011
[c]Thailand National Technical Committee on Product Carbon Footprint, 2015
[d]IPCC, 2006
[e]Suwannarit, 2010

2.2.5 The calculation of greenhouse gas emissions

Greenhouse gas emissions were calculated in every step by multiplying the emission factor of the material by the energy of that process (Equation 1) and recorded in terms of greenhouse gas emissions per unit of product.

$$CO_2 \text{ Emission} = \text{Activity data} \times \text{Emission factor} \quad (1)$$

where the activity data is energy used in each step such as raw materials (tons), and emission factor is the coefficient of pollutant emissions.

If the greenhouse gases were other gases, their emission was adjusted to a carbon dioxide equivalent by using GWP (Equation 2).

$$CO_2 \text{ Emission} = \text{Emission} \times GWP \quad (2)$$

where GWP is potential of global warming in term of carbon dioxide equivalent (CO_2=1, CH_4=25 and N_2O=298) (IPCC, 2007).

The N_2O Emissions from synthetic fertilizer and manure application-direct emission. N_2O Emissions from N fertilizer utilization was represented in Equation 3 (IPCC, 2006).

$$N_2O\text{-}NN_{input} = F_{SN} + F_{ON} \times EF_1 \quad (3)$$

where $N_2O\text{-}NN_{inputs}$ is annual direct N_2O-N emissions from N inputs to manage soils (kg N_2O-N/year). F_{SN} is annual amount of synthetic fertilizer N applied to soils (kg N/year). F_{ON} is annual amount of manure applied to soils (kg N/year). EF_1 is emission factor for N_2O emissions from N inputs (kg N_2O-N /kg N input). This is 0.01 kg N_2O-N/kg N input (IPCC, 2006)

N_2O Emissions from atmospheric deposition of N volatilized from managed soil were represented in Equation 4. The equation for this purpose is given below (IPCC, 2006).

$$N_2O_{(ATD)}\text{-}N = [(F_{SN} \times Frac_{GASF}) + (F_{ON} + F_{PRP} \times Frac_{GASM})] \times EF_4 \quad (4)$$

where $N_2O_{(ATD)}$-N is annual amount of N_2O-N produced from atmospheric deposition of N volatilized from managed soils, kg N_2O-N/year. F_{SN} is annual amount of synthetic fertilizer N applied to soils, kg N/year. $Frac_{GASF}$ is fraction of synthetic fertilizer N that volatilizes as NH_3 and NOx, kg N volatilized (kg of N applied)$^{-1}$; 0.10 kg NH_3-N + NO_x-N (IPCC, 2006). F_{ON} is annual amount of managed animal manure, compost, sewage sludge and other organic N additions applied to soils, kg N/y. F_{PRP} is annual amount of urine and dung N deposited by grazing animals on pasture, range and paddock, kg N/year. $Frac_{GASM}$ is fraction of applied organic N fertilizer materials (F_{ON}) and of urine and dung N deposited by grazing animals (F_{PRP}) that volatilizes as NH_3 and NOx, kg N volatilized (kg of N applied or deposited)$^{-1}$; 0.20 kg NH_3-N + NO_x-N (IPCC, 2006). EF_4 is emission factor for N_2O emissions from atmospheric deposition of N on soils and water surfaces, [kg N-N_2O/(kg NH_3-N + NO_x-N volatilized)]; 0.010 kg N_2O-N (IPCC, 2006)

N_2O Emissions from N fertilizer utilization and manure by leaching and runoff were estimated according to the methodology of IPCC (2006) and were represented in Equation 5. The equation for this purpose is given below (IPCC, 2006).

$$N_2O(L)\text{-}N = (F_{SN} + F_{ON}) \times Frac_{LEACH-(H)} \times EF_5 \quad (5)$$

where $N_2O(L)$-N is annual amount of N_2O-N produced from leaching and runoff of N additions to managed soils in regions where leaching/runoff occurs, kg N_2O-N/year. F_{SN} is annual amount of synthetic fertilizer N applied to soils in regions where leaching/runoff occurs, kg N/year. F_{ON} is annual amount of managed animal manure, compost, sewage sludge and other organic N additions applied to soils in regions where leaching/runoff occurs, kg N/year. $Frac_{LEACH-(H)}$ is fraction of all N added to/mineralized in managed soils in regions where leaching/runoff=0.30. EF_5 is emission factor for N_2O emissions from N leaching and runoff, kg N_2O-N (kg N leached and runoff)$^{-1}$ (TabIPCC 2006)=0.0075 kg N_2O-N (kg leaching/runoff). All emission factors and data use for calculation were listed in Tables 1-3.

3. RESULTS AND DISCUSSION

3.1 Input, yields and emissions from crop management

3.1.1 Characteristics of Chinese kale production in Nakhon Pathom province

Agricultural practices in organic and conventional Chinese kale production during the study period are shown in Table 1 and Table 2. Calculation of GHG emissions by the crop was based on the farmer's work schedule, the time taken for each operation, the number of labourers and machines, and all inputs used for field operations (fertilizer applications, insect trapping, etc.). To calculate CF from this activity, we recorded the use of materials and fuel consumption, as well as the time needed to complete each operation (Table 3). The differences between the two practices were the amounts of fertilizer, herbicide and insecticide applied; the type of chemical and methodology to control weeds and pests; energy and fossil fuel use; markets; product price; and the quantity of product (Table 1 and Table 2).

Information on chemical farming, the general features of farms, farm operations and energy utilization from 11 questionnaires (or farms) shows a wide range of the amount of resource inputs (Table 2). The yield per hectares range was 12.5-31.25 tons/ha. From the interviews, most of the farmers have continued growing their Chinese kale for 3-30 years. Thus, the emissions from land used changed to Chinese kale was not accounted for in this study. Chinese kale yield was sent to Talad Thai market located in Patum Thani province, Thailand. On average, the farms were located about 200 km from the market. Average diesel consumption was 50-3.75 L/ha. It is worth noting that the N fertilizer application rate range was 250-625 kg/ha, urea was 62.5-1,250 kg/ha and organic fertilizer was 312.5-1,875 kg/ha. Irrigation was usually carried out during the start of the growing season and 2-3 days after Chinese kale planting. Energies required for trucks and pumps to spray water were diesel and gasoline. Herbicide and insecticide was applied by the type of bioactive and chemical compound to control weed and pest (Buakum, Hachi Hahi, Simtrack and Abamethene etc.) (Table 2).

The general features of organic farms differed from farms that used chemical fertilizer. Responses about energy utilization from 4 questionnaires (or farms) show a wide range of resource inputs (Table 1). The yield per hectares range was 10 tons/ha. From the interviews, the farmers have grown their Chinese kale for 1-2 years. Chinese kale yield was sent to the market located within Nakom Pathom province, Thailand. On average, the farms were located about 24-30 km from the market. The organic fertilizer was applied at 625-3,175 kg/ha. Irrigation was similar with chemical farming. Bioactive compounds (Pyroligneous acid, Buvaria and Effective microorganisms (EM)) were used as herbicide and insecticide to control weeds and pests (Table 1).

3.2 CF from organic farming (raw material, cultivation and transportation to central market)

The CF of organic farming included emissions from fossil fuel for irrigation and fertilizer as represented by the unit of kg CO_2e/kg of Chinese kale. The number of CF was 0.195±0.122 kg CO_2e/ kg of Chinese kale (N=4) (Table 4 and Figure 4). The highest emissions came from transportation (0.091 kg CO_2e/kg of fresh product, 81%) followed by organic fertilizer (0.113 kg CO_2e/kg of Chinese kale, 12%) and fossil fuel for irrigation (0.008 kg CO_2e/kg of Chinese kale, 7%), respectively (Figure 4).

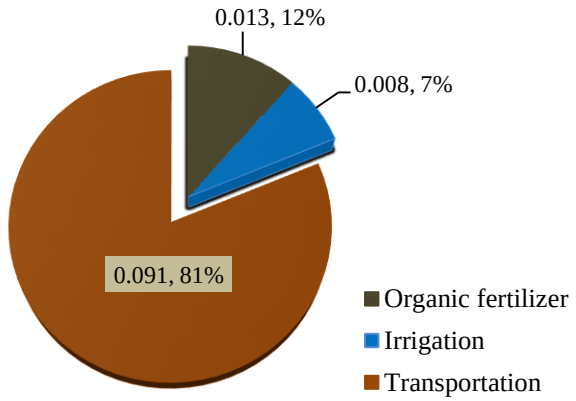

Figure 4. The proportion of emission from organic farming (kg CO_2e/kg of Chinese kale)

Table 4. Carbon footprint of organic Chinese kale (including emission from raw material, utilization, cultivation and transportation)

No.	Emission sources kg CO_2e/ha				Total emission (kg CO_2e/kg of Chinese kale)
	Organic fertilizer[a]	Irrigation[b]	Transportation[c]	Total emission	
1	1,598.19	441.5	1,180.25	3,219.88	0.322
2	360.75	441.5	944.19	1,746.44	0.175
3	239.81	110.38	Planting for household	350.19	0.035
4	1,082.31	331.13	1,062.19	2,475.63	0.248
Mean	820.27	331.13	1,062.21	1,948.04	0.195
S.D.	638.21	156.09	118.03	1,223.34	0.122

[a]Organic fertilizer utilization (direct and indirect N_2O emission) and organic fertilizer production
[b]Energy for irrigation system; fossil fuel and electricity (utilization and production)
[c]Energy for transportation of product to central market (utilization and production)

3.3 CF from conventional farming (raw material, cultivation practice and transportation to central market)

The CF of conventional farming included the emissions from tillage, organic and chemical fertilizer, herbicides, insecticides, irrigation and transportation. The total emission was 0.402±0.47 kg CO_2e/kg of Chinese kale (N=11) (Table 5). The highest emission came from chemical fertilizer (0.22 kg CO_2e/kg of Chinese kale, 51%) followed by transportation (0.092 kg CO_2e/kg of Chinese kale, 21%), irrigation (0.084 kg CO_2e/kg of Chinese kale, 19%), tillage (0.020 kg CO_2e/kg of Chinese kale, 5%), organic fertilizer (0.009 kg CO_2e/kg of Chinese kale, 2%), herbicide (0.004 kg CO_2e/kg of Chinese kale, 1%) and insecticide (0.003 kg CO_2e/kg of Chinese kale, 1%) (Table 5 and Figure 5).

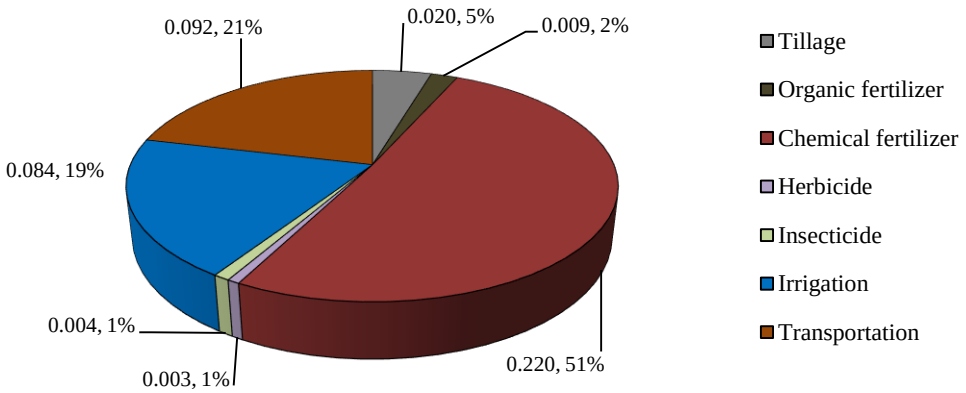

Figure 5. The proportion of emission from conventional farming (kg CO_2e/kg of Chinese kale)

Table 5. Carbon footprint of conventional farming (including emission from raw material, utilization, cultivation and transportation)

No.	Emission sources kg CO_2e /ha								Total emission (kg CO_2e/kg of Chinese kale)
	Tillage[a]	Organic Fertilizer[b]	Chemical fertilizer[c]	Insecti-cide[d]	Herbicide[e]	Irrigation[f]	Transporta-tion[g]	Total	
1	294.13	-	988.00	135.97	-	882.38	1,290.38	3,590.63	0.287
2	294.13	59.31	1476.00	54.40	72.53	441.19	1,290.38	3,687.69	0.197
3	176.50	243.38	885.63	16.78	45.37	1,617.69	1,290.38	4,275.56	0.342
4	294.13	-	2,180.00	18.15	-	1,307.25	1,290.38	5,089.94	0.204
5	294.13	-	8,206.50	-	9.07	1,307.25	1,290.38	11,107.31	1.777
6	294.13	-	2,952.00	181.35	72.53	1,176.50	1,290.38	5,966.44	0.318
7	294.13	-	5,470.19	38.19	116.59	1,176.50	1,290.38	8,385.69	0.447
8	294.13	59.31	1,095.88	19.09	116.59	1,176.50	1,290.38	4,051.69	0.216
9	294.13	-	662.13	2.00	18.15	-	1,290.38	2,266.69	0.121
10	294.13	-	1,366.94	12.08	89.86	-	1,290.38	3,053.25	0.326
11	294.13	-	1,848.81	19.09	89.86	-	1,290.38	3,542.13	0.189
Mean	283.43	120.67	2,466.55	45.19	70.06	1,135.66	1,290.38	5,001.55	0.402
S.D.	35.47	106.27	2,338.35	59.01	38.97	346.96	-	2,611.95	0.470

[a]Fossil fuel for farm machinery (production and utilization)
[b]Organic fertilizers (production and utilization)
[c]Chemical fertilizers (production and utilization)
[d]Energy for insecticide application (production and utilization) and insecticide production
[e]Energy for herbicide application (production and utilization) and herbicide production
[f]Energy for irrigation system; fossil fuel and electricity (production and utilization)
[g]Fossil fuel for transportation of product to central market (production and utilization)

3.4 Comparison between CF from organic and conventional farming

In conclusion, the CF of conventional farming was 0.402±0.47 kg CO_2e/kg of Chinese kale (N=11), (Table 5) and the CF of organic farming was 0.195±0.122 kg CO_2e/kg of Chinese kale (N=4), (Table 4). The difference in emissions related to farm management. The CF of conventional farming was about double that of organic farming. Because conventional farming was cultivated by applying a large amount of chemical fertilizer, fossil fuel for farm operation and management, use of herbicide and insecticide to get more production and further product shipment to a central market (higher demand from consumer). In contrast, the organic farmers did not plant for sale to a central market, but for home consumption or for a nearby community market. The distances involved in the two systems differed, and so emission levels and CF were affected.

Conventional cultivation was found to be less environmentally friendly than organic cultivation when results are presented per unit of product

(Kaltasas et al., 2007; Florence et al., 2015; Sonia et al., 2017). Moreover, the researcher presented the results of energy analysis that indicate ways to decrease energy inputs without losses in production and profits. The choice of management style in organic olive groves can decrease energy inputs without losses in production, and different uses of fossil energy tend to result in lower CO_2 emissions (Kaltasas et al., 2007). Florence et al. (2015) studied organic and conventional wheat farming. Organic wheat is more environmentally friendly than conventional wheat in terms of global warming, photo-oxidant formation and energy demand. Sonia et al. (2017) compared the energy and environmental impacts of organic and conventional apples cultivated in northern Italy. The results showed that conventional apples could help to reduce environmental impacts, and detailed analysis of the farming step showed that a significant share of the overall energy and environmental impacts was from the use of fertilizers and pesticides, and the diesel consumption of agricultural machines. The CF and the key of CF hotspots of organic and conventional cultivation systems in Chinese kale in this study indicate that fossil fuel for transportation plays a very important role for organic cultivation, while chemical fertilizer utilization plays a very important role for conventional cultivation. There were similar results in a sugarcane plantation in Thailand, crop production in China, coffee in Costa Rica and spring wheat in Canada. These studies found the very large amount of conventional cultivation emissions come from chemical fertilizer use (Yuttitham et al., 2011; Kun et al., 2011; Martin et al., 2012; Yantai et al., 2012). In China, crop emissions analysis showed that the largest contribution (~60%) comes from fertilizers (Kun et al., 2011). The CF results in coffee comparing conventional and organic management revealed that 1 kg of fresh coffee cherries in conventional systems accounted for between 0.26 and 0.67 kg CO_2e and organic systems accounted for between 0.12 and 0.52 kg CO_2e. The main contributor to GHG emissions for all management systems were the inputs of organic and inorganic nitrogen (Martin et al., 2012).

Total GHG emissions and environmental impacts from organic cultivation were lower than that in conventional cultivation. These results are similar to that of previous studies assessing organic versus conventional agriculture in many types of agricultural crops (Harpinder et al., 2010; Matthias et al., 2015; Spyros and Efthalia, 2016). One previous study of apple supply chains showed that 1 kg of apples had a GWP of 0.20 kg CO_2e. The main contribution to the CF during cultivation was consumption of fuel for machinery, which changed significantly according to the distance from the farm center and the field size (Sessa et al., 2014). Some research output from the USA studying small organic vegetable farms found fuel use, organic fertilizer, soil emissions and irrigation as the major hotspots in CF in organic farming management (Adewale et.al, 2016).

In this study, the CF of organic Chinese kale was 0.195±0.122 kg CO_2e/kg of Chinese kale, as mentioned above. A review of other organic crops in Thailand found the CF of organic crop cultivation ranged from 0.0019 to 0.8780 kg CO_2/kg of fresh product. This range includes the CF from acacia (0.0019 kg CO_2/kg), hamate bean (0.0044 kg CO_2/kg), garlic (0.0560 kg CO_2/kg), string bean (0.0565 kg CO_2/kg), guangdong (0.0739 kg CO_2/kg), cabbage (0.1202 kg CO_2/kg), Chinese cabbage (0.1621 kg CO_2/kg), soybean (0.2496 kg CO/kg) and asparagus (0.8780 kg CO_2/kg) (Thailand Greenhouse Gas Management Organization, 2018). The CF of organic Chinese kale in this study has a relatively high footprint if compared with other crops in the Thailand database. The CF of conventional Chinese kale was 0.402±047 kg CO_2e/kg of Chinese kale. When compared with other conventionally farmed products in the Thailand database, the CF sum ranged from 0.1223 to 2.5862 kg CO_2/kg of fresh product. Table 6 shows the footprint from many types of crops (Thailand Greenhouse Gas Management Organization, 2018).

The CF from this study show relatively moderate values when compared with others. One CF from Chinese kale in the Thailand database showed a total CF of 0.159 kg CO_2/kg of Chinese kale; this included emissions from cultivation (excluding emissions from transportation to the central market) (Thailand Greenhouse Gas Management Organization, 2018). The difference was mainly due to the inclusion of emissions from the use of materials in the cultivation process.

Table 6. The carbon footprint from conventional farming in Thailand database.

No.	Crop	Carbon footprint kg CO_2/kg	No.	Crop	Carbon footprint kg CO_2/kg
1	galangal	0.1074	16	sesame	0.3154
2	potato	0.1223	17	sweet corn	0.3262
3	guangdong	0.1338	18	tomato	0.3486
4	cauliflower	0.1457	19	paprika	0.3676
5	lemon grass	0.1494	20	black eyed peas	0.3684
6	carrot	0.1872	21	sweet pepper	0.3910
7	string bean	0.1897	22	garlic	0.4229
8	onion	0.2018	23	sweet basil	0.4447
9	lentils	0.2229	24	peanut	0.5528
10	kaffir lime fruit	0.2381	25	green beans	0.6999
11	cabbage	0.2555	26	lettuce	0.7771
12	shallots	0.2522	27	bamboo shoot	0.9272
13	maize	0.2670	28	pepper	1.1271
14	soybean	0.2898	29	kaffir lime leaves	2.5862
15	cucumber	0.3062			

4. CONCLUSIONS

This study aimed to estimate the CF from organic and conventional farming of Chinese kale in Nakhon Pathom province, Thailand. In conventional farming, more than 50% of GHG emissions come from the use of chemical fertilizers. In organic farming, more than 80% of GHG emissions come from the use of fossil fuel transportation. The results are similar to those in previous studies. Chemical fertilizers accounted for the highest GHG emissions found in conventional farming. To reduce GHG emissions, therefore, farmers should reduce use of chemical fertilizers or be recommended to use the appropriate quantity of fertilizer. We already know that organic farming maintains land in good agricultural and environmental conditions and is beneficial to food safety, and animal health and welfare. The results of this study could be used to promote the planting of Chinese kale by organic farmers. More survey data are needed to study the sensitivity of the CF to such large variations in input data. Lack of specific data meant that stock changes in soil organic carbon and soil pollution were not accounted for in this study, and further research should consider these.

ACKNOWLEDGEMENTS

This research was supported by Faculty of Environment and Resource Studies, Mahidol University. The authors gratefully acknowledge the contribution to Chinese kale farmers in Nakhon Pathom Province, Thailand for their kind answers to questionnaires and data support on their farm managements and operation and Dr. Wipawan Tinnungwattana for her support for data collection in field. The protocol No: MU-CIRB 2015/086.0206 certificate of approval by Mahidol University Central Institutional Review Board (MU-CIRB) for this study. We thank Elaine Monaghan, BSc (Econ), from Edanz Group (www.edanzediting.com/ac) for editing a draft of this manuscript.

REFERENCES

Adewale C, Higgins S, Granatstein D, Stockle C, Carloson BR. Identifying hotspots in the footprint of small scale organic vegetable farm. Agricultural Systems 2016;149:112-21.

Chaimanuskul K, Punnakanta L, Sonchaem W, Sukreeyapongse P, Hutacharoen RA. Practice model for sustainable agriculture assessment: a case study of the sustainable cultivation of Thai Hom Mali (Jasmine) rice in Thailand. Environment and Natural Resources Journal 2011;9:12-28.

Dalgaard T, Hakberg N, Porter JR. A model for fossil energy use in Danish agriculture used to compare organic and conventional farming. Agriculture Ecosystems and Environment 2001;87(1):51-65.

Florence VS, Astrid L, Michael M, Viviane P, Didier S, Frederic D. Organic *versus* conventional farming: the case of wheat production in Wallonia (Belgium). Procedia 2015;7:272-9.

Intergovernmental Panel on Climate Change (IPCC). IPCC Guidelines for National Greenhouse Gas Inventories: Volume 1-5. Hayama, Japan: Institute for Global Environmental Strategies; 2006.

Intergovernmental Panel on Climate Change (IPCC). Climate change 2007: The physical science basis. In: Solomon S, Qin D, Manning M, Chen Z, Marquis M, Averyt KB, Tignor M, Miller HL, editors. Contribution of Working Group I to the Fourth Assessment Report to the Intergovernmental Panel on Climate Change. Cambridge, USA; Cambridge University Press: 2007.

Kaltasas AM, Mamolos AP, Tsatsarelis CA, Nanos GD, Kalburtji KL. Energy budget in organic and conventional olive groves. Agriculture Ecosystems and Environment 2007;122:243-51.

Kaufman A, Watanasak S. Farmers and fertilizers: a socio-ecological exploration of the alternative agriculture movement in Northeastern Thailand. Environment and Natural Resources Journal 2011;9:1-11.

Kerdnoi1 T, Prabudhanitisarn S, Sangawongse S, Prapamontol T, Santasup C. The struggle of organic rice in Thailand: a multi - level perspective of barriers and opportunities for up scaling. Environment and Natural Resources Journal 2014;12:95-115.

Kun K, Genxing P, Pete S, Ting L, Lianqing Li, Jinwei Z, Xuhui Z, Xiaojun H, Ming Y. Carbon footprint of China's crop production: an estimation using agro-statistics data over 1993-2007. Agriculture, Ecosystems and Environment 2011;142:231-7.

Martin RAN, Gareth EJ, Jeremy PH, Gabriela S, Nicola A, John RH. Greenhouse gas emissions in coffee grown with differing input levels under conventional and organic management. Agriculture, Ecosystems and Environment 2012;151:6-15.

Matthias SM, Franziska S, Niel J, Rinnie J, Christian S, Matthias S. Environmental impacts of organic and conventional agricultural products: are the differences captured by life cycle assessment? Journal of Environmental Management 2015;149:193-208.

Meisterling K, Samaras C, Schweizer V. Decisions to reduce greenhouse gases from agriculture and product transport: LCA case study of organic and conventional wheat. Journal of Cleaner Production 2009;17:222-30.

Ministry of Agriculture and Cooperatives. Bureau of Agriculture Development Policy and Planning, Central of Philosopher Community. Ministry of Agriculture and Cooperatives; Bangkok, Thailand. 2010. (in Thai)

Mungkung R, Gheewala SH, Tomnantong A. Carbon footprint of IQF peeled Tail-On breaded shrimp (*Litopenaeusvannamei*): how big is it compared to other aquatic products? Environment and Natural Resources Journal 2012;10:31-6.

Office of Agricultural Economics (OAE). Farmer database in Thailand cropping years 2015 [Internet]. 2015 [cited 2015 Dec 10]. Available from: http://www.oae.go.th.

Prapaspongsa T, Løkke S. Framework for LCI modelling towards green logistic systems. Environment and Natural Resources Journal 2012;10:58-65.

Rewlay-Ngoen C, Papong S, Piumsomboon P, Malakul P, Sampattagul S. Life cycle impact modeling of global warming on net primary production: a case study of biodiesel in Thailand. Environment and Natural Resources Journal 2013;11:21-30.

Sandrhu HS, Wratten SD, Cullen R. The role of supporting ecosystem in conventional and organic arable farmland. Ecological Complexity 2010;7:302-10.

Thailand Greenhouse Gas Management Organization (Public Organization), (TGO). Thailand [Internet]. 2018 [cited 2018 Jun 15]. Available from: http://www.tgo.or.th.

Thailand National Technical Committee on Product Carbon Footprint. Carbon footprint of product. Bangkok, Thailand: Amarin Printing; 2009.

Thailand National Technical Committee on Product Carbon Footprint. Carbon footprint of product. Bangkok, Thailand: Amarin Printing; 2011.

Thailand National Technical Committee on Product Carbon Footprint. Carbon footprint of product. Bangkok, Thailand: Amarin Printing; 2015.

Thailand Research Fund (TRF). The development of the sufficient economy for mitigate greenhouse gases emission by Eastern Wisdom. Bangkok; 2010.

The British Standards Institution (BSI). Specification for the assessment of the life cycle greenhouse gas emissions of goods and services. London, UK: British Standards Institution; 2008.

The Joint Graduated School of Energy and Environment (JGSEE). Thailand greenhouse gases inventory report. Bangkok; 2009.

Sessa F, Marino M, Montanaro G, Dal Piaz A, Zanotelli D, Mazzetto F, Tagliavini M. Life cycle assessment of apples at a country level. Proceeding of the 9th International Conference on Life Cycle Assessment in Ari-food Sector (LCA Food 2014); 2014 Oct 8-10; Vashon, USA: American Center for Life Cycle Assessment; 2014.

Sinden G. The contribution of PAS 2050 to the evolution of international greenhouse gas emissions standards. International Journal of Life Cycle Assessment 2009;14(3):195-203.

Sonia L, Marina M, Francesco G, Maurizio G. Life cycle assessment of organic and conventional apple supply chains in the North of Italy. Journal of Cleaner Production 2017;140:654-63.

Spyros F, Efthalia C, Life cycle assessment of organic versus conventional agriculture: a case study of lettuce cultivation in Greece. Journal of Cleaner Production 2016;112:2462-71.

Suwannarit A. Fertilizer with Agriculture and Environment. 3rd ed. Bangkok: Kasetsart University; 2010.

Yantai G, Chang L, Con AC, Robert PZ, Reynald LL, Hong W, Chao Y. Carbon footprint of spring wheat in response to fallow frequency and soil carbon changes over 25 years on the semiarid Canadian prairie. European Journal of Agronomy 2012;43:175-84.

Yuttitham M, Gheewala SH, Chidthaisong A. Carbon footprint of sugar produced from sugarcane in Eastern Thailand. Journal of Cleaner Production 2011;19: 2119-27.

Mahidol University

Wisdom of the Land

Research and Academic Service Section, Faculty of Environment and Resource Studies, Mahidol University
999 Phutthamonthon 4 Rd, Salaya, Nakhon Pathom 73170, Phone +662 441-5000 ext. 2108 Fax. +662 441 9509-10
E-mail: ennrjournal@gmail.com Website: https://www.tci-thaijo.org/index.php/ennrj